Supporting Information

Divergent Fe-mediated C-H Activation paths driven by Alkali Cations

Vincent Wowk,[a] Alexis K. Bauer,[b] Aleksa Radovic,[b] Lise-Marie Chamoreau,[c] Michael L. Neidig,[d] and Guillaume Lefèvre*[a]*

[a] Chimie ParisTech, PSL University, CNRS, Institute of Chemistry for Life and Health Sciences, CSB2D, 75005 Paris, France

[b] Department of Chemistry, University of Rochester, Rochester, NY, 14627, USA

[c] Sorbonne Université, CNRS, Institut Parisien de Chimie Moléculaire, F-75252, Paris, France

[d] Inorganic Chemistry Laboratory, Department of Chemistry, University of Oxford, South Parks Road, Oxford OX1 3QR, United Kingdom

E-mail: guillaume.lefevre@chimieparistech.psl.eu ; michael.neidig@chem.ox.ac.uk

Table of Contents.

1) General information

All the samples were prepared in a Jacomex Campus glovebox under inert atmosphere of argon and vacuum Schlenk lines. Glassware was dried overnight at 120 ºC before use. Deuterated solvents were thoroughly degassed by Freeze-Thaw cycles and dried overnight on 4Å molecular sieves. Non-deuterated solvents were dried over a Na/benzophenone mixture and distilled before use. NMR tubes equipped with a J. Young valve were used for all ^{1}H NMR, ^{31}P NMR and ^{11}B NMR experiments. Chemicals were obtained from commercial sources and used as purchased, unless specified otherwise or after drying when necessary. A modified synthesis from the literature was applied for the synthesis of $Fe(Cl)_2(dmpe)_2$.

NMR spectra were recorded using a Bruker Avance III HD 400 MHz spectrometer. Chemical shifts (δ) are given in ppm and coupling constants (*J*) in Hz. The peak patterns are indicated as follow: (s, singlet; d, doublet; t, triplet; q, quartet; quin, quintet; m, multiplet, and br, for broad). Chemical shifts for ^{1}H NMR spectra were referenced using the residual solvent signal as internal standard (^{1}H: $CDCl_3$ = 7.26 ppm, THF-d8 = 3.58 ppm, 1.72 ppm and C_6D_6 = 7.16 ppm). ^{31}P NMR (162 MHz) spectra were referenced against external 85 % H_3PO_4 standard and ^{11}B NMR (128 MHz) spectra against external BF_3•OEt_2.

A Thorlabs' M365LP1 LED (nominal wavelength = 365 nm, FWHM = 9 nm) mounted to the end of a 57 mm heat sink enabling heat dissipation has been used for irradiation setup.

Low-resolution (LRMS) analysis were performed on GCMS-QP2010 SE device, equipped with AOC-20i injector, AOC-20s autosampler (Shimadzu Corporation) and electronic impact ionization technology (70 eV). Compounds were eluted on a ZB-5MS capillary column (length = 20 m ; intern diameter = 0.18 mm ; film thickness = 0.18 µm ; nature of the stationary phase = 5 % phenylarylene, 95 % dimethylpolysiloxane) using helium as carrier gas. Chromatograms were processed using LabSolutions software with GCMSsolution package v 4.52 (Shimadzu Corporation).

Elemental analyses were recorded in sealed tin capsules, prepared in a glovebox, by the analytical facilities of the Laboratoire de Chimie de Coordination (Isabelle Borget, Toulouse, France).

2) Preparation of the iron complexes: $Fe(Cl)_2(dmpe)_2$ and $FeBr(C_6H_5)(dmpe)_2$

a) $Fe(Cl)_2(dmpe)_2$ (1)

$Fe(Cl)_2(dmpe)_2$ was prepared according to the synthesis described by Chatt and Hayter[R1] but with some modification:

In an argon-filled glovebox, a 50 mL flask fitted with a J. Young valve was charged with anhydrous $FeCl_2$ finely ground (160 mg, 1.26 mmol, 1 equiv.). The flask was attached to the Schlenk line and anhydrous EtOH (15 mL) was added. The mixture was heated at 40 °C until $FeCl_2$ was completely dissolved, the color changed to yellow/orange. To the stirred mixture a solution of dmpe (420 µL, 2.52 mmol, 2 equiv.) in toluene (3 mL) (previously prepared in the glovebox) was added dropwise, the color change instantly to dark purple. The reaction mixture was stirred overnight at 40 °C, EtOH was removed under vacuum and the crude residue was dissolved in THF. The dark solution was filtered through a Pasteur pipette charged with Celite® 545 and glass wool. The resulting dark green solution was evaporated to dryness to afford an emerald-green powder (501 mg, 1,17 mmol, 93 %). ^{1}H NMR (400 MHz, THF-d8): δ = 2.21 (quin, 8H, -C*H*$_2$C*H*$_2$-), 1.45 (quin, 24H, -C*H*$_3$). ^{31}P{^{1}H} NMR (162 MHz, THF-d8): δ = 59.34 (s, 4P).

b) $FeBr(C_6H_5)(dmpe)_2$ ($2_{Ph'}$)

In an argon-filled glovebox, a 50 mL flask fitted with a J. Young valve was charged with $FeCl_2(dmpe)_2$ (80,1 mg, 187.6 µmol, 1 equiv.) and C_6H_6 (2 mL). The mixture was cooled at -30 °C and a 1M solution of PhMgBr in THF (93.8 µL, 93.8 µmol, 0.5 equiv.) was added dropwise. The reaction mixture was vigorously shaken and left 1 h at room temperature. The color gradually turned yellow/orange. The same process was repeated to a total of 1 equiv. of PhMgBr. The flask was left at room temperature overnight. The dark solution was filtered through a Pasteur pipette charged with Celite® 545 and glass wool. The resulting dark pink/red solution was concentrated (ca. 0.5 mL) and was layered with 2 mL of *n*-pentane. This was placed in the glovebox freezer at -35 °C for 3 days. The solution was evaporated to dryness to afford red crystals (51.7 mg, 100.8 µmol, 54 %). ^{1}H NMR (400 MHz, C_6D_6): δ = 6.81 (d, 2H, *o*-*H*$_{Ar}$, *J*(^{1}H-^{1}H) = 7.4 Hz), 6.71 (t, 1H, *p*-*H*$_{Ar}$, *J*(^{1}H-^{1}H) = 6.8 Hz), 6.63 (t, 2H, *m*-*H*$_{Ar}$, *J*(^{1}H-^{1}H) = 7.2 Hz), 1.85 (br, 8H, -C*H*$_2$C*H*$_2$-), 1.56 (s, 12H, -C*H*$_3$), 1.11 (s, 12H, -C*H*$_3$). ^{31}P{^{1}H} NMR (162 MHz, C_6D_6): δ = 67.12 (s, 4P).

Anal. Calcd. For $C_{18}H_{37}BrFeP_4$ (513.14 g.mol^{-1}): C, 42.13; H, 7.27; Found: C, 41.19; H, 7.03.

The same procedure was applied for the synthesis of $^{57}FeBr(C_6H_5)(dmpe)_2$ (**^{57}Fe-2$_{Ph'}$**). ^{1}H NMR (400 MHz, C_6D_6): δ = 6.80 (d, 2H, *o*-H_{Ar}, $J(^1H\text{-}^1H)$ = 7.4 Hz), 6.70 (t, 1H, *p*-H_{Ar}, $J(^1H\text{-}^1H)$ = 7.0 Hz, $J(^1H_{para}\text{-}^{57}Fe)$ = 3 Hz), 6.61 (t, 2H, *m*-H_{Ar}, $J(^1H\text{-}^1H)$ = 7.2 Hz, $J(^1H_{meta}\text{-}^{57}Fe)$ = 4 Hz), 1.86 (br, 8H, -CH_2CH_2-), 1.55 (s, 12H, -CH_3), 1.11 (s, 12H, -CH_3). $^{31}P\{^1H\}$ NMR (162 MHz, C_6D_6): δ = 67.16 (d, 4P, $J(^{31}P\text{-}^{57}Fe)$ = 42 Hz).

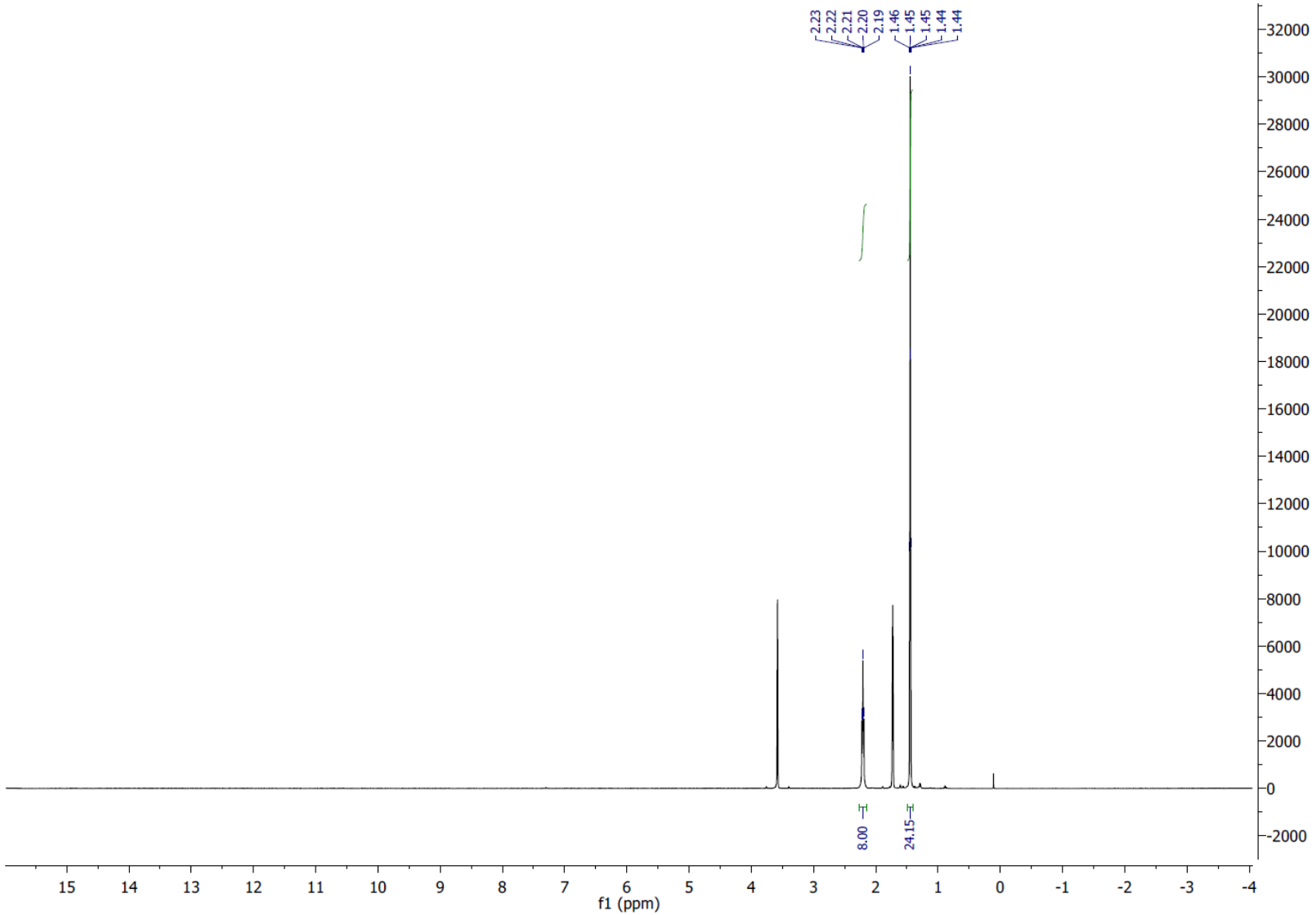

Figure S1: ^{1}H NMR (400 MHz, 298 K, THF-d8) of $Fe(Cl)_2(dmpe)_2$ (**1**).

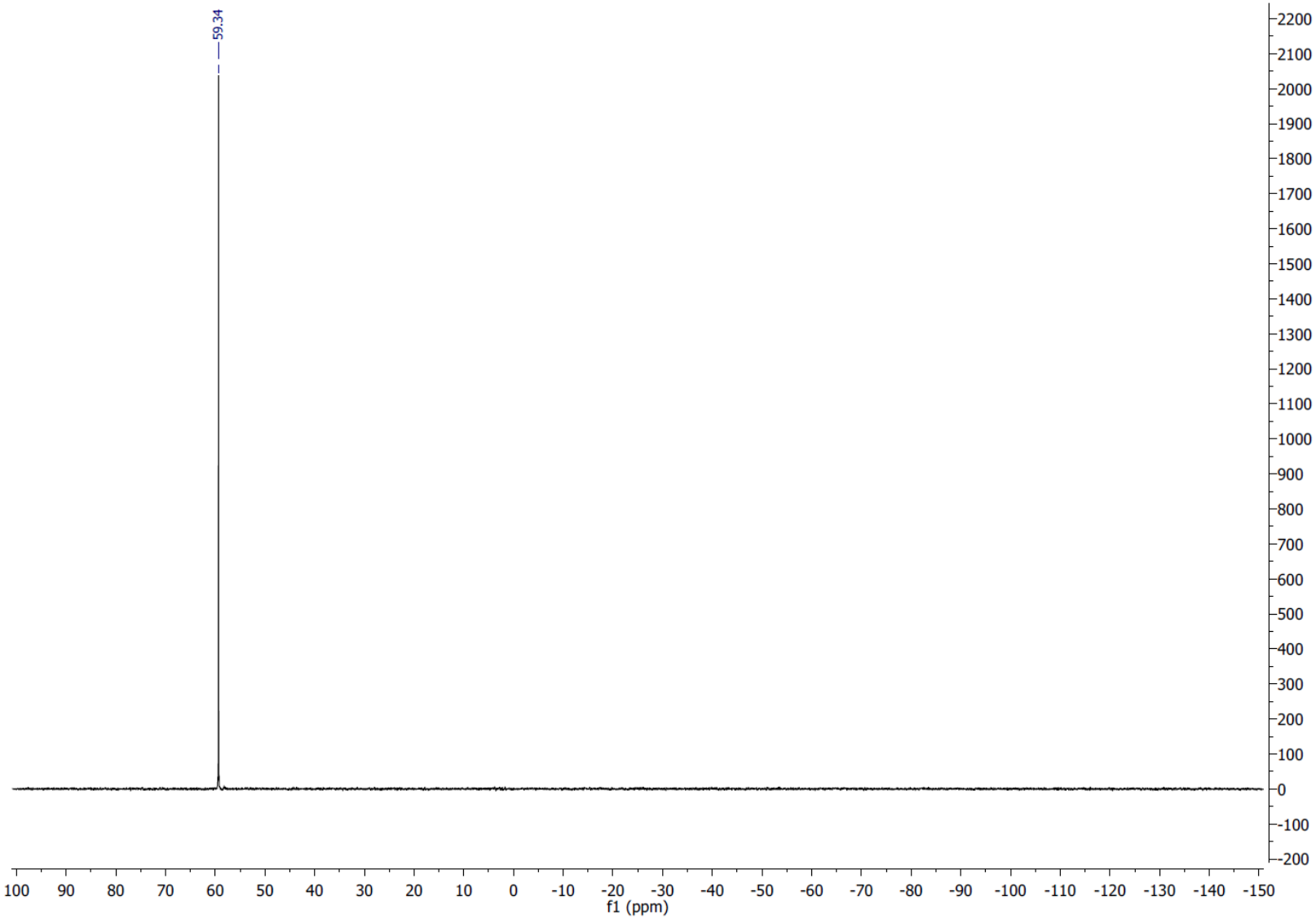

Figure S2: $^{31}P\{^{1}H\}$ NMR (162 MHz, 298 K, THF-d8) of $Fe(Cl)_2(dmpe)_2$ (**1**).

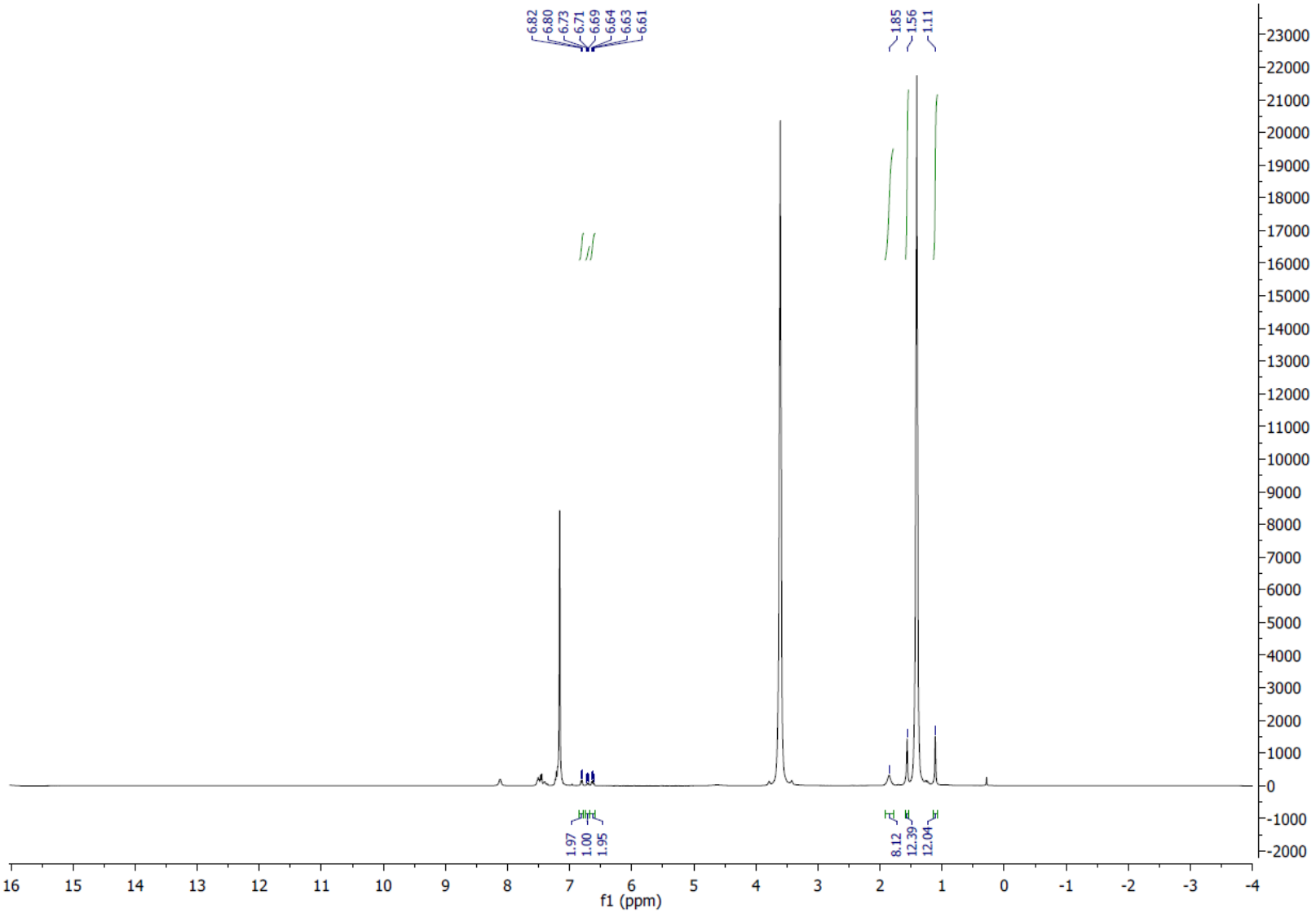

Figure S3: ^{1}H NMR (400 MHz, 298 K, C_6D_6) of $FeBr(C_6H_5)(dmpe)_2$ (**2$_{Ph'}$**).

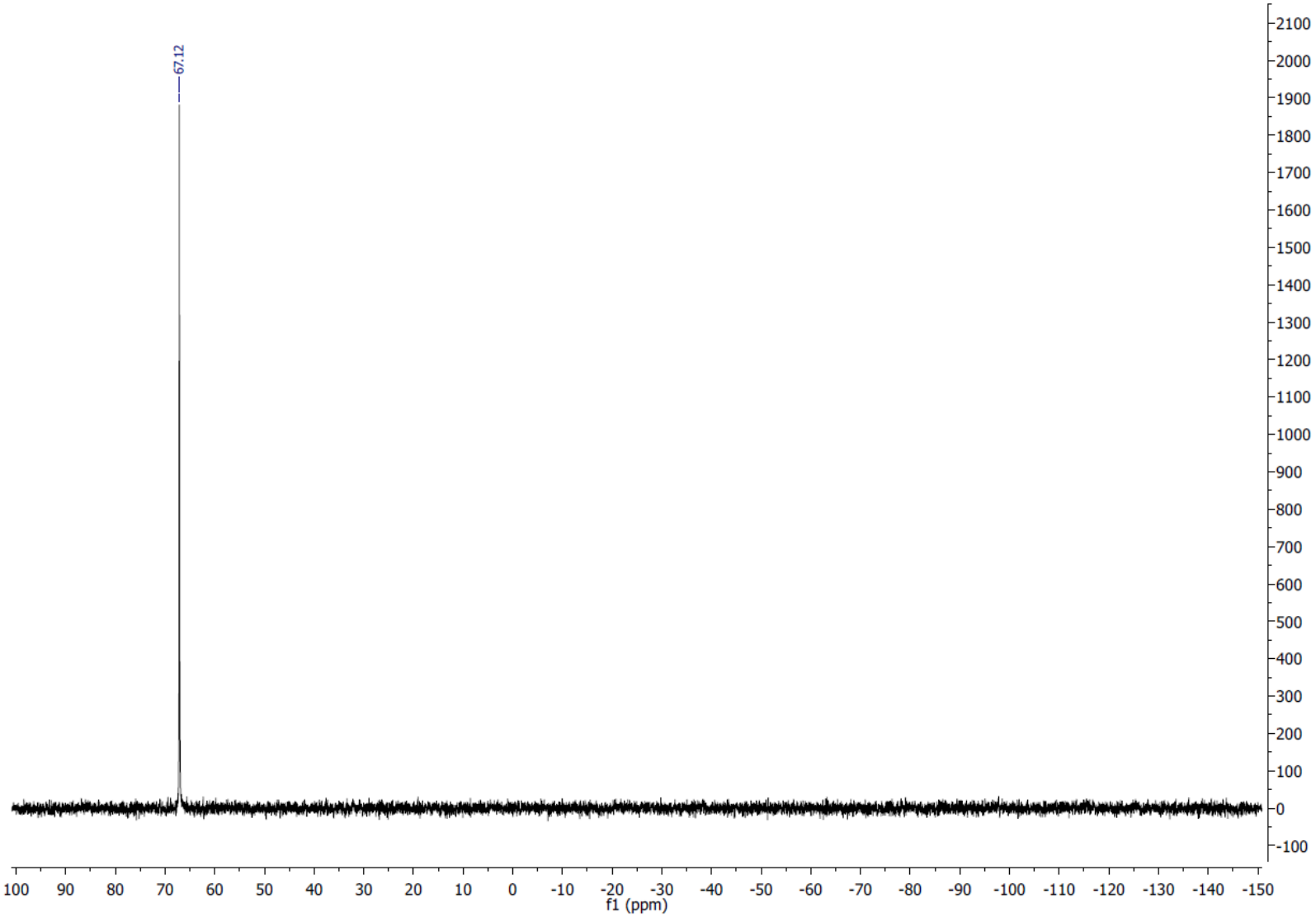

Figure S4: $^{31}P\{^{1}H\}$ NMR (400 MHz, 298 K, C_6D_6) of $FeBr(C_6H_5)(dmpe)_2$ (**2$_{Ph'}$**).

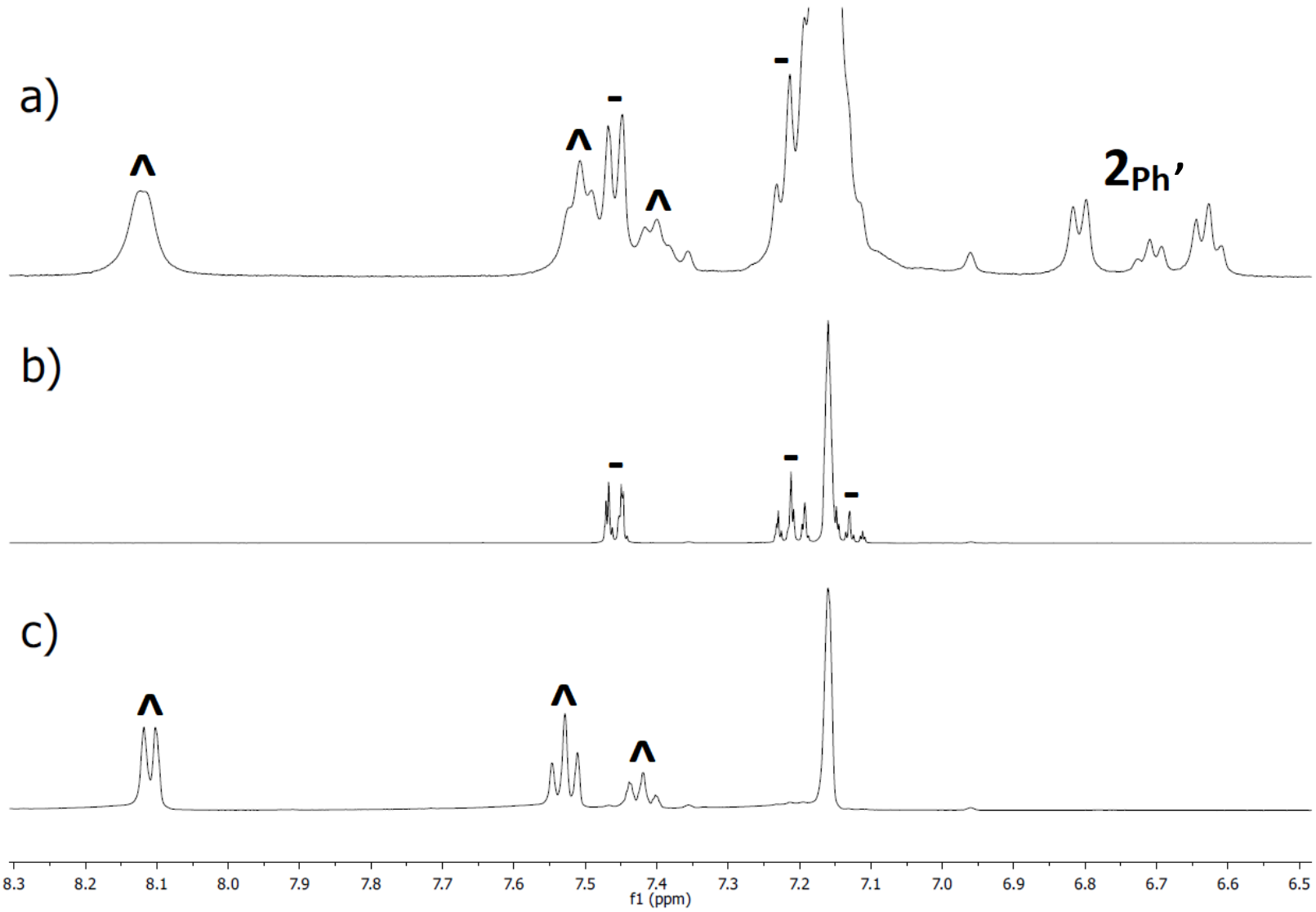

Figure S5: ^{1}H NMR (400 MHz, 298 K, C_6D_6) of $Fe(Cl)_2(dmpe)_2$ (**1**) treated by 1 equiv. of PhMgBr after one night at 20 °C (a), 1,1′-Biphenyl (-) (b) and a 1M solution of PhMgBr (^) in THF (c).

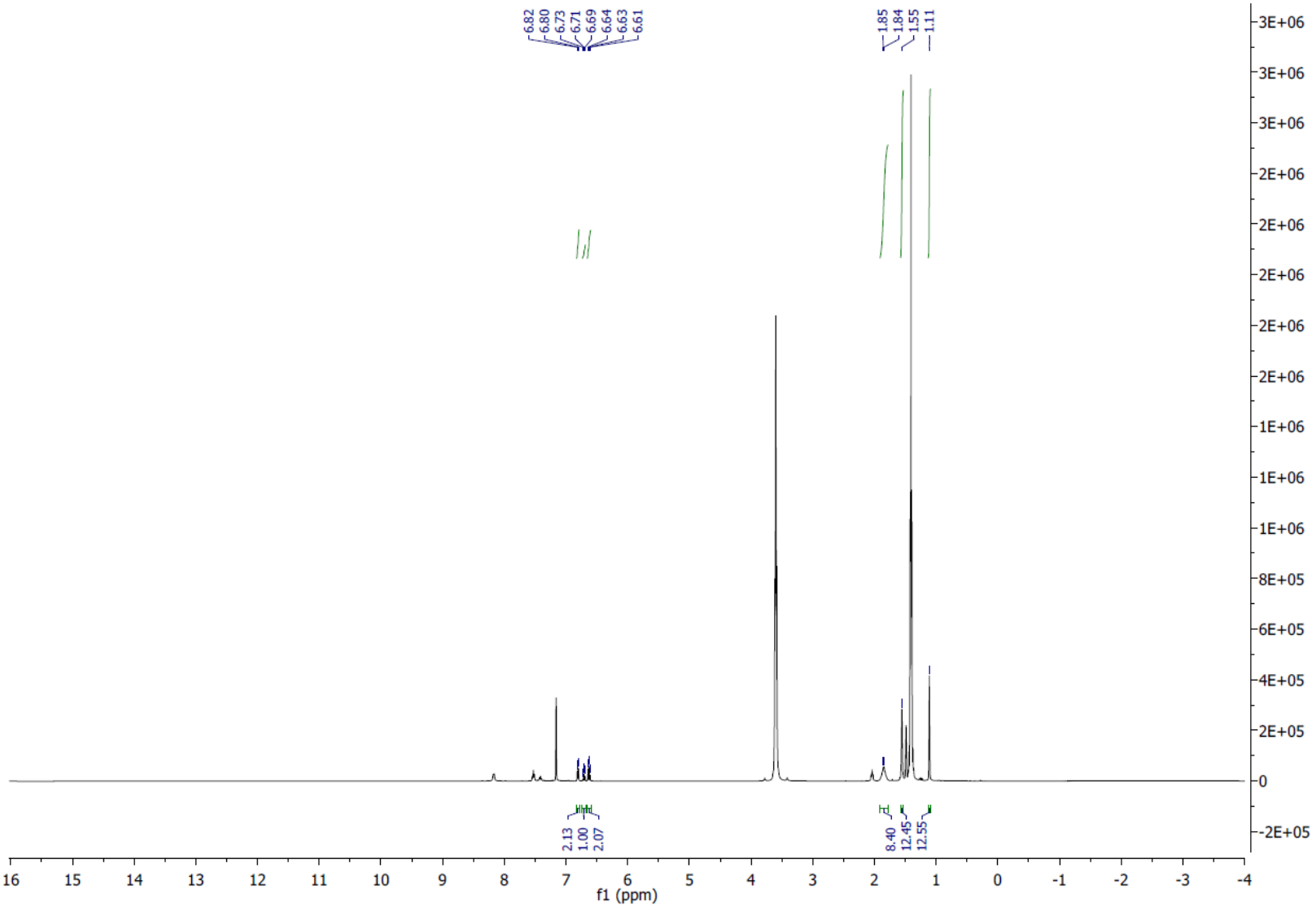

Figure S6: ^{1}H NMR (400 MHz, 298 K, C_6D_6) of $^{57}FeBr(C_6H_5)(dmpe)_2$ (**^{57}Fe-2$_{Ph'}$**).

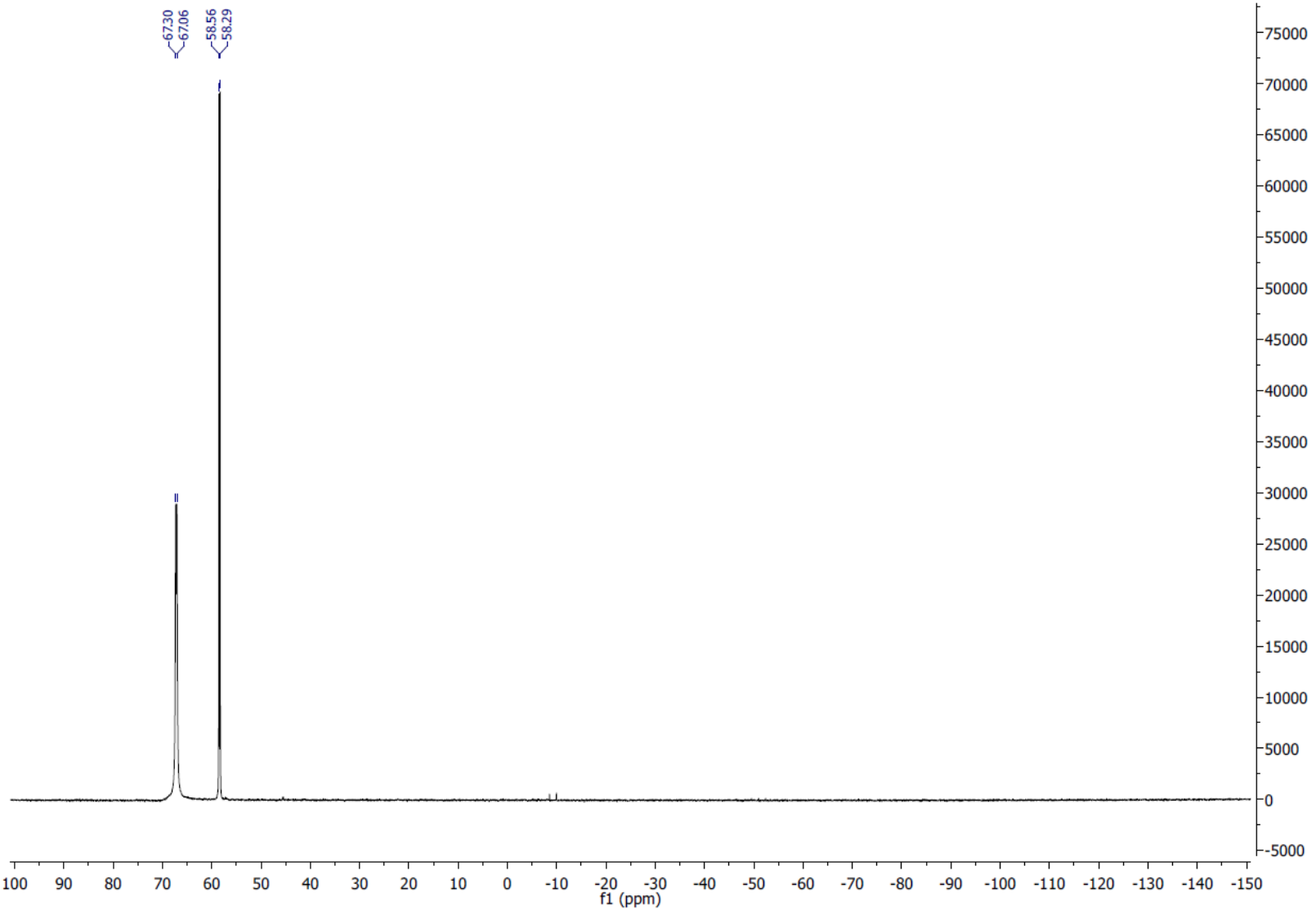

Figure S7: $^{31}P\{^{1}H\}$ NMR (400 MHz, 298 K, C_6D_6) of $^{57}FeBr(C_6H_5)(dmpe)_2$ (**^{57}Fe-2$_{Ph'}$**). Starting $^{57}Fe(Cl)_2(dmpe)_2$ (**^{57}Fe-1**) is still present.

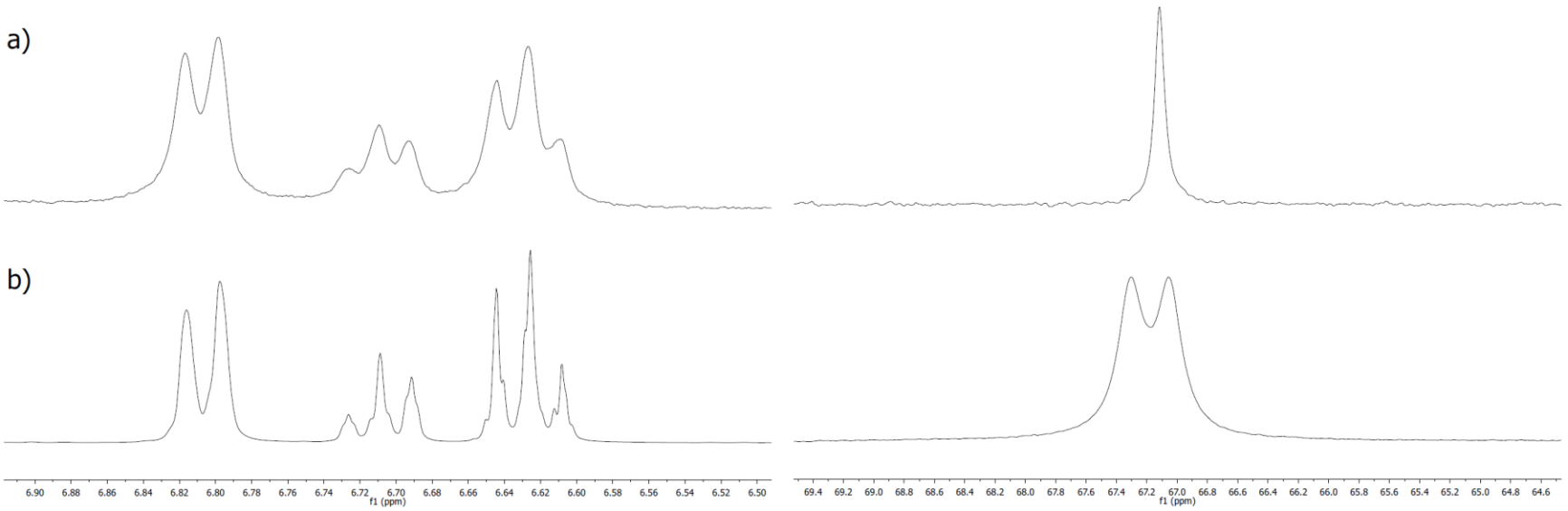

Figure S8: ^{1}H (left) and $^{31}P\{^{1}H\}$ NMR (right) (298 K, C_6D_6) of complexes **2$_{Ph}$**, (a) and **^{57}Fe-2$_{Ph}$**, (b) generated by addition of 1 equiv. of PhMgBr onto **1** and **^{57}Fe-1**

3) Speciation of the iron-containing species upon treatment of $Fe(Cl)_2(dmpe)_2$ by M(hmds) (M = Li, Na, K)

Entry	Complexes	^{1}H NMR and ^{31}P NMR	References
1	**1**	^{1}H NMR: *trans*: 1.95 ppm (m), 1.35 (br) $^{31}P\{^1H\}$ NMR: *trans:* 58.8 ppm (s)	[R2]
2	$\mathbf{2_{Ph}}$	$^{31}P\{^1H\}$ NMR: *trans:* 68.4 ppm (s)	[R3]
3	**3'**	$^{31}P\{^1H\}$ NMR: 60.4 ppm (d, J_{PP} = 10 Hz) and 7.2 ppm (quin, J_{PP} = 10 Hz)	[R2]
4	**3''**	$^{31}P\{^1H\}$ NMR: 60.4 ppm (d, J_{PP} = 10 Hz), 10.2 ppm (dq, J_{PP} = 10, 20 Hz) and -49.8 ppm (d, J_{PP} = 20 Hz)	[R2]
5	$\mathbf{4_{C6D5,D}}$	$^{31}P\{^1H\}$ NMR: *trans*: 74.7 ppm (t, J_{PD} = 7.5 Hz) *cis*: unresolved ABCD pattern	[R3]
6	$\mathbf{4_{C6H5,H}}$	^{1}H NMR: *trans*: -19,7 ppm (quin, J_{PH} = 48.5 Hz) *cis*: -13.4 ppm (m, J_{PH} = 68, 53, 53, 38 Hz) $^{31}P\{^1H\}$ NMR: *trans*: 74.5 ppm (s) *cis*: unresolved ABCD pattern	[R3]
7	$\mathbf{5^-}$	^{1}H NMR: -4.72 ppm (br)	[R4]

Table S1: ^{1}H NMR and $^{31}P\{^1H\}$ NMR (C_6D_6, 298K) diagnostic signals of $FeCl_2(dmpe)_2$ (**1**), $FeCl(C_6H_5)(dmpe)_2$ ($\mathbf{2_{Ph}}$), $Fe^0{}_2(dmpe)_5$ (**3'**), $Fe^0(dmpe)_3$ (**3''**), $Fe(D)(C_6D_5)(dmpe)_2$ ($\mathbf{4_{C6D5,D}}$), $Fe(H)(C_6H_5)(dmpe)_2$ ($\mathbf{4_{C6H5,H}}$) and $Fe(hmds)_3^-$ ($\mathbf{5^-}$) reported in the literature

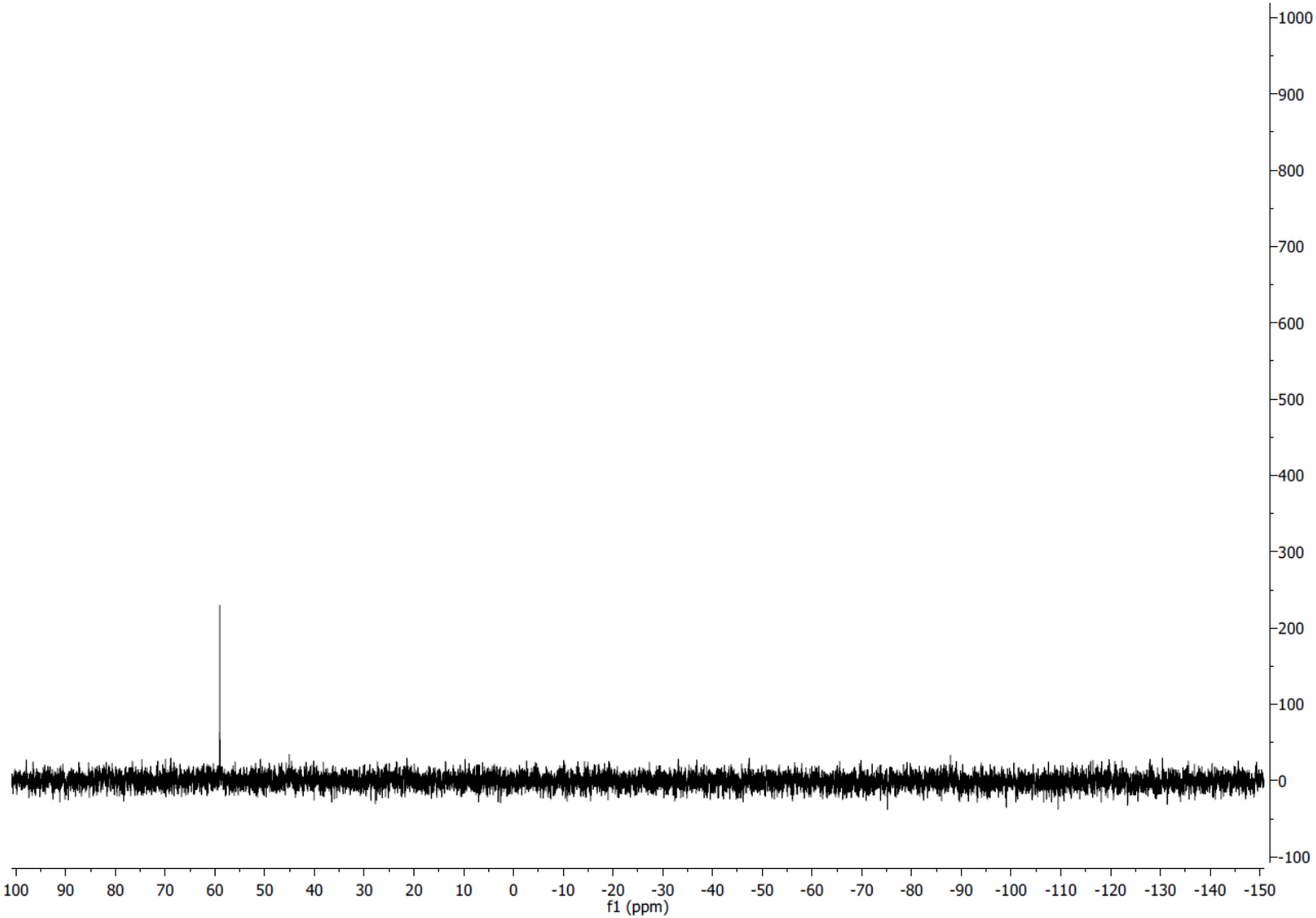

Figure S9: $^{31}P\{^{1}H\}$ NMR (162 MHz, 298 K, C_6D_6) of $Fe(Cl)_2(dmpe)_2$ (**1**) (8.7 µmol) treated by 2 equiv. of Li(hmds) after 72 h at 20 °C.

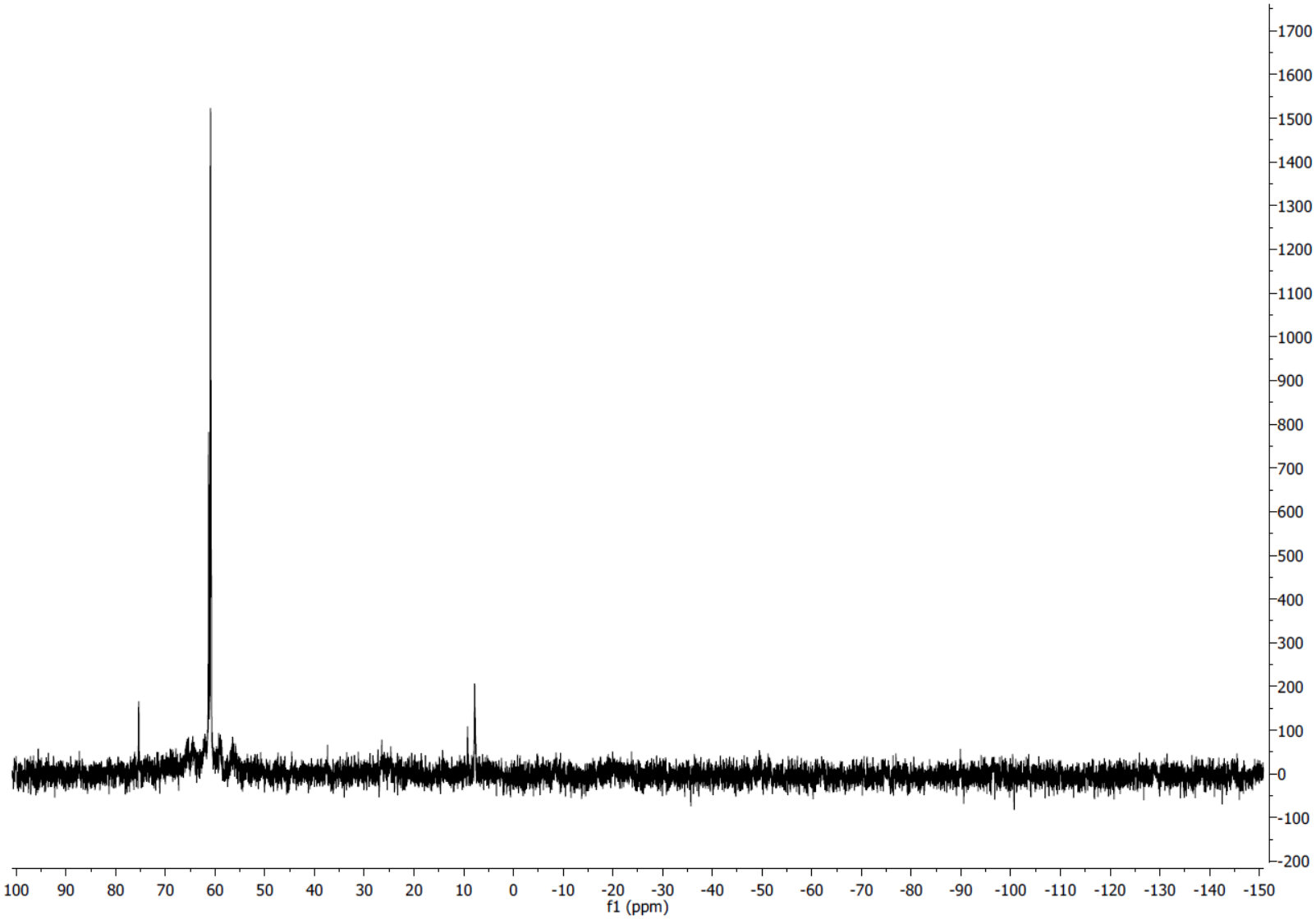

Figure S10: $^{31}P\{^{1}H\}$ NMR (162 MHz, 298 K, C_6D_6) of $Fe(Cl)_2(dmpe)_2$ (**1**) (8.9 µmol) treated by 2 equiv. of Na(hmds) after 72 h at 20 °C.

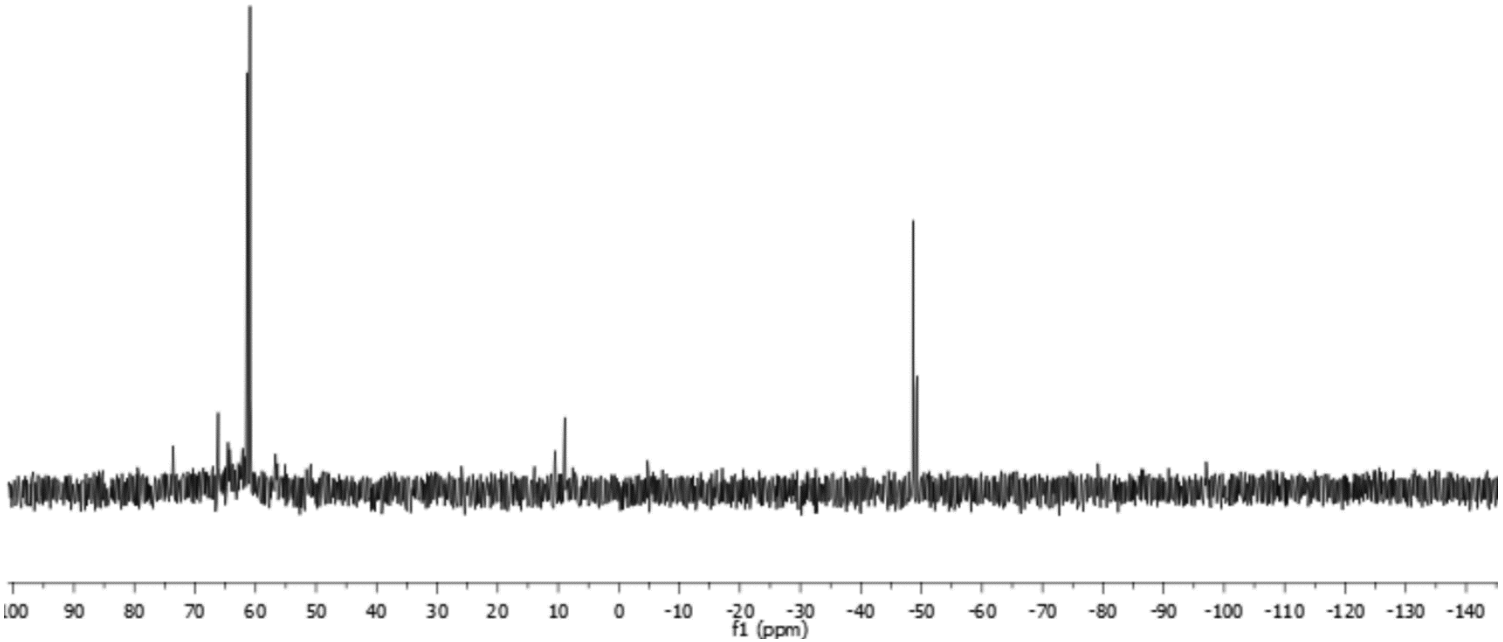

Figure S11: $^{31}P\{^{1}H\}$ NMR (162 MHz, 298 K, C_6D_6) of $Fe(Cl)_2(dmpe)_2$ (**1**) (8.9 µmol) treated by 2 equiv. of K(hmds) after 72 h at 20 °C.

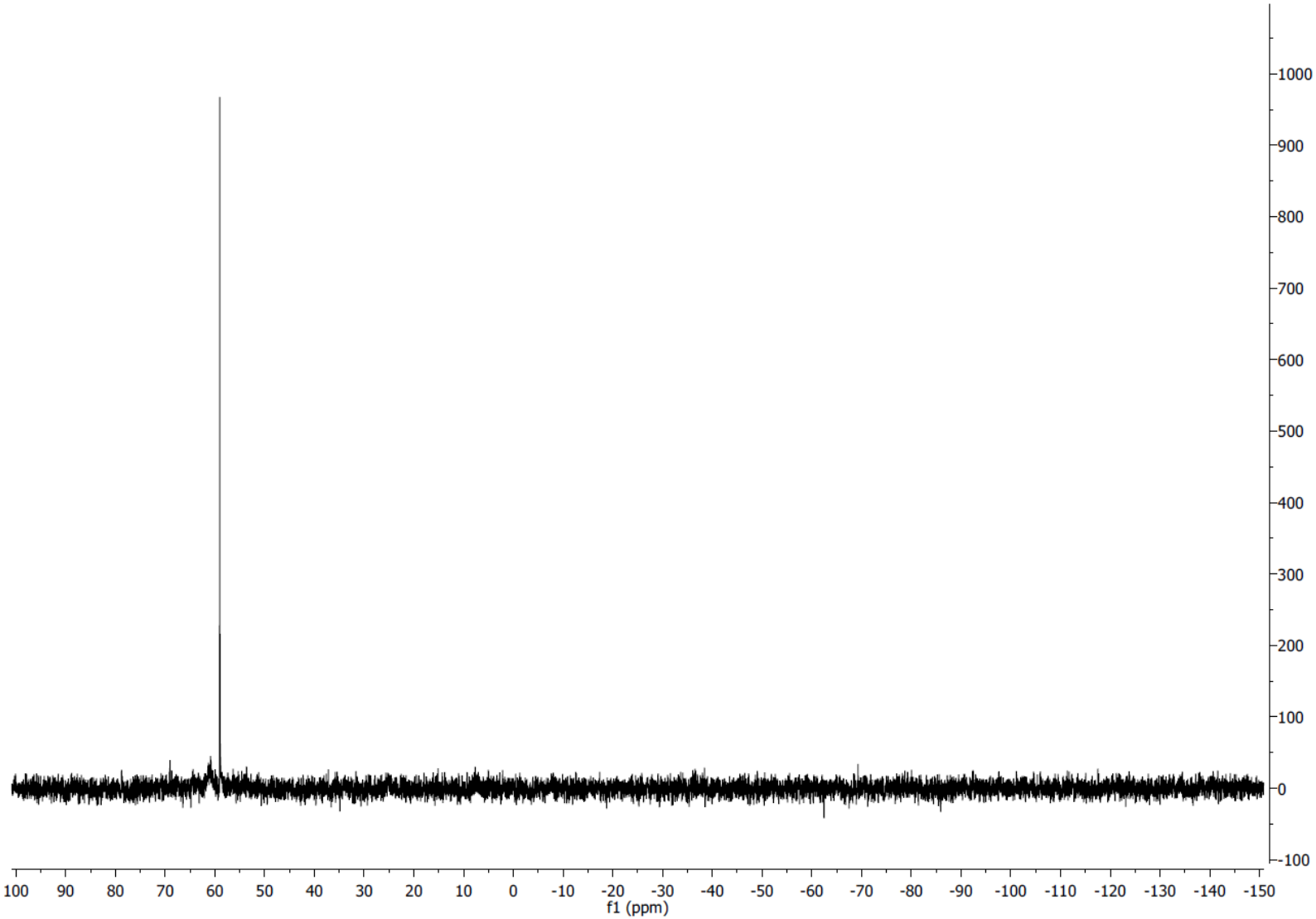

Figure S12: $^{31}P\{^{1}H\}$ NMR (162 MHz, 298 K, C_6D_6/THF 9:1) of $Fe(Cl)_2(dmpe)_2$ (**1**) (8.7 µmol) treated by 2 equiv. of Li(hmds) after 72 h at 20 °C.

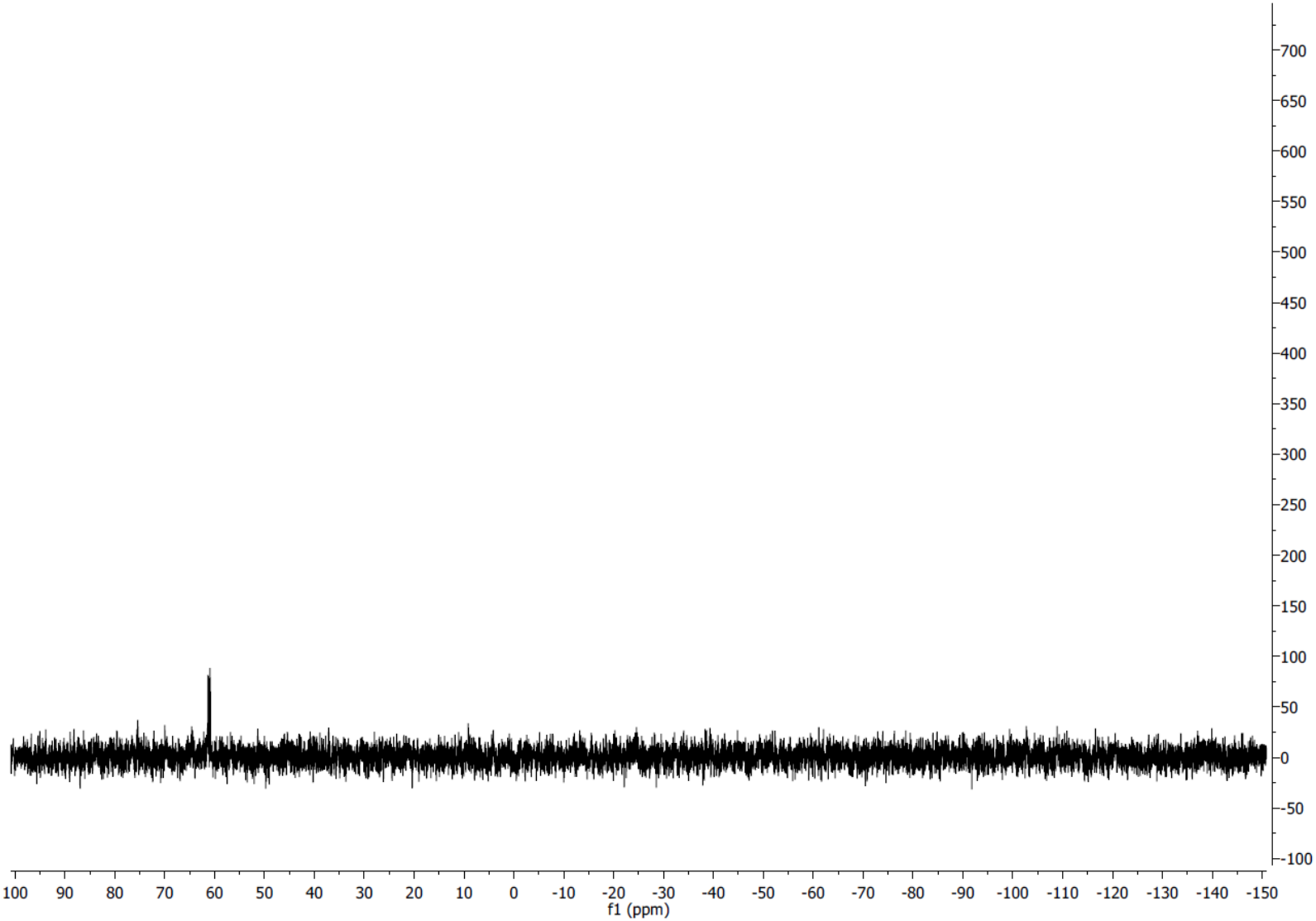

Figure S13: $^{31}P\{^{1}H\}$ NMR (162 MHz, 298 K, C_6D_6/THF 9:1) of $Fe(Cl)_2(dmpe)_2$ (**1**) (8.7 µmol) treated by 2 equiv. of Na(hmds) after 72 h at 20 °C.

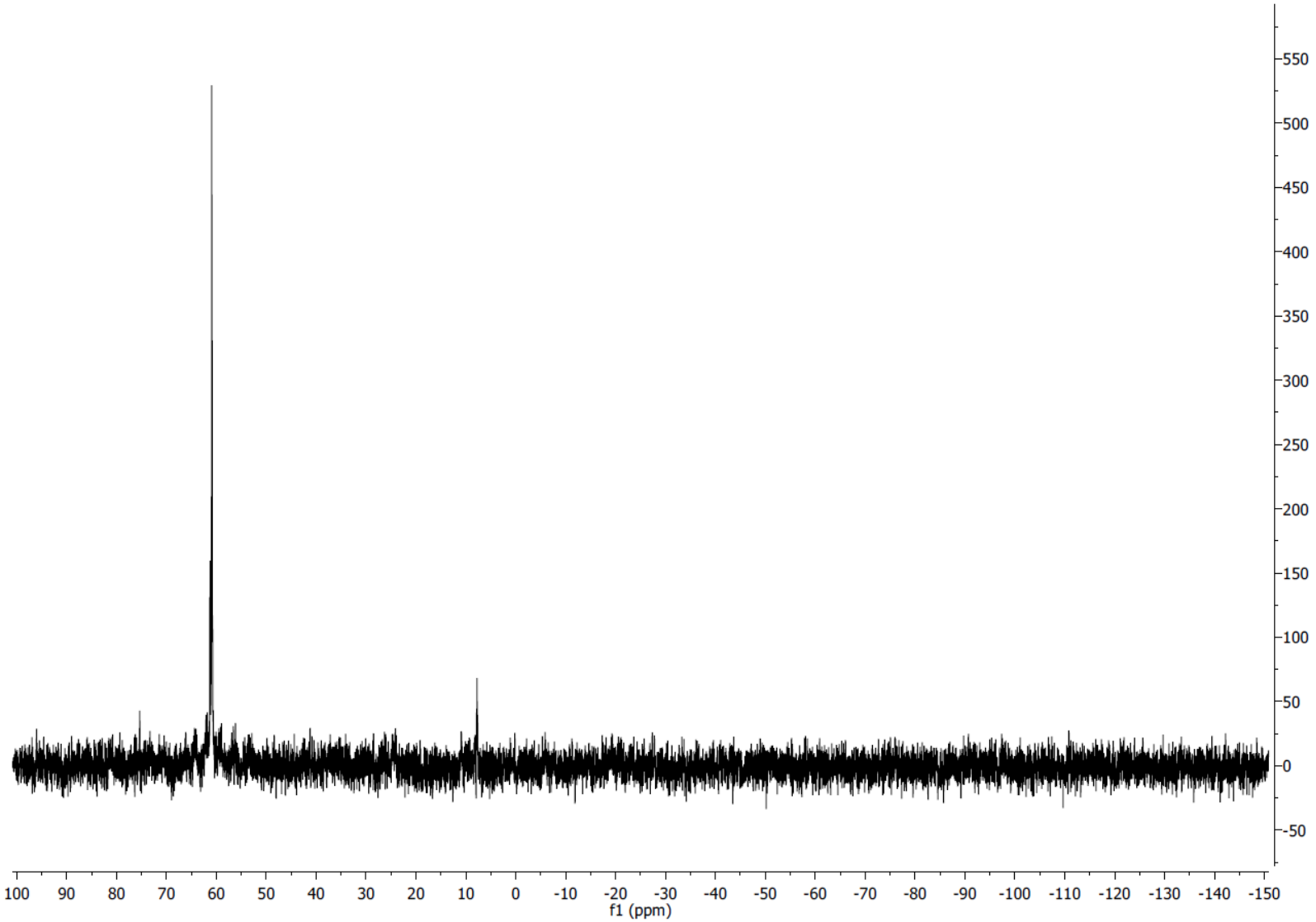

Figure S14: $^{31}P\{^{1}H\}$ NMR (162 MHz, 298 K, C_6D_6/THF 9:1) of $Fe(Cl)_2(dmpe)_2$ (**1**) (8.7 µmol) treated by 2 equiv. of K(hmds) after 72 h at 20 °C.

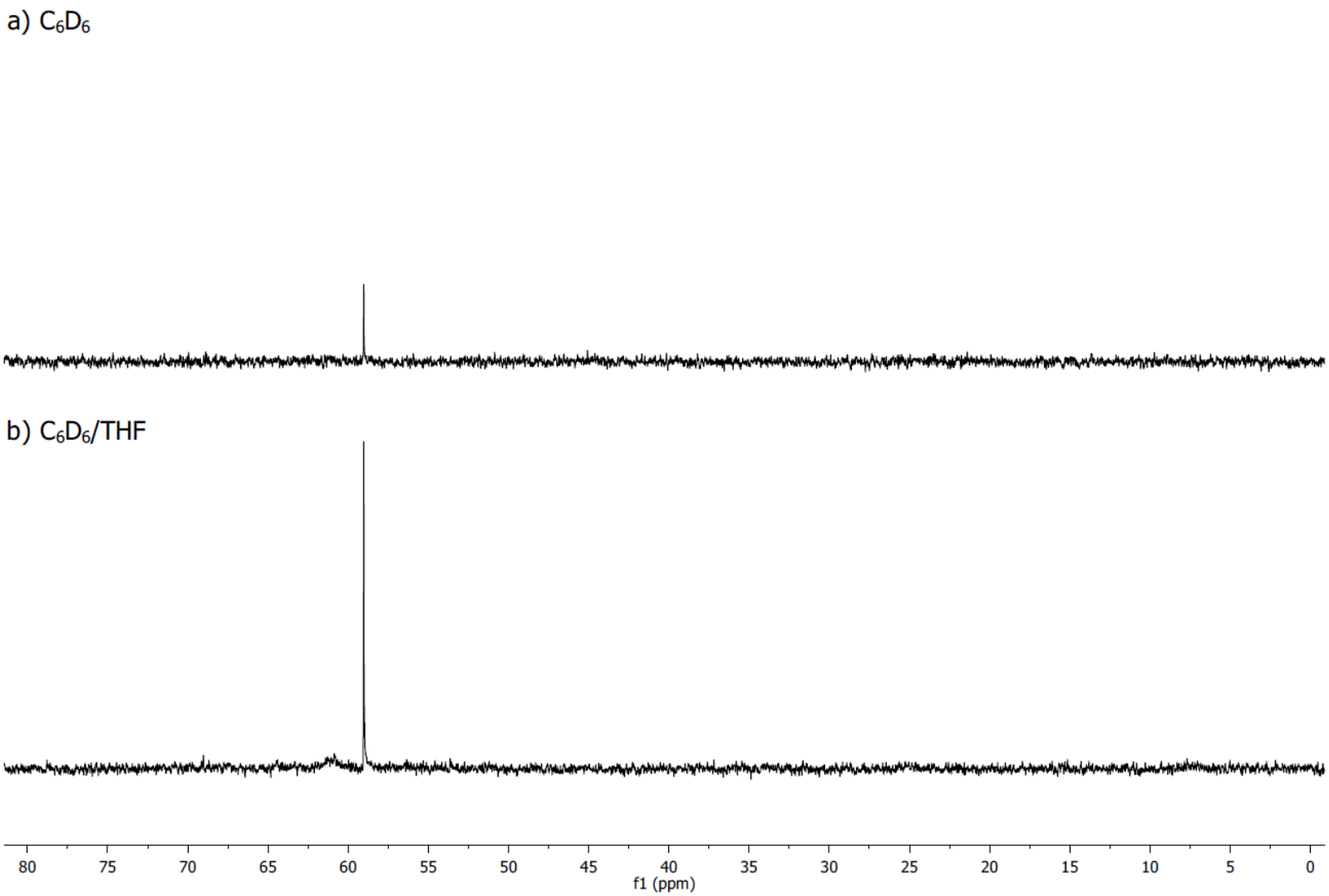

Figure S15: $^{31}P\{^{1}H\}$ NMR (162 MHz, 298 K, C_6D_6) of $Fe(Cl)_2(dmpe)_2$ treated by 2 equiv. of Li(hmds) after 72 h at 20 °C without THF (a) and with THF (b).

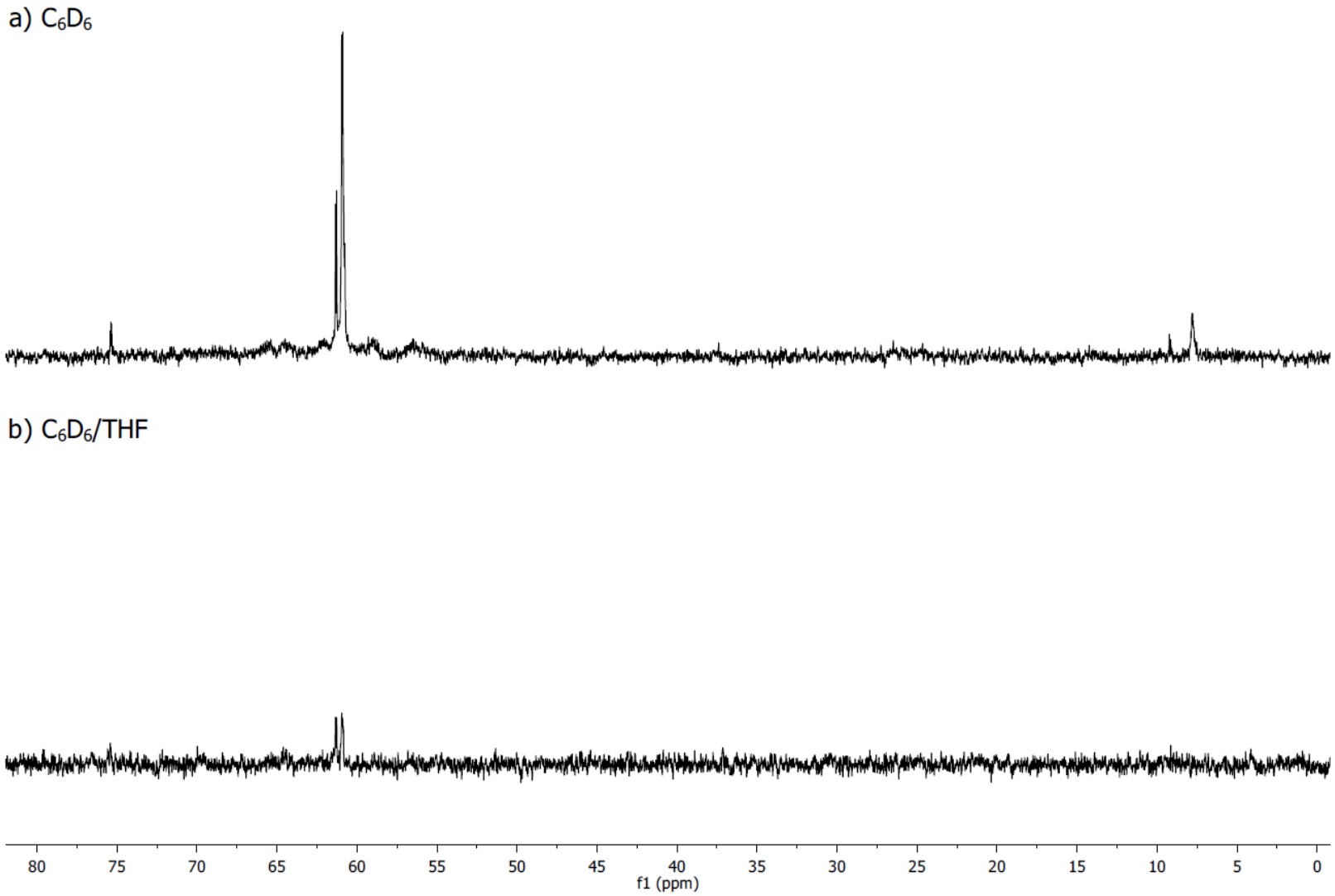

Figure S16: $^{31}P\{^{1}H\}$ NMR (162 MHz, 298 K, C_6D_6) of $Fe(Cl)_2(dmpe)_2$ treated by 2 equiv. of Na(hmds) after 72 h at 20 °C without THF (a) and with THF (b).

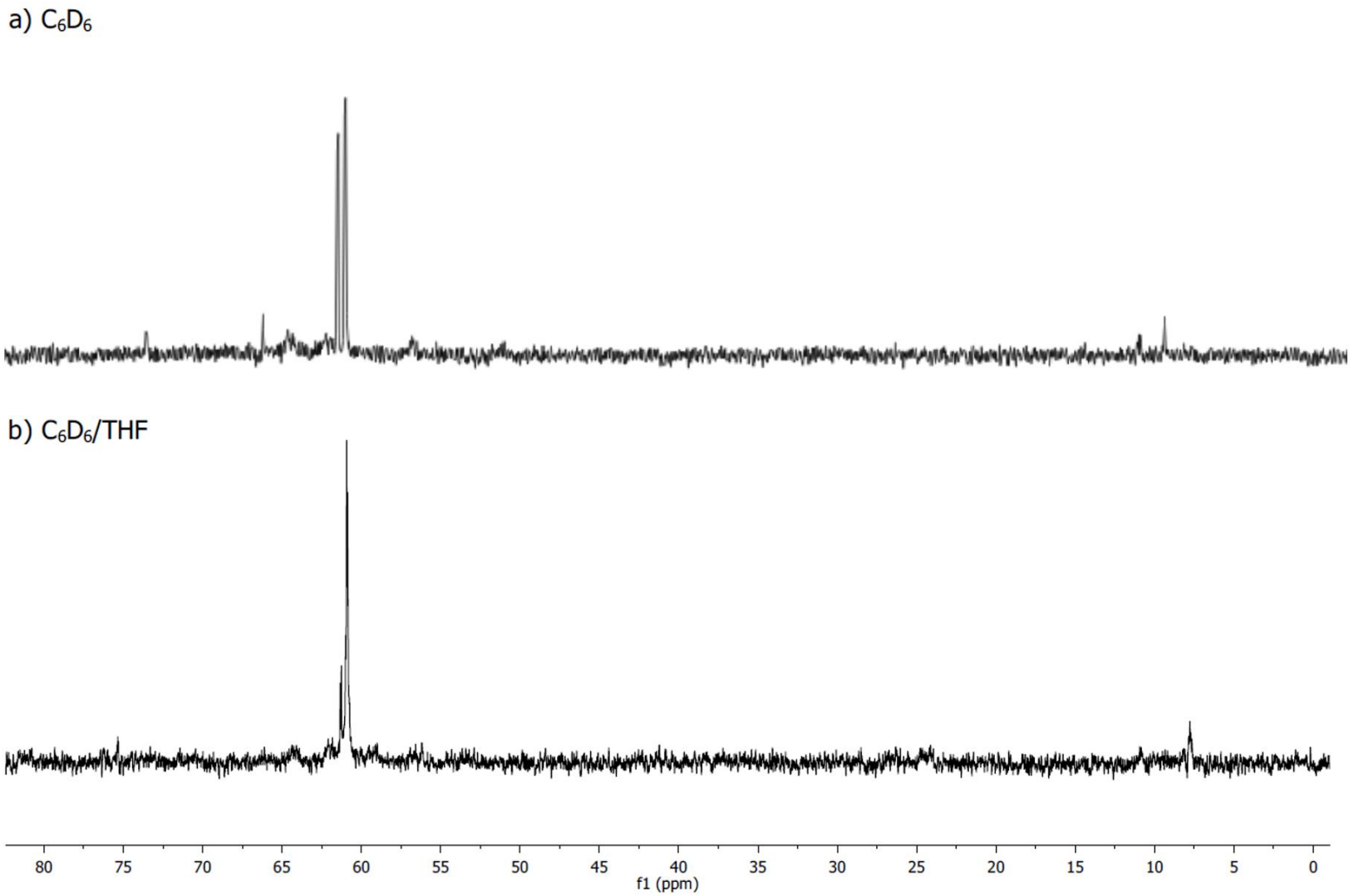

Figure S17: $^{31}P\{^{1}H\}$ NMR (162 MHz, 298 K, C_6D_6) of $Fe(Cl)_2(dmpe)_2$ treated by 2 equiv. of K(hmds) after 72 h at 20 °C without THF (a) and with THF (b).

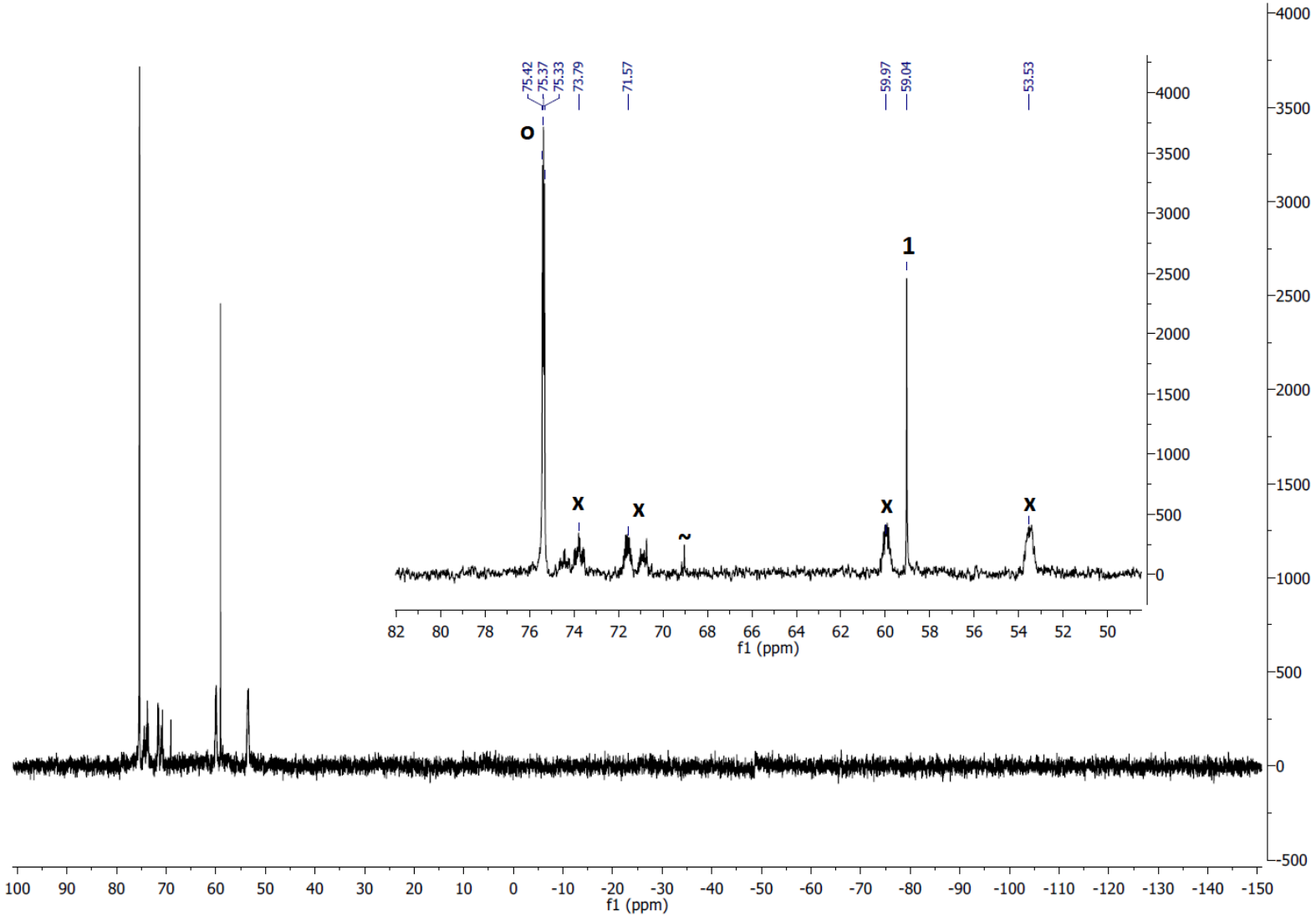

Figure S18: $^{31}P\{^{1}H\}$ NMR (162 MHz, 298 K, C_6D_6) of $Fe(Cl)_2(dmpe)_2$ (**1**) (8.7 µmol) treated by 2 equiv. of Li(hmds) after 72 h upon photolysis (350 nm). It shows the presence of *trans*- (**O**) and *cis*- (**X**) $Fe(D)(C_6D_5)(dmpe)_2$ ($\mathbf{4_{C6D5,D}}$), starting $Fe(Cl)_2(dmpe)_2$ (**1**) and unknown species (~).

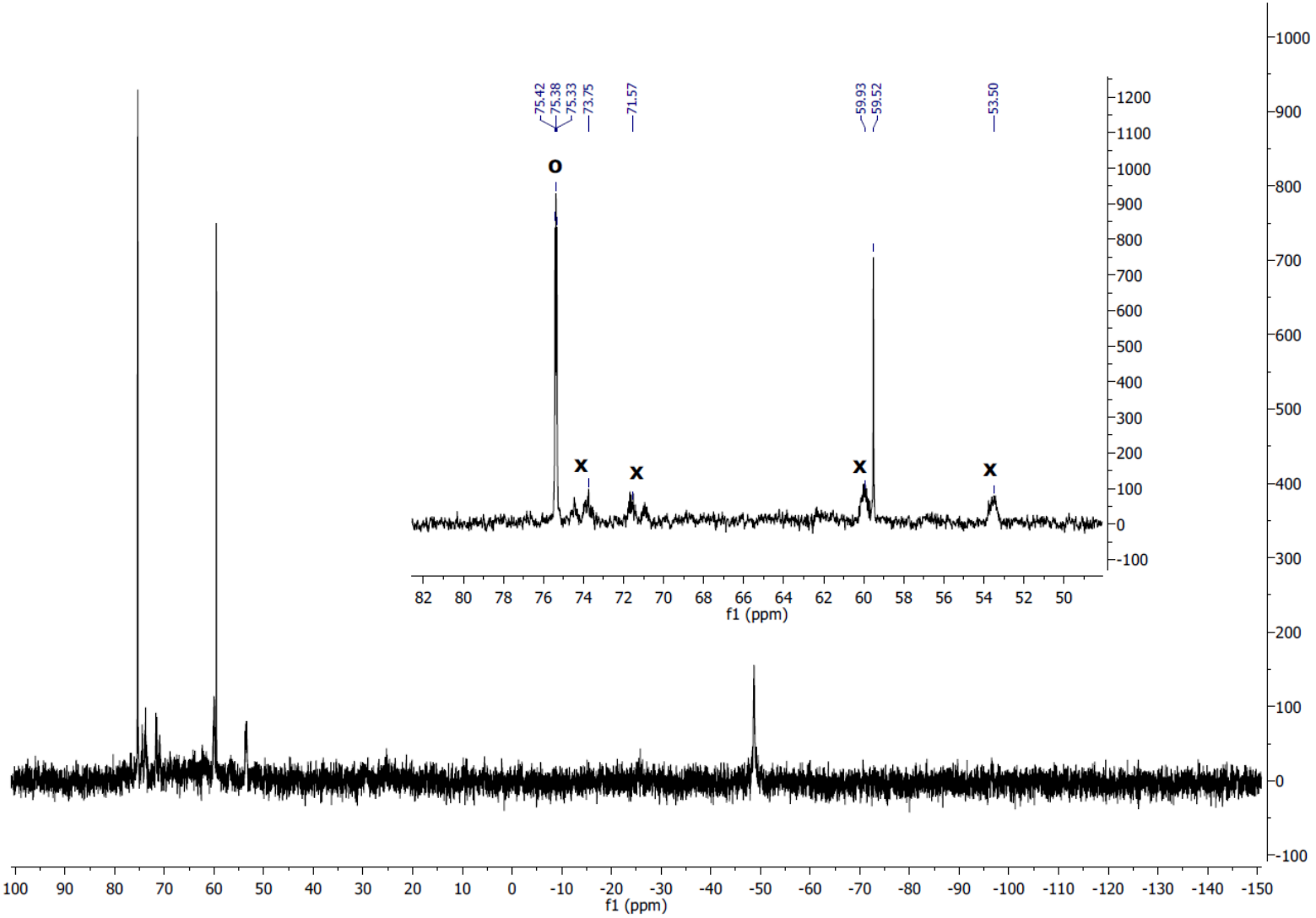

Figure S19: $^{31}P\{^{1}H\}$ NMR (162 MHz, 298 K, C_6D_6) of $Fe(Cl)_2(dmpe)_2$ (**1**) (8.9 µmol) treated by 2 equiv. of Na(hmds) after 72 h upon photolysis (350 nm). It shows the presence of *trans*- (**O**) and *cis*- (**X**) $Fe(D)(C_6D_5)(dmpe)_2$ ($\mathbf{4_{C6D5,D}}$).

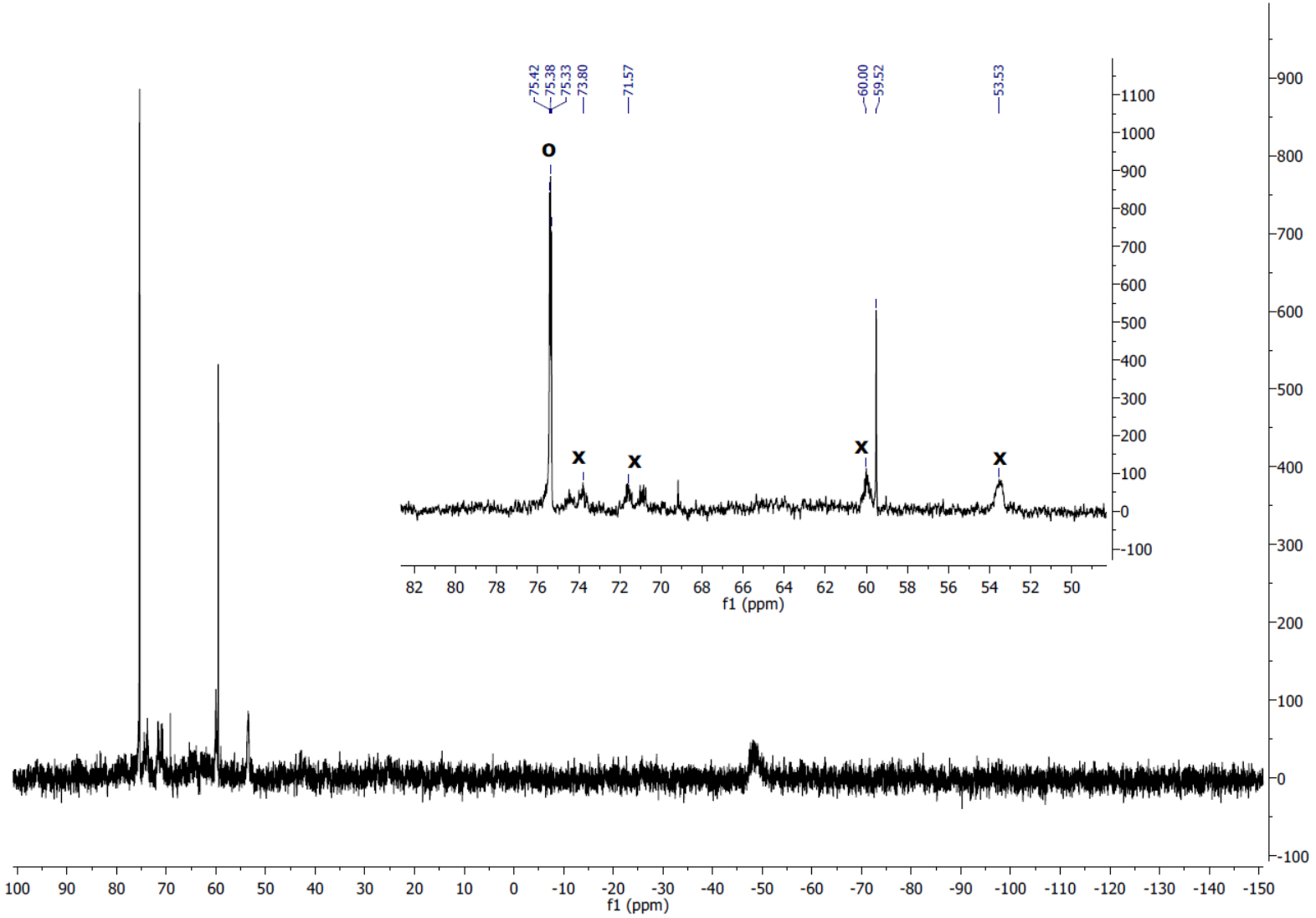

Figure S20: $^{31}P\{^{1}H\}$ NMR (162 MHz, 298 K, C_6D_6) of $Fe(Cl)_2(dmpe)_2$ (**1**) (8.9 µmol) treated by 2 equiv. of K(hmds) after 72 h upon photolysis (350 nm). It shows the presence of *trans*- (**O**) and *cis*- (**X**) $Fe(D)(C_6D_5)(dmpe)_2$ ($\mathbf{4_{C6D5,D}}$).

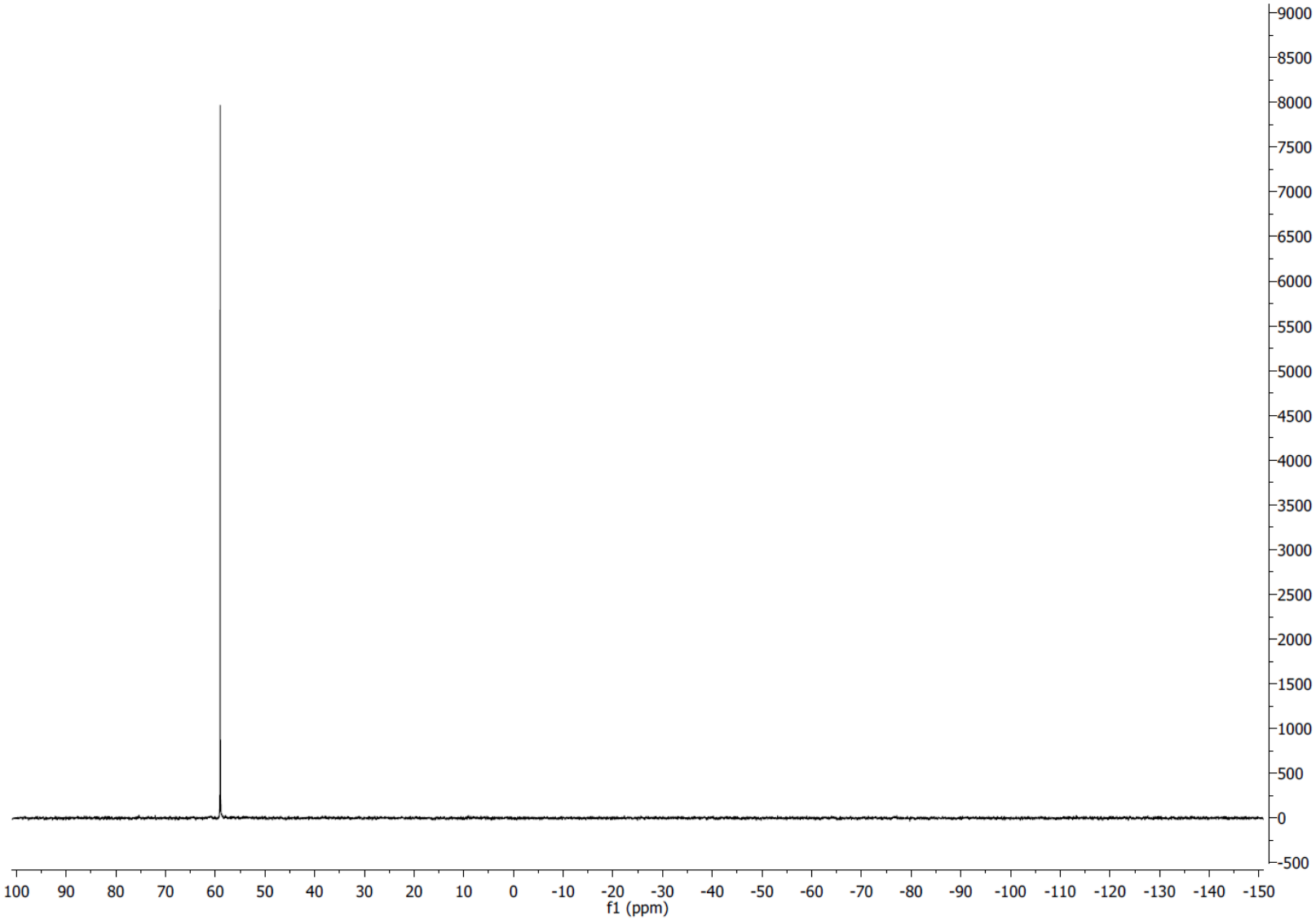

Figure S21: $^{31}P\{^{1}H\}$ NMR (162 MHz, 298 K, C_6D_6/THF 9:1) of $Fe(Cl)_2(dmpe)_2$ (**1**) (9.1 µmol) treated by 10 equiv. of Li(hmds) after 22 h at 20 °C.

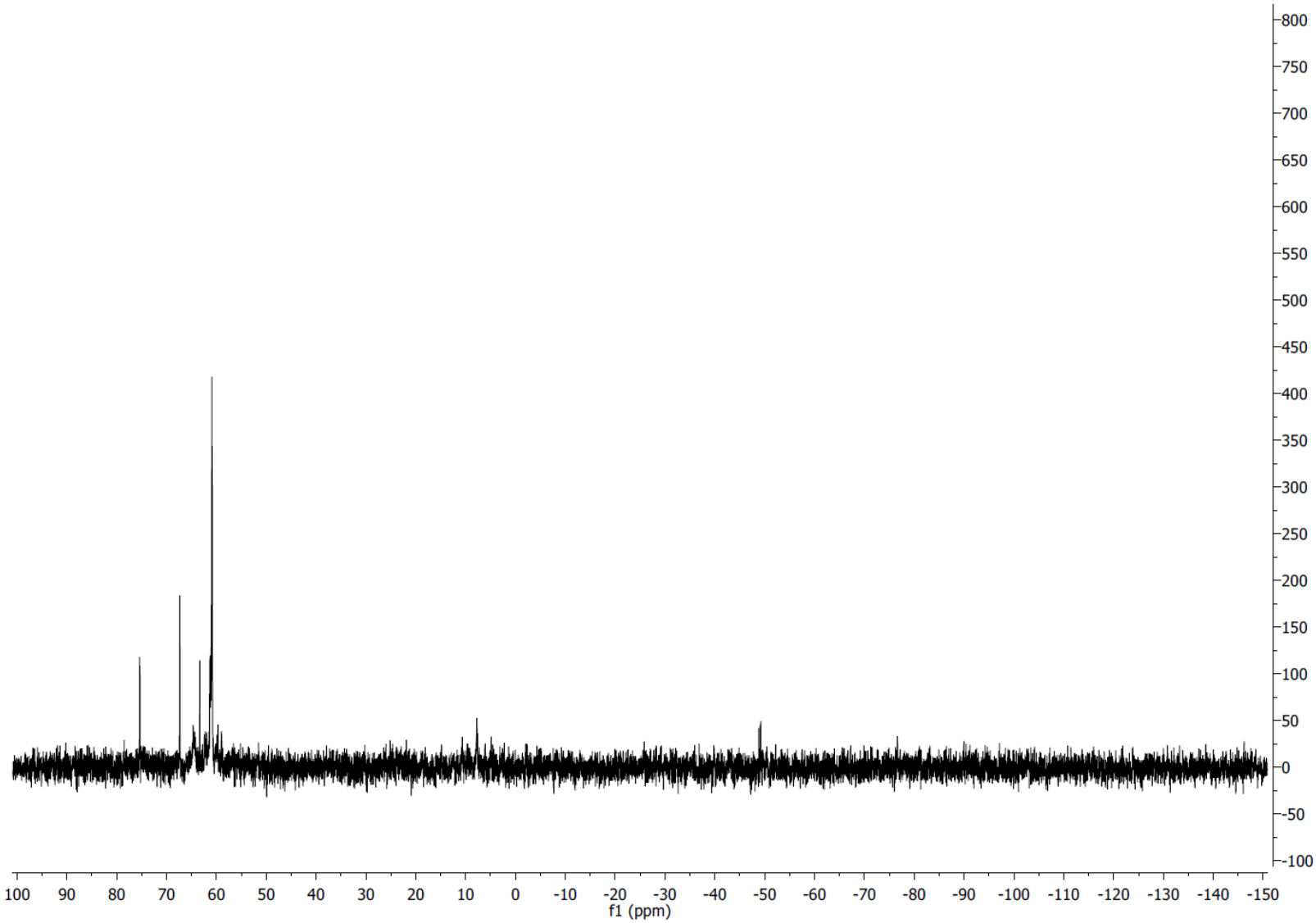

Figure S22: $^{31}P\{^{1}H\}$ NMR (162 MHz, 298 K, C_6D_6/THF 9:1) of $Fe(Cl)_2(dmpe)_2$ (**1**) (8.4 µmol) treated by 10 equiv. of Na(hmds) after 22 h at 20 °C.

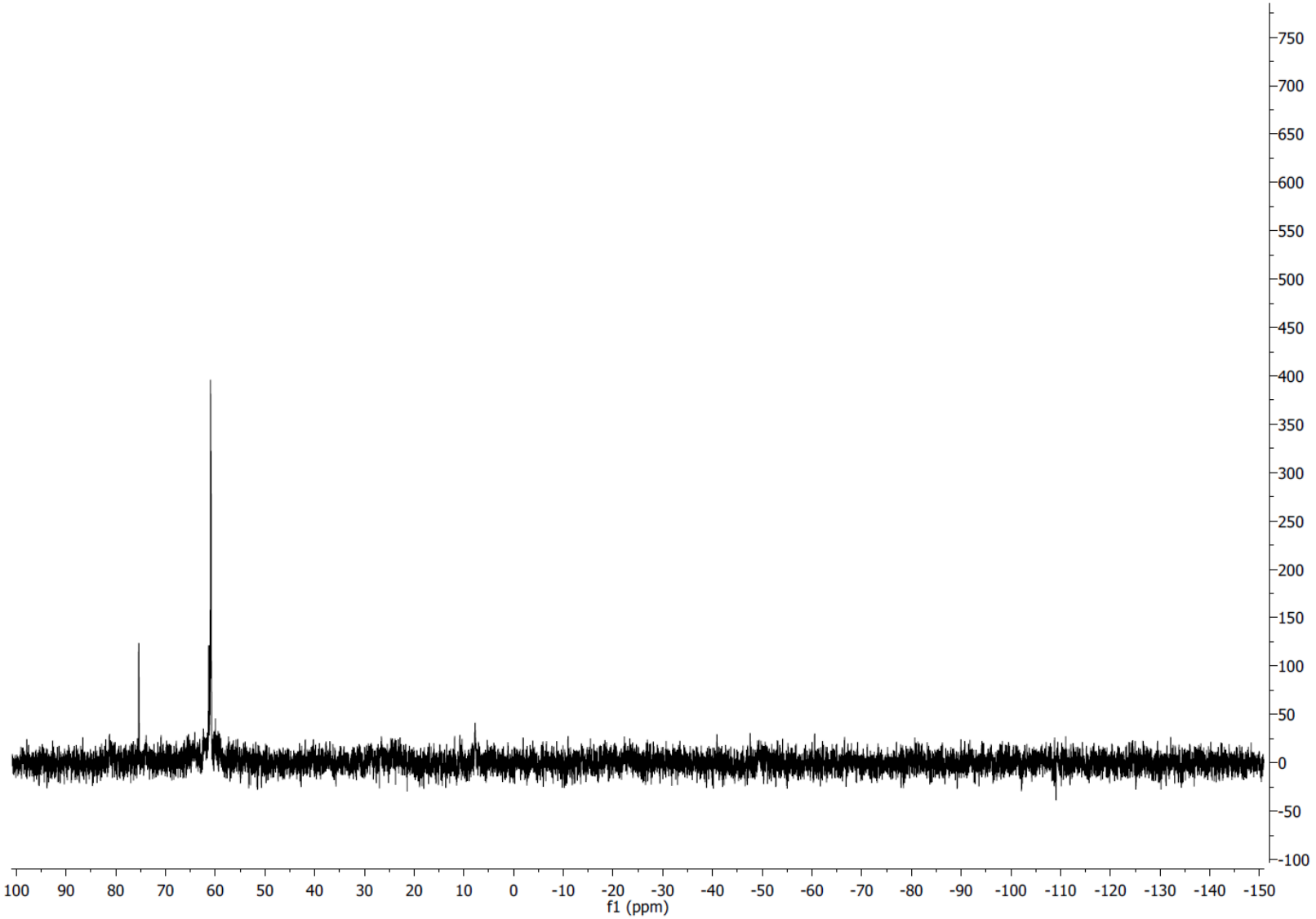

Figure S23: $^{31}P\{^{1}H\}$ NMR (162 MHz, 298 K, C_6D_6/THF 9:1) of $Fe(Cl)_2(dmpe)_2$ (**1**) (8.9 µmol) treated by 10 equiv. of K(hmds) after 22 h at 20 °C.

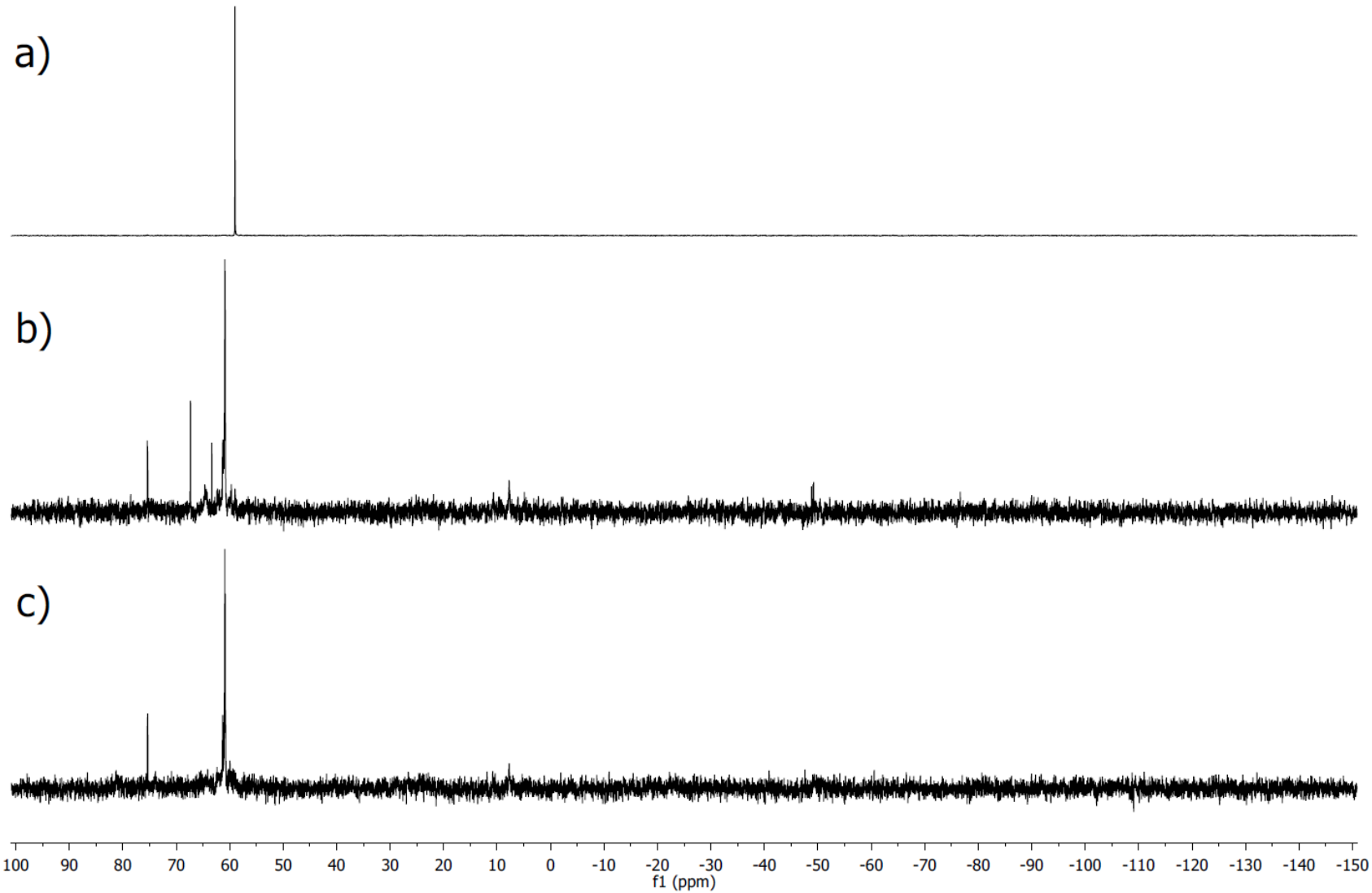

Figure S24: $^{31}P\{^{1}H\}$ NMR (162 MHz, 298 K, C_6D_6/THF 9:1) of $Fe(Cl)_2(dmpe)_2$ (**1**) treated by 10 equiv. of M(hmds) after 22 h at 20 °C. M = Li (a), Na (b) and K (c).

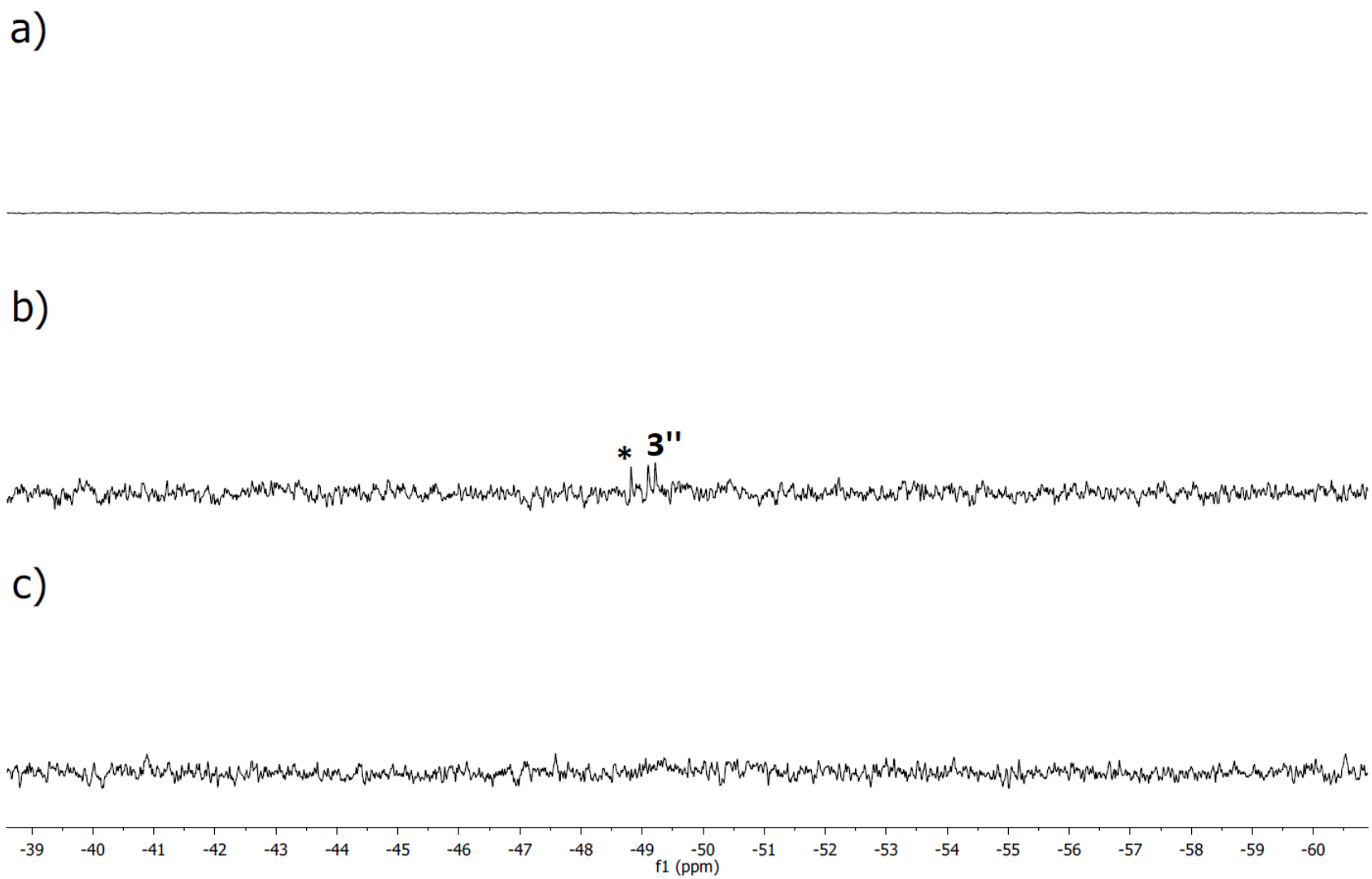

Figure S25: -40 ppm to -60 ppm area $^{31}P\{^{1}H\}$ NMR (162 MHz, 298 K, C_6D_6/THF 9:1) of $Fe(Cl)_2(dmpe)_2$ (**1**) treated by 10 equiv. of M(hmds) after 22 h at 20 °C. M = Li (a), Na (b) and K (c); * = free dmpe and $Fe^0(dmpe)_3$ (**3''**).

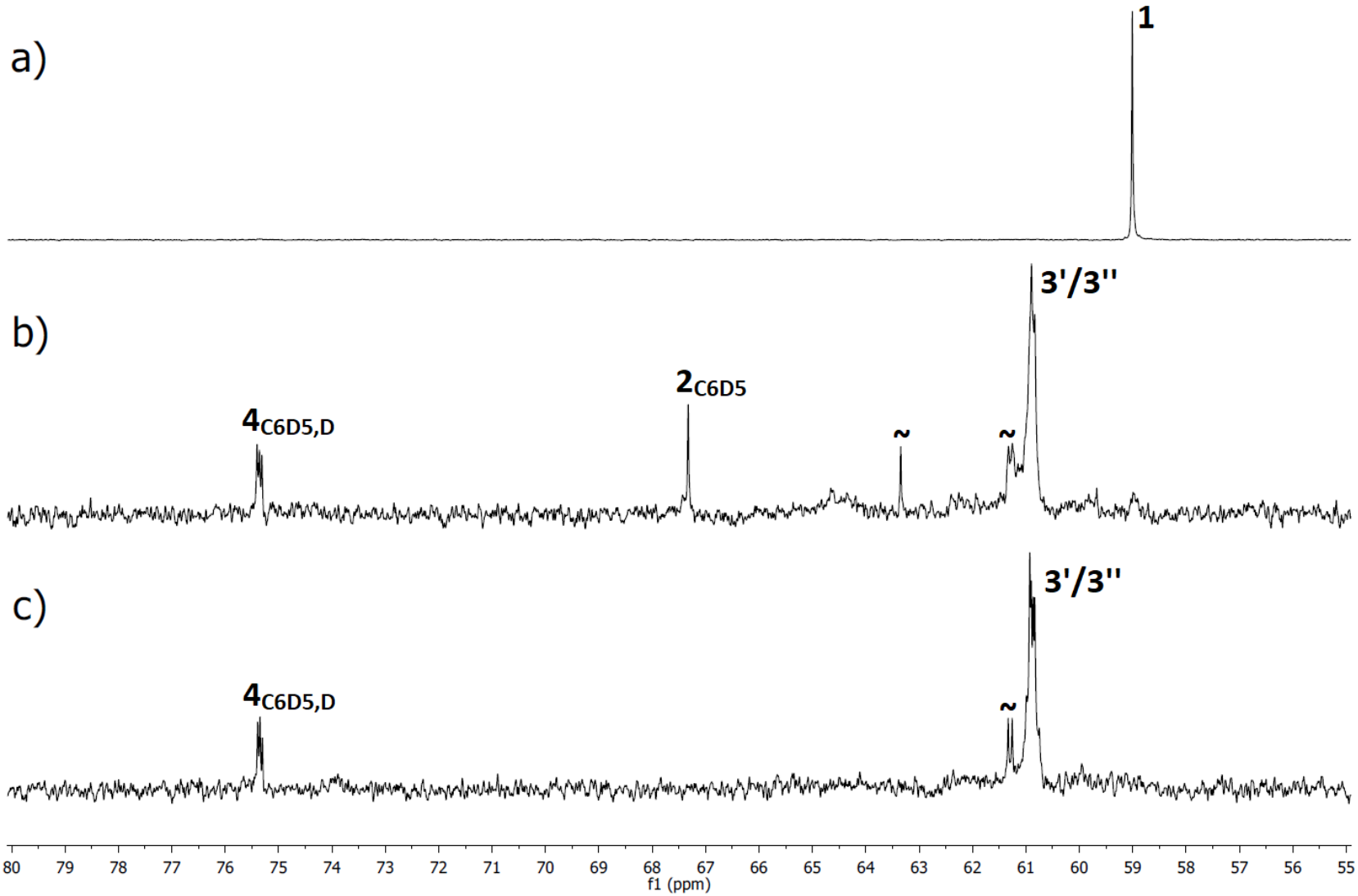

Figure S26: 80 ppm to 55 ppm area $^{31}P\{^{1}H\}$ NMR (162 MHz, 298 K, C_6D_6/THF 9:1) of $Fe(Cl)_2(dmpe)_2$ (**1**) treated by 10 equiv. of M(hmds) after 22 h at 20 °C. M= Li (a), Na (b) and K (c); $Fe^0{}_2(dmpe)_5$ (**3'**); $Fe^0(dmpe)_3$ (**3''**); *trans*- $Fe(D)(C_6D_5)(dmpe)_2$ (**$4_{C6D5,D}$**); $FeCl(C_6D_5)(dmpe)_2$ (**2_{C6D5}**) and (~) = unknown species **3***.

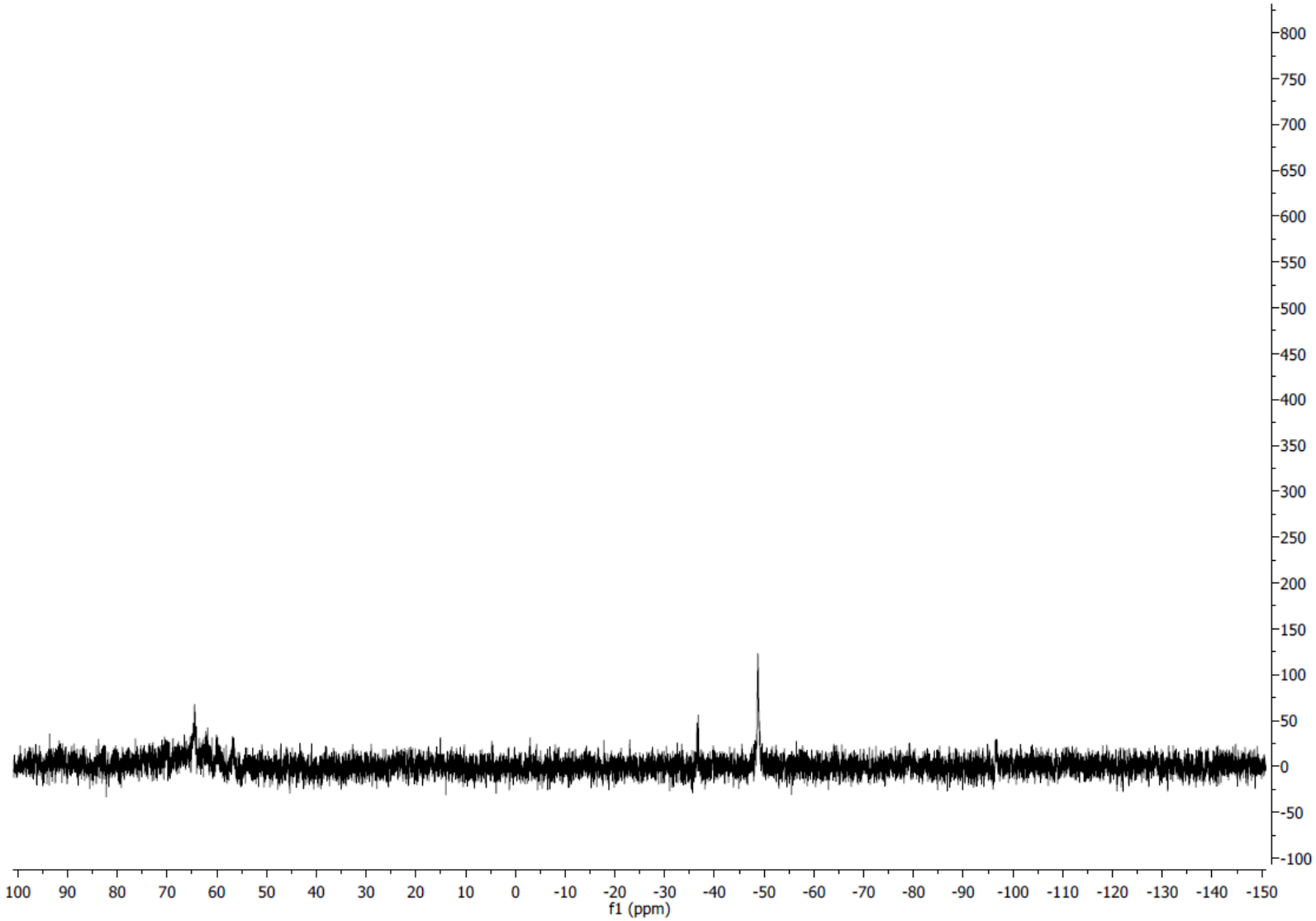

Figure S27: $^{31}P\{^{1}H\}$ NMR (162 MHz, 298 K, C_6D_6/THF 9:1) of $Fe(Cl)_2(dmpe)_2$ (**1**) (8.7 µmol) treated by 10 equiv. of Li(hmds) after 22 h at 80 °C.

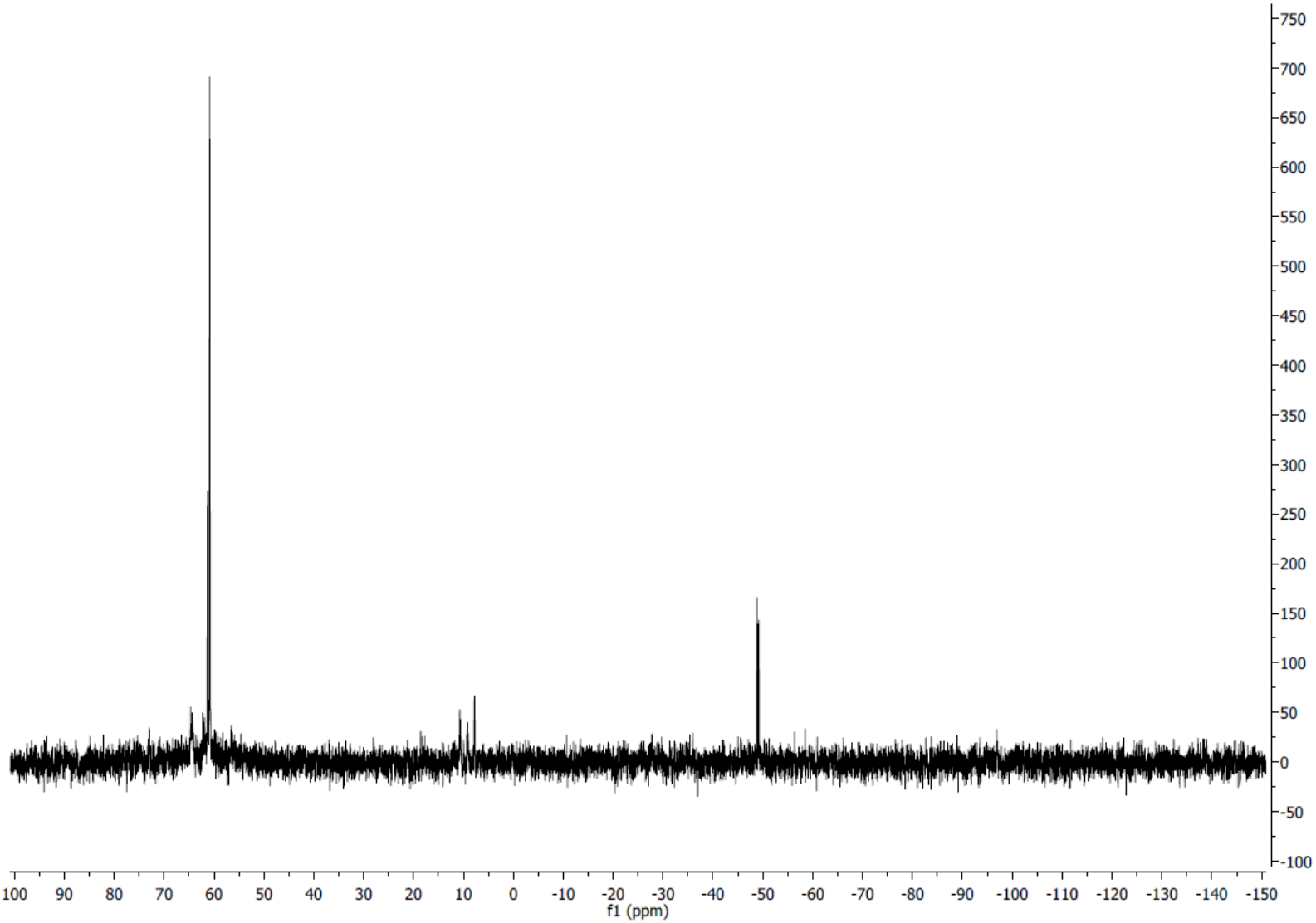

Figure S28: $^{31}P\{^{1}H\}$ NMR (162 MHz, 298 K, C_6D_6/THF 9:1) of $Fe(Cl)_2(dmpe)_2$ (**1**) (8.9 µmol) treated by 10 equiv. of Na(hmds) after 22 h at 80 °C.

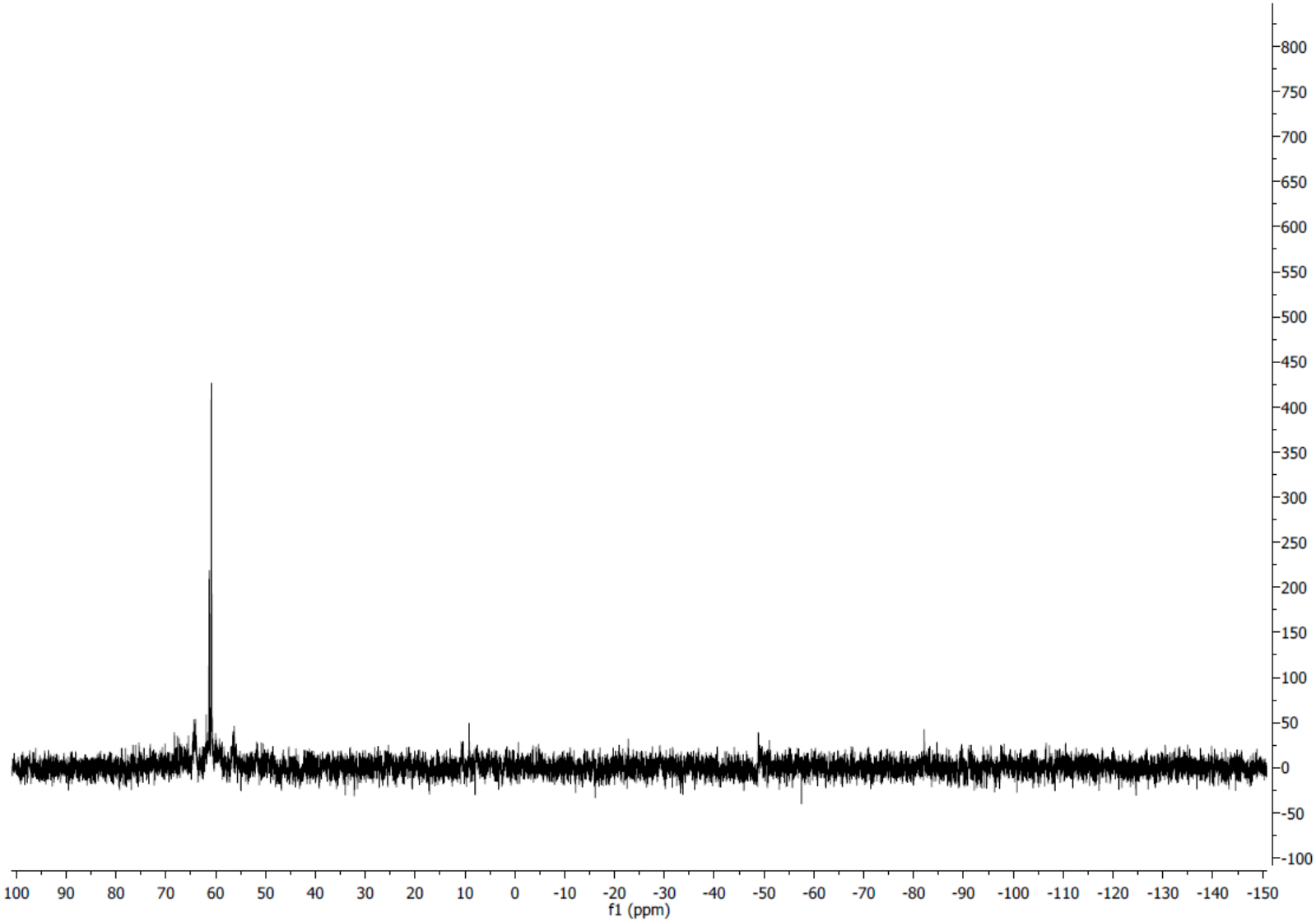

Figure S29: $^{31}P\{^{1}H\}$ NMR (162 MHz, 298 K, C_6D_6/THF 9:1) of $Fe(Cl)_2(dmpe)_2$ (**1**) (8.9 µmol) treated by 10 equiv. of K(hmds) after 22 h at 80 °C.

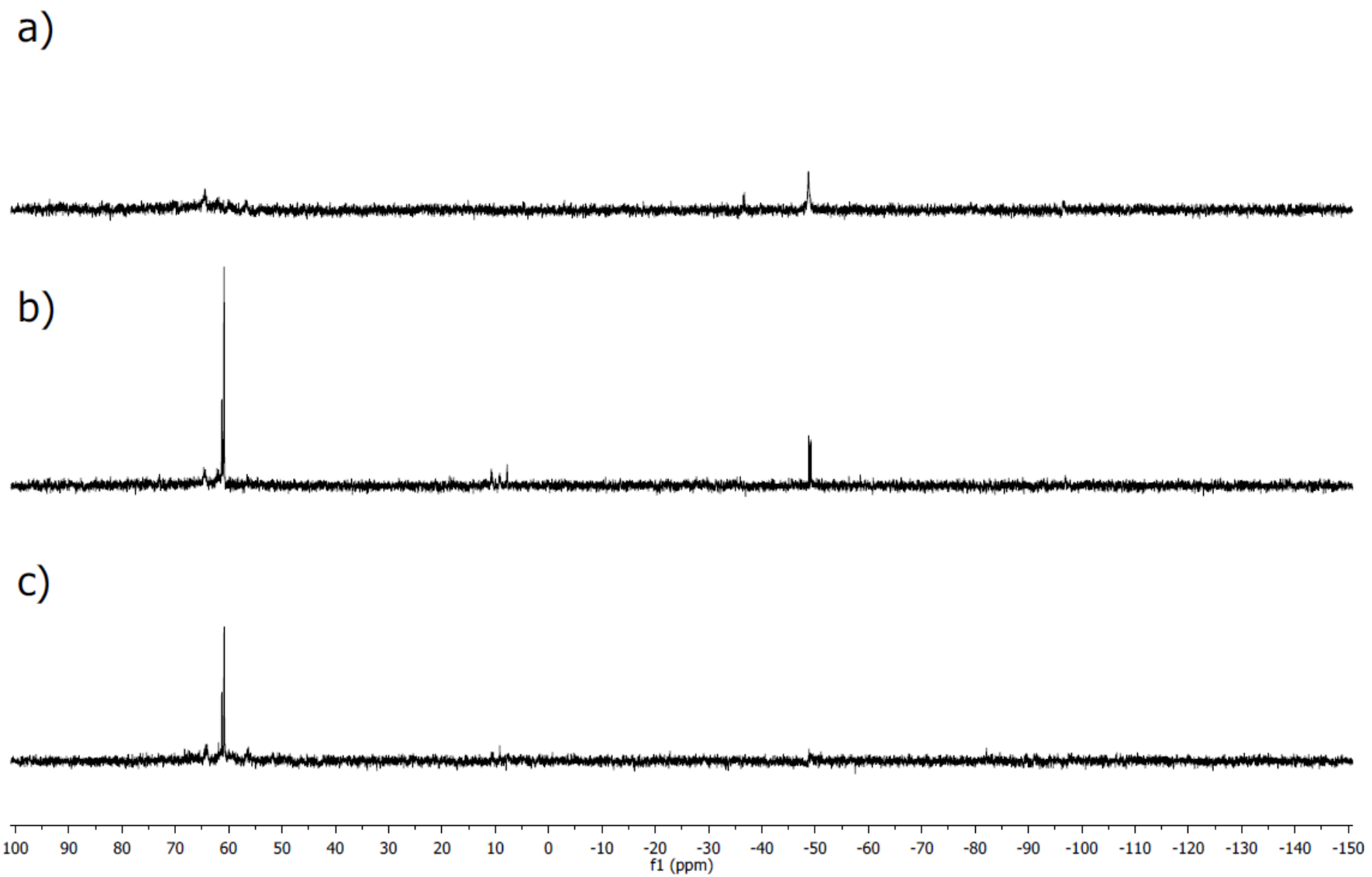

Figure S30: $^{31}P\{^{1}H\}$ NMR (162 MHz, 298 K, C_6D_6/THF 9:1) of $Fe(Cl)_2(dmpe)_2$ (**1**) treated by 10 equiv. of M(hmds) after 22 h at 80 °C. M = Li (a), Na (b) and K (c).

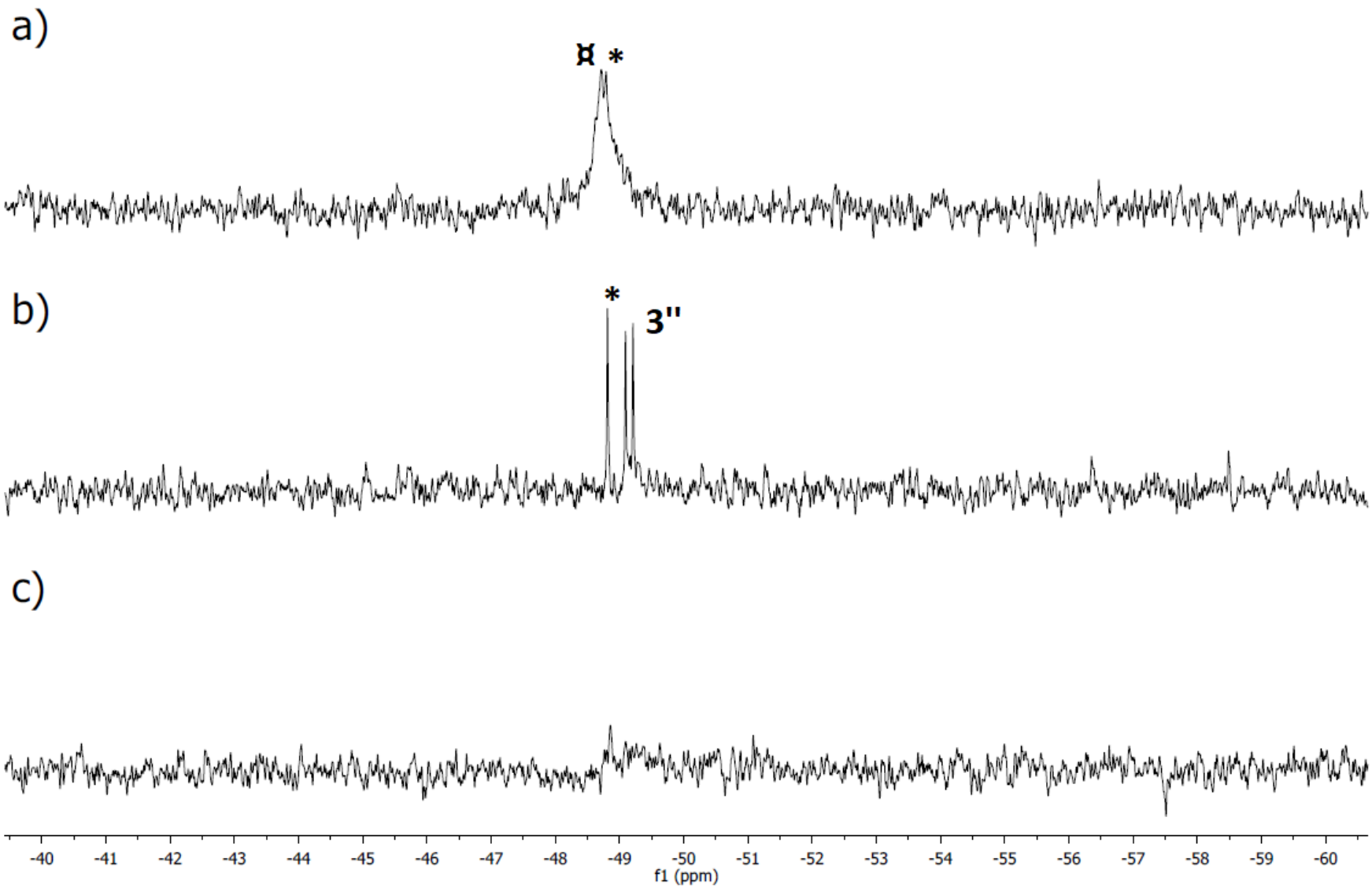

Figure S31: -40 ppm to -60 ppm area $^{31}P\{^{1}H\}$ NMR (162 MHz, 298 K, C_6D_6/THF 9:1) of $Fe(Cl)_2(dmpe)_2$ (**1**) treated by 10 equiv. of M(hmds) after 22 h at 80 °C. M = Li (a), Na (b) and K (c); * = free dmpe, ¤ = [dmpe•Li^{I}] adduct and $Fe^{0}(dmpe)_3$ (**3''**).

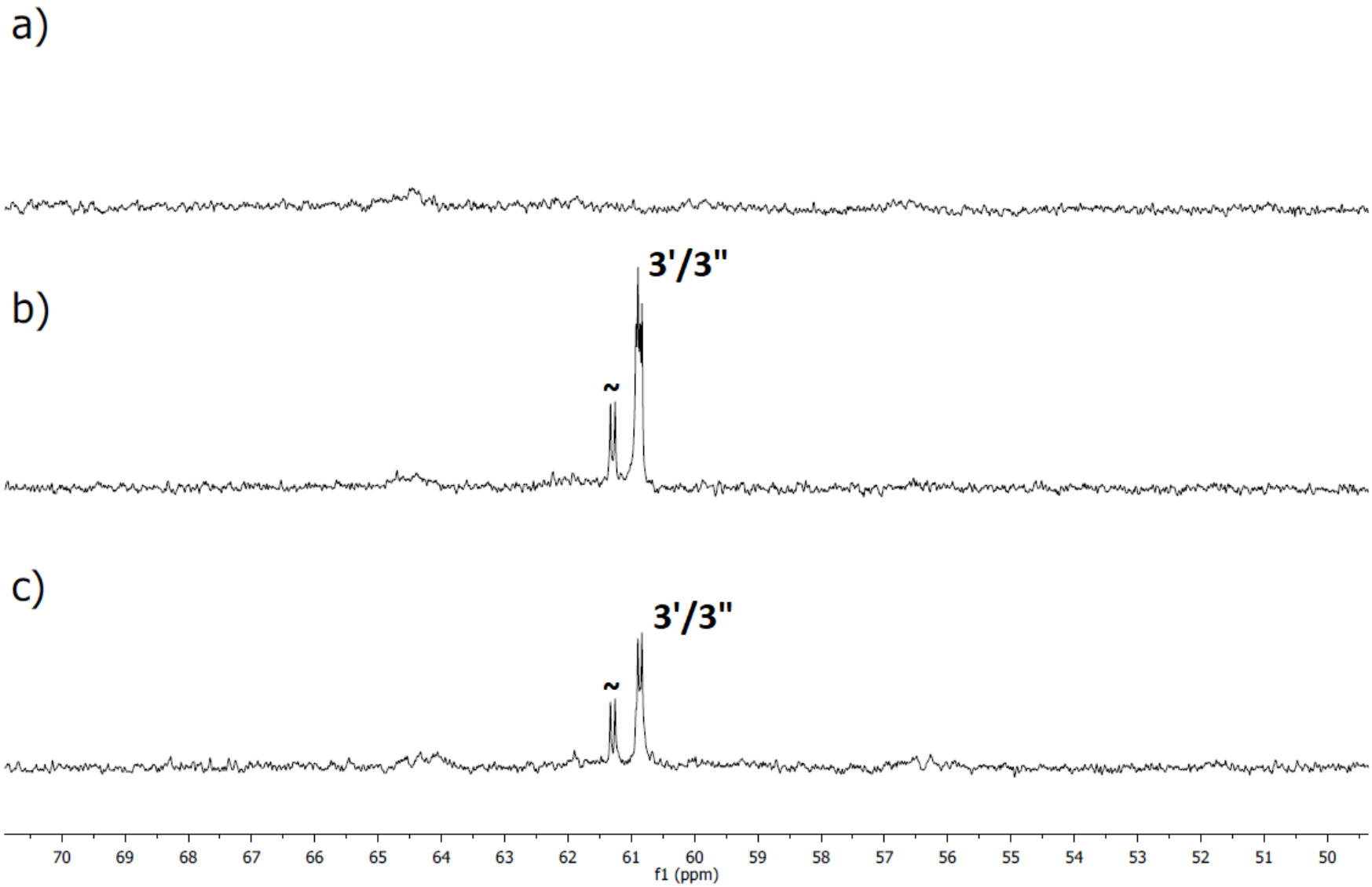

Figure S32: 70 ppm to 50 ppm area $^{31}P\{^{1}H\}$ NMR (162 MHz, 298 K, C_6D_6/THF 9:1) of $Fe(Cl)_2(dmpe)_2$ (**1**) treated by 10 equiv. of M(hmds) after 22 h at 80 °C. M= Li (a), Na (b) and K (c); $Fe^0{}_2(dmpe)_5$ (**3'**); $Fe^0(dmpe)_3$ (**3''**) and (**~)** = unknown species **3***.

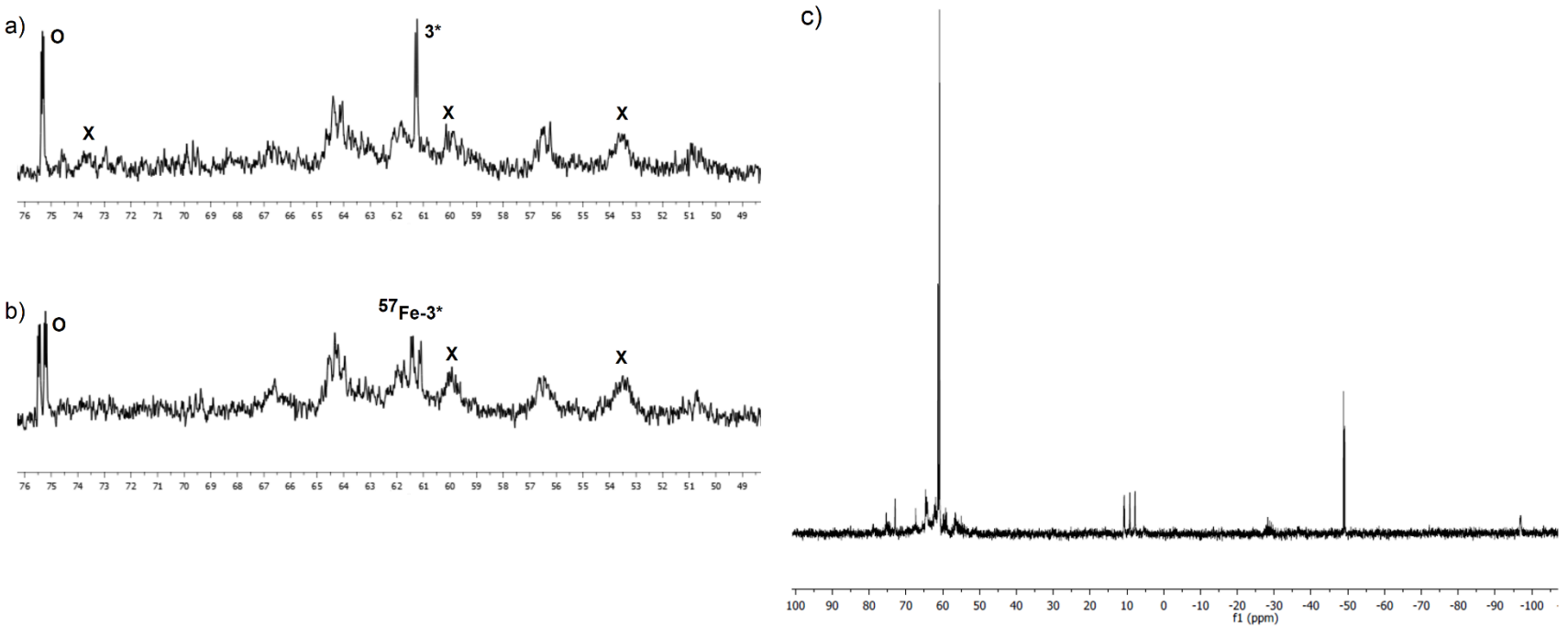

Figure S33: $^{31}P\{^{1}H\}$ NMR (162 MHz, 298 K, C_6D_6/THF 9:1) of $Fe(Cl)_2(dmpe)_2$ (**1**) (9.4 µmol) treated by 10 equiv. Li(hmds) after 22 h at 80 °C followed by 10 additionnal hours at 20 °C (a); same than (a) but with **^{57}Fe-1** as starting material (b); $Fe(Cl)_2(dmpe)_2$ (**1**) (9.4 µmol) treated by 10 equiv. of Na(hmds) after 22 h at 80 °C then cooled 72 h at room temperature (c); *trans*- (**O**) and *cis*- (**X**) $Fe(D)(C_6D_5)(dmpe)_2$ (**4$_{C6D5,D}$**).

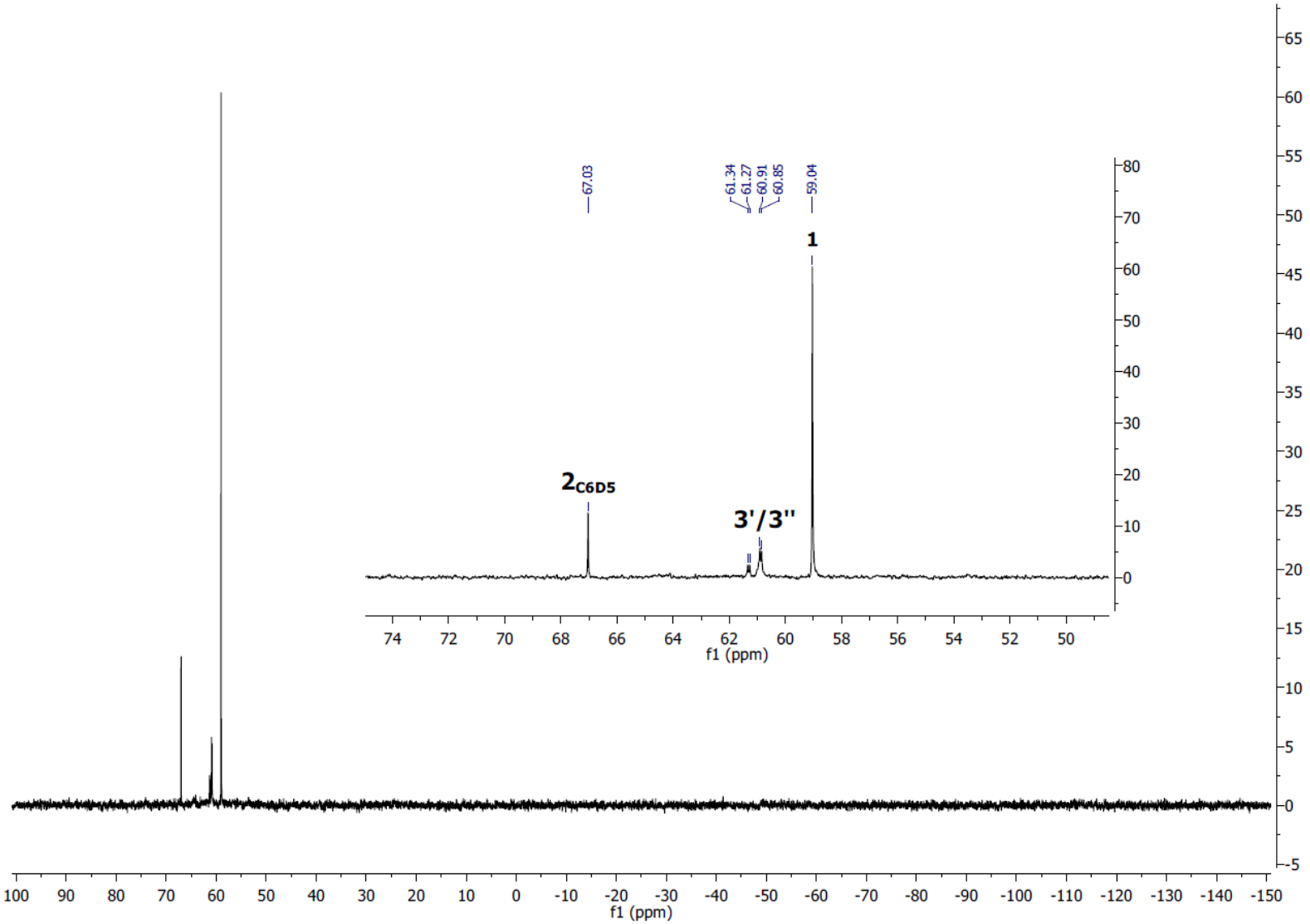

Figure S34: $^{31}P\{^{1}H\}$ NMR (162 MHz, 298 K, C_6D_6) of $Fe(Cl)_2(dmpe)_2$ (**1**) (9.4 µmol) treated by 2 equiv. of Li(hmds) and 2 equiv. of 15-C-5 after 72 h at 20 °C. It shows the presence of $FeCl(C_6D_5)(dmpe)_2$ (**2$_{C6D5}$**), starting $Fe(Cl)_2(dmpe)_2$ (**1**) and Fe^0 species (**3'/3''**).

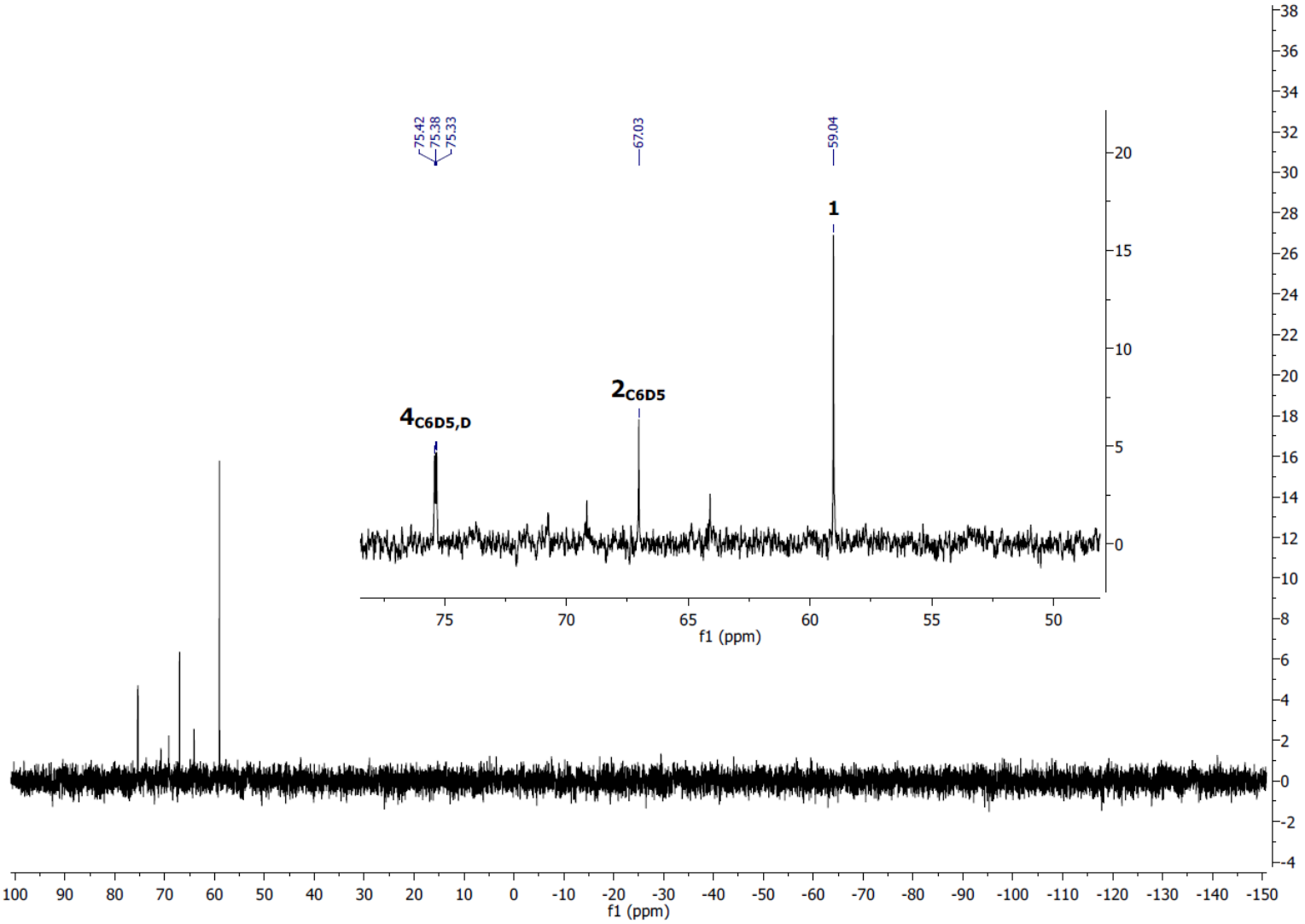

Figure S35: $^{31}P\{^{1}H\}$ NMR (162 MHz, 298 K, C_6D_6) of $Fe(Cl)_2(dmpe)_2$ (**1**) (9.4 µmol) treated by 2 equiv. of Li(hmds) and 2 equiv. of 15-C-5 after 72 h upon photolysis (350 nm). It shows the presence of $FeCl(C_6D_5)(dmpe)_2$ (**2**$_{C6D5}$), starting $Fe(Cl)_2(dmpe)_2$ (**1**) and *trans*-$Fe(D)(C_6D_5)(dmpe)_2$ (**4**$_{C6D5,D}$).

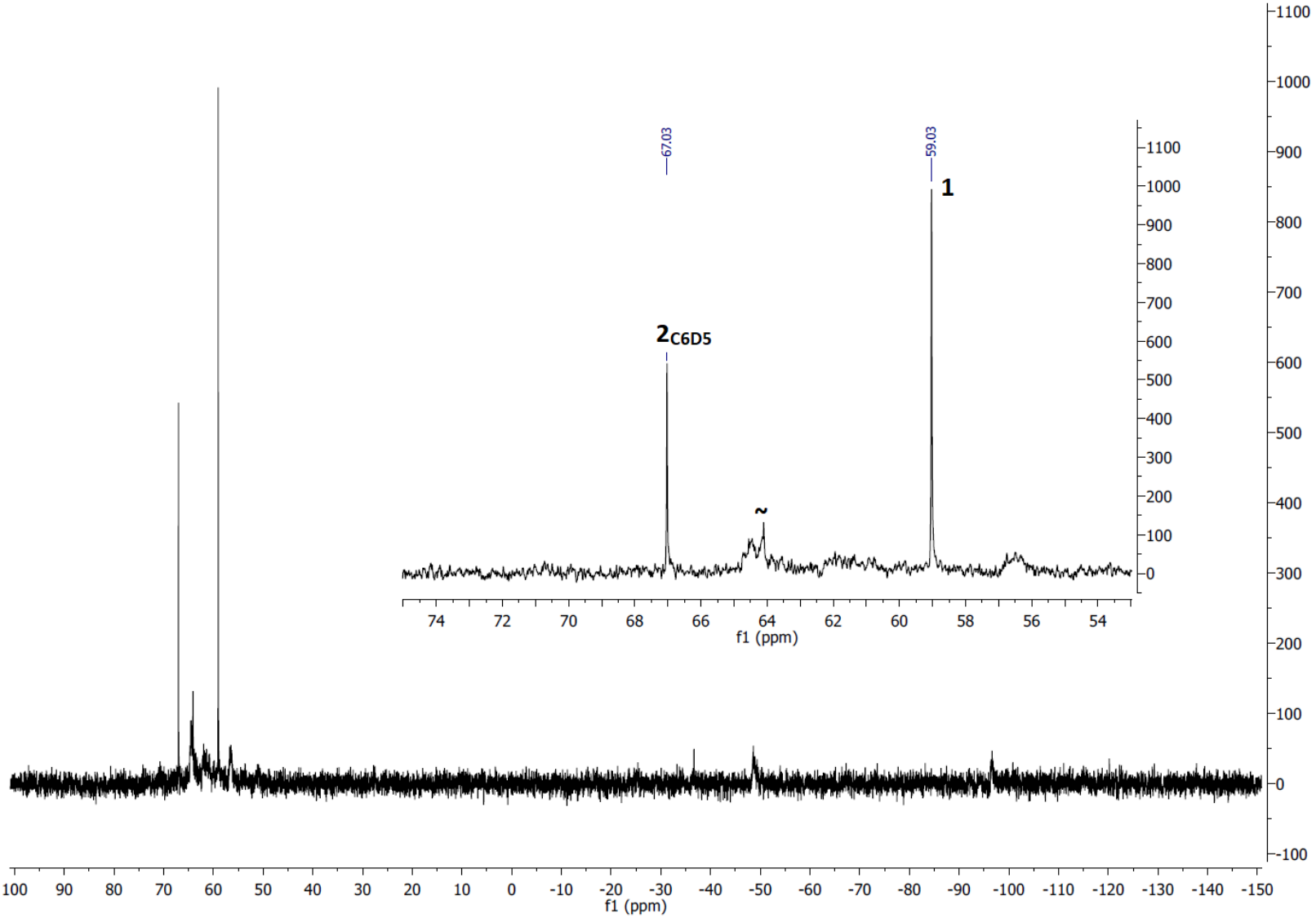

Figure S36: $^{31}P\{^{1}H\}$ NMR (162 MHz, 298 K, C_6D_6) of $Fe(Cl)_2(dmpe)_2$ (**1**) (9.4 µmol) treated by 2 equiv. of Li(hmds) and 2 equiv. of 15-C-5 after 22 h at 80 °C. It shows the presence of $FeCl(C_6D_5)(dmpe)_2$ (**2**$_{C6D5}$), starting $Fe(Cl)_2(dmpe)_2$ (**1**) and unknown species (~).

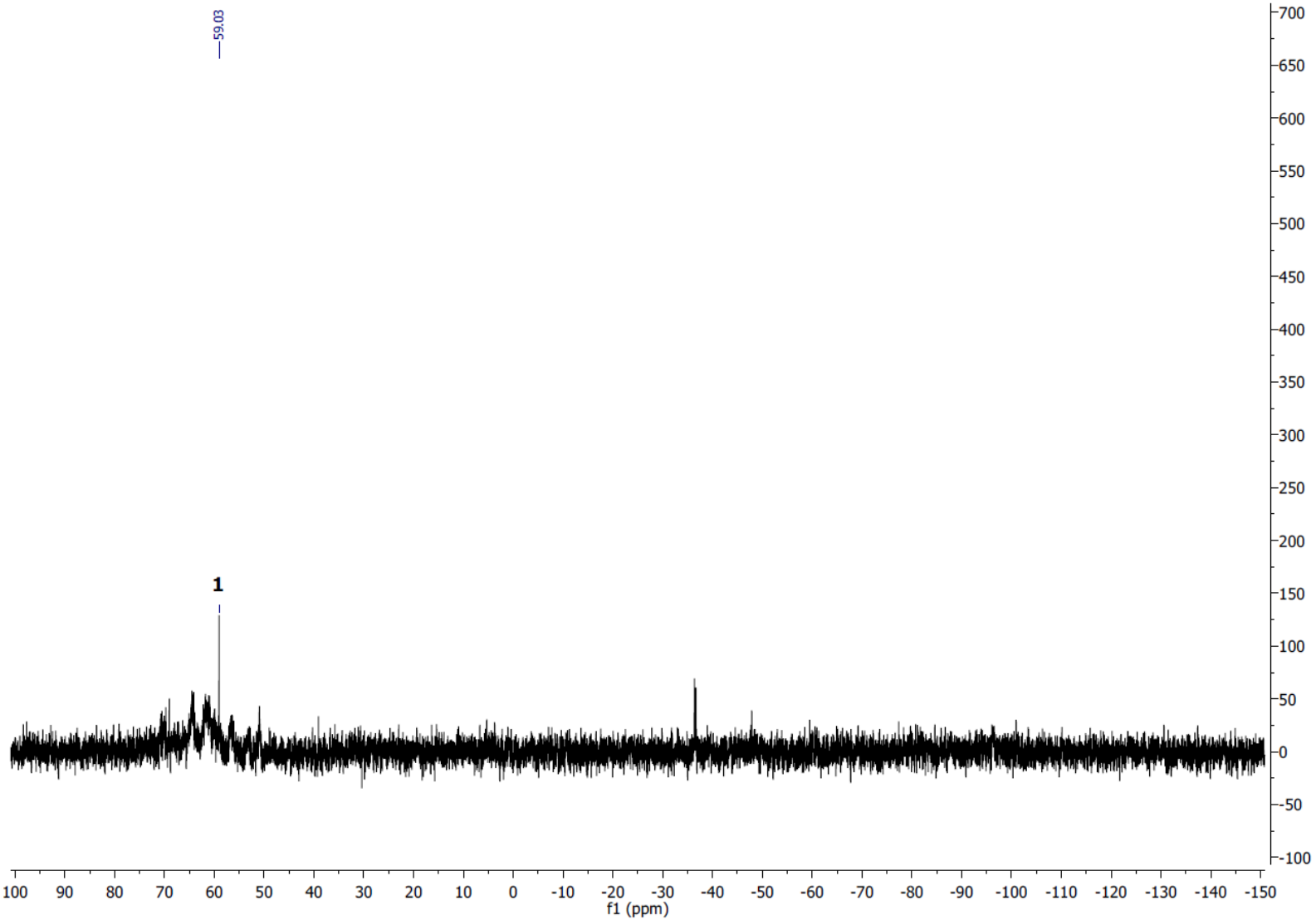

Figure S37: $^{31}P\{^{1}H\}$ NMR (162 MHz, 298 K, C_6D_6) of $Fe(Cl)_2(dmpe)_2$ (**1**) (8.4 µmol) treated by 2 equiv. of Li(hmds) after 22 h at 80 °C. It shows the presence of starting $Fe(Cl)_2(dmpe)_2$ (**1**) and unknown species.

4) Catalytic applications

a) General procedure for cross-coupling reactions with *n*-$C_{12}H_{25}$I and iodocyclohexane

All the cross-coupling reactions discussed in the main article, involving either benzene or fluorobenzene (PhF), were carried out using the following procedure (Figure S38a). Yields were determined by both GC-MS (optimization and screening and the conditions) and NMR analysis of the purified products. NMR analysis for Ph(*n*-$C_{12}H_{25}$) and Ph(cyclohexyl) match with reported data.[**R5**] The ^{19}F NMR spectrum of the purified fraction containing the three isomers formed by cross-coupling attempt between PhF and *n*-$C_{12}H_{25}$I is given in Figure S38b.

a)

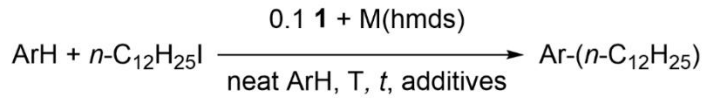

b)

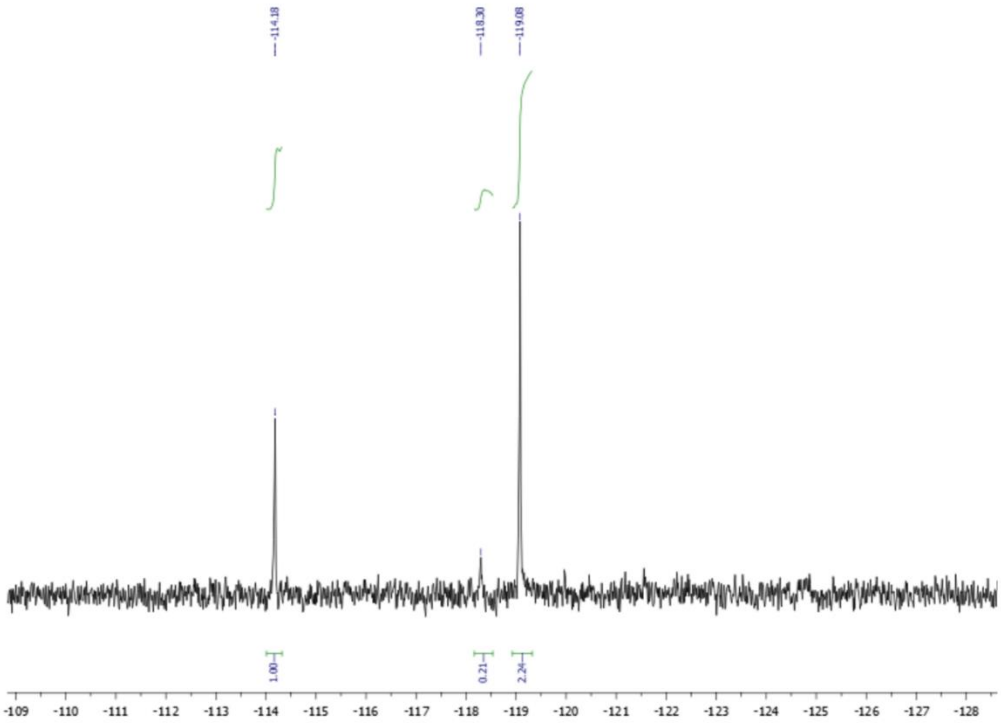

Figure S38: Cross-coupling between ArH and *n*-$C_{12}H_{25}$I mediated by **1** in the presence of M(hmds) (a); ^{19}F NMR spectrum ($CDCl_3$, 377 MHz) of the purified mixture of cross-coupling products between PhF and *n*-$C_{12}H_{25}$I (δ = -119.1 (*ortho*, 65%); -114.2 (*meta*, 29%); -118.3 (*para*, 6%)) (b).

General coupling procedure for GC-MS-monitored coupling experiments :

The reaction with $Fe(Cl)_2(dmpe)_2$ (**1**) and Li(hmds) at 80 °C is given as an example (main article, Table 3, Entry 2). In an argon-filled glove box, a 12 mL vial equipped with a magnetic stir bar was loaded with $Fe(Cl)_2(dmpe)_2$ (3.5 mg, 8.4 µmol, 0.1 equiv.), ArH (1.5 mL) and decane as an internal standard for GC-MS analysis. The mixture was placed under stirring and *n*-$C_{12}H_{25}I$ (20.2 µL, 82 µmol, 1 equiv.) was added dropwise followed by Li(hmds) (15.0 mg, 82 µmol, 1 equiv.). The color of the reaction medium gradually changed from emerald green to yellow/orange. The reaction mixture was stirred for 5 min and transferred into an NMR tube fitted with a J.Young valve. The tube was placed in an oil bath at 80°C and left for 72 h. The color turned pale yellow. The tube was cooled to room temperature and quenched with 2 mL of H_2O. The solution was extracted with 2 mL of MTBE and analyzed by GC-MS.

Procedure and analytical data for cross-coupling between benzene and n-$C_{12}H_{25}I$:

In an argon-filled glove box, a 50 mL J. Young flask equipped with a magnetic stir bar was loaded with $Fe(Cl)_2(dmpe)_2$ (43.9 mg, 102.8 µmol, 0.1 equiv.), C_6H_6 (16 mL) and decane as an internal standard for GC-MS analysis. The mixture was placed under stirring and *n*-$C_{12}H_{25}I$ (253.6 µL, 1028 µmol, 1 equiv.) was added dropwise followed by Li(hmds) (172.0 mg, 1028 µmol, 1 equiv.). The color of the reaction medium gradually changed from emerald green to yellow/brown. The reaction mixture was stirred for 5 min at room temperature then placed in an oil bath at 80°C and left for 72 h. The color turned dark brown with a white precipitate in suspension. The flask was cooled to room temperature and quenched with 10 mL of H_2O. The solution was extracted with DCM (3 x 10 mL) and the organic fractions were combined. The organic layer was dried over $MgSO_4$ and concentrated under vacuum. The crude product purified by silica gel chromatography (100 % cyclohexane as eluent).

Standard analysis conditions: 40 °C (hold 1 min) to 250 °C (hold 6 min), heating rate: 7.5 °C/min.

GC-MS (LRMS):

n-$C_{12}H_{26}$: t_R = 10.777 min, m/z = 170.2 (calcd. = 170.2).

n-$C_{12}H_{25}I$: t_R = 19.074 min, m/z = 296.2 (calcd. = 296.1).

Ph(*n*-$C_{12}H_{25}$): t_R = 22.415 min, m/z = 246.2 (calcd. = 246.2).

Procedure and analytical data for cross-coupling between PhF and n-$C_{12}H_{25}I$:

In an argon-filled glove box, a 50 mL J. Young flask equipped with a magnetic stir bar was loaded with $Fe(Cl)_2(dmpe)_2$ (42.9 mg, 101.4 µmol, 0.1 equiv.), C_6H_5F (16.5 mL) and decane as an internal standard for GC-MS analysis. The mixture was placed under stirring and *n*-$C_{12}H_{25}I$ (250.1 µL, 1014 µmol, 1 equiv.) was added dropwise followed by Li(hmds) (169.7 mg, 1014 µmol, 1 equiv.). The color of the reaction medium gradually changed from emerald green to orange/brown. The reaction mixture was stirred for 5 min at room temperature then placed in an oil bath at 80°C and left for 72 h. The color turned dark brown with a white precipitate in suspension.. The flask was cooled to room temperature and quenched with 10 mL of H_2O. The solution was extracted with DCM (3 x 10 mL) and the organic fractions were combined. The organic layer was dried over $MgSO_4$ and concentrated under vacuum. The crude product purified by silica gel chromatography (100 % cyclohexane as eluent); overall yield for the three *ortho* / *meta* / *para* isomers : 15% (11:5:1).

^{19}F NMR analytical data (Figure S24b) of the pure fraction containing the three coupling isomers was analyzed by GC-MS, and is in agreement with reported literature (comparison with *meta*-C_6H_4F(*n*-C_6H_{13}),[**R5**] *para*-C_6H_4F(*n*-$C_{12}H_{25}$),[**R6**] and *ortho*-C_6H_4F(*n*-C_6H_{13}),[**R7**]).

b) General procedure for cross-coupling reactions with radical clock: $Br(CH_2)_4CH=CH_2$

All the cross-coupling reactions below were carried out using the following procedure. The reaction with $Fe(Cl)_2(dmpe)_2$ (**1**) and Li(hmds) without additives at 80 °C is given as an example (Entry 1) and was analyzed by GC-MS using pure compounds as internal standards.

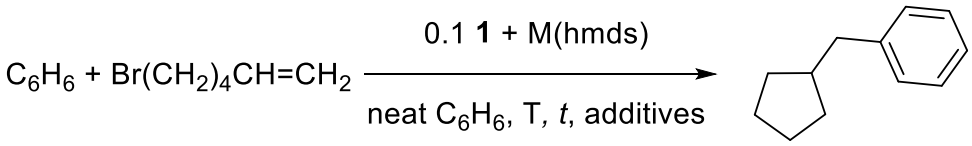

Entry	M	T / °C	*t* / h	additives	Yield (%)
1	Li	80	24	-	8
2	Li	80	24	dmpe 1 equiv.	3
3	Li	80	24	dmpe 5 equiv.	1
4[a]	Li	80	24	dmpe 1 equiv.	8

Figure S39: Cross-coupling between C_6H_6 and $Br(CH_2)_4CH=CH_2$ mediated by **1** in the presence of Li(hmds); other iron sources: [a] = 0.1 equiv. $FeCl_2$.

In an argon-filled glove box, a 12 mL vial equipped with a magnetic stir bar was loaded with $Fe(Cl)_2(dmpe)_2$ (3.1 mg, 7.3 µmol, 0.1 equiv.), C_6H_6 (1.5 mL) and decane as an internal standard for GC-MS analysis. The mixture was placed under stirring and $Br(CH_2)_4CH=CH_2$ (9.7 µL, 72.6 µmol, 1 equiv.) was added dropwise followed by Li(hmds) (12.2 mg, 72.6 µmol, 1 equiv.). The color of the reaction medium gradually changed from emerald green to brown. The reaction mixture was stirred for 5 min and transferred into an NMR tube fitted with a J.Young valve. The tube was placed in an oil bath at 80°C and left for 24 h. The color turned dark orange. The tube was cooled to room temperature and quenched with 2 mL of H_2O. The solution was extracted with 2 mL of MTBE and analyzed by GC-MS.

Standard analysis conditions: 40 °C (hold 1 min) to 250 °C (hold 6 min), heating rate: 7.5 °C/min.

GC-MS (LRMS):
$Br(CH_2)_4CH=CH_2$: t_R = 5.168 min, m/z = 162.0 (calcd. = 162.0).

$C_{12}H_{16}$: t_R = 12.810 min, m/z = 160.1 (calcd. = 160.1).

c) General procedure for cross-coupling reactions with $\mathbf{2_{Ph'}}$ and *n*-$\mathbf{C_{12}H_{25}I}$

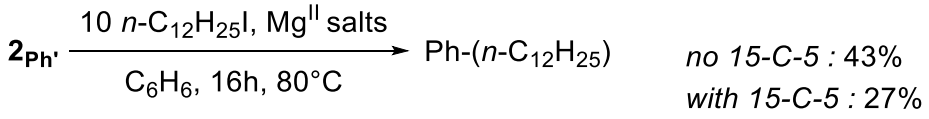

Figure S40: Cross-coupling between $\mathbf{2_{Ph'}}$ and *n*-$C_{12}H_{25}I$ with or without 15-C-5; yields based on GC-MS analysis.

$FeBr(C_6H_5)(dmpe)_2$ was synthesized using the procedure previously described with $Fe(Cl)_2(dmpe)_2$ (12 mg, 28.1 µmol, 1 equiv.), C_6H_6 (1.4 mL) and PhMgBr (14.1 µL, 14.05 µmol, 0.5 equiv.) in a 12 mL vial equipped with a magnetic stir bar. After one night at room temperature in the glove box, the solution was separated into two NMR tubes fitted with a J. Young valve. In the first tube (T1), *n*-$C_{12}H_{25}I$ (34.7 µL, 140.5 µmol, 5 equiv.) was added dropwise and then the tube was vigorously shaken. The solution turned pink. In the second tube (T2), *n*-$C_{12}H_{25}I$ (34.7 µL, 140.5 µmol, 5 equiv.) was also added dropwise followed by 15-C-5 (2.8 µL, 14.05 µmol, 0.5 equiv.) then vigorously shaken. The solution remained yellow/orange. Both tubes were placed in an oil bath at 80°C and left for 16 h. The tube (T1) turned pale green and the tube (T2) turned

green/yellow. Tubes were cooled to room temperature and quenched with 1 mL H_2O. They were extracted with 1 mL of MTBE and analyzed by GC-MS.

5) C-H / B-H bond metathesis: reductive dehydrocoupling

a) General procedure for borylation of C-H bonds

All the borylation reactions present in the main article, Table 4 were carried out using the following procedure. The reaction with $Fe(Cl)_2(dmpe)_2$ (**1**) and Li(hmds) is given as an example (Entry 4).

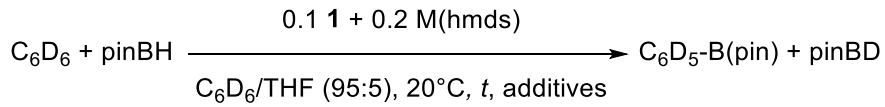

Figure S41: Borylation between C_6D_6 and pinBH mediated by **1** in the presence of M(hmds); composition of the crude mixture was determined by ^{11}B NMR integration.

In an argon-filled glove box, a 12 mL vial equipped with a magnetic stir bar was loaded with $Fe(Cl)_2(dmpe)_2$ (3.7 mg, 8.7 µmol, 0.1 equiv.), C_6D_6 (0.6 mL) and THF in a 9:1 ratio. The mixture was placed under stirring and Li(hmds) (2.9 mg, 17.3 µmol, 0.2 equiv.) was added. The color of the reaction medium gradually changed from emerald green to yellow/orange. The reaction mixture was stirred for 3 days at room temperature in order to afford the expected distribution of **3**, **3'** and $\mathbf{4_{C6D5,D}}$ species. Pinacolborane (12.6 µL, 87 µmol, 1 equiv.) was added dropwise and the mixture was transferred into an NMR tube fitted with a J.Young valve. The tube was irradiated, and the reaction was followed by ^{11}B, $^{31}P\{^1H\}$ and ^1H NMR.

The ^1H and ^{11}B NMR data are in agreement with the literature**[R8]**.

Ph-Bpin: ^1H NMR (400 MHz, $CDCl_3$): δ = 7.79-7.76 (m, 2H), 7.44-7.40 (m, 1H), 7.35-7.31 (m, 2H), 1.31 (s, 12H). ^{11}B NMR (128 MHz, $CDCl_3$): δ = 31.02 (br. s).

Standard GC-MS analysis conditions: 40 °C (hold 1 min) to 250 °C (hold 6 min), heating rate: 7.5 °C/min.

GC-MS (LRMS):
Ph-Bpin: t_R = 13.945 min, m/z = 204.1 (calcd. = 204.1).

b) ^{11}B, $^{31}P\{^1H\}$ and ^1H NMR data for borylation experiments

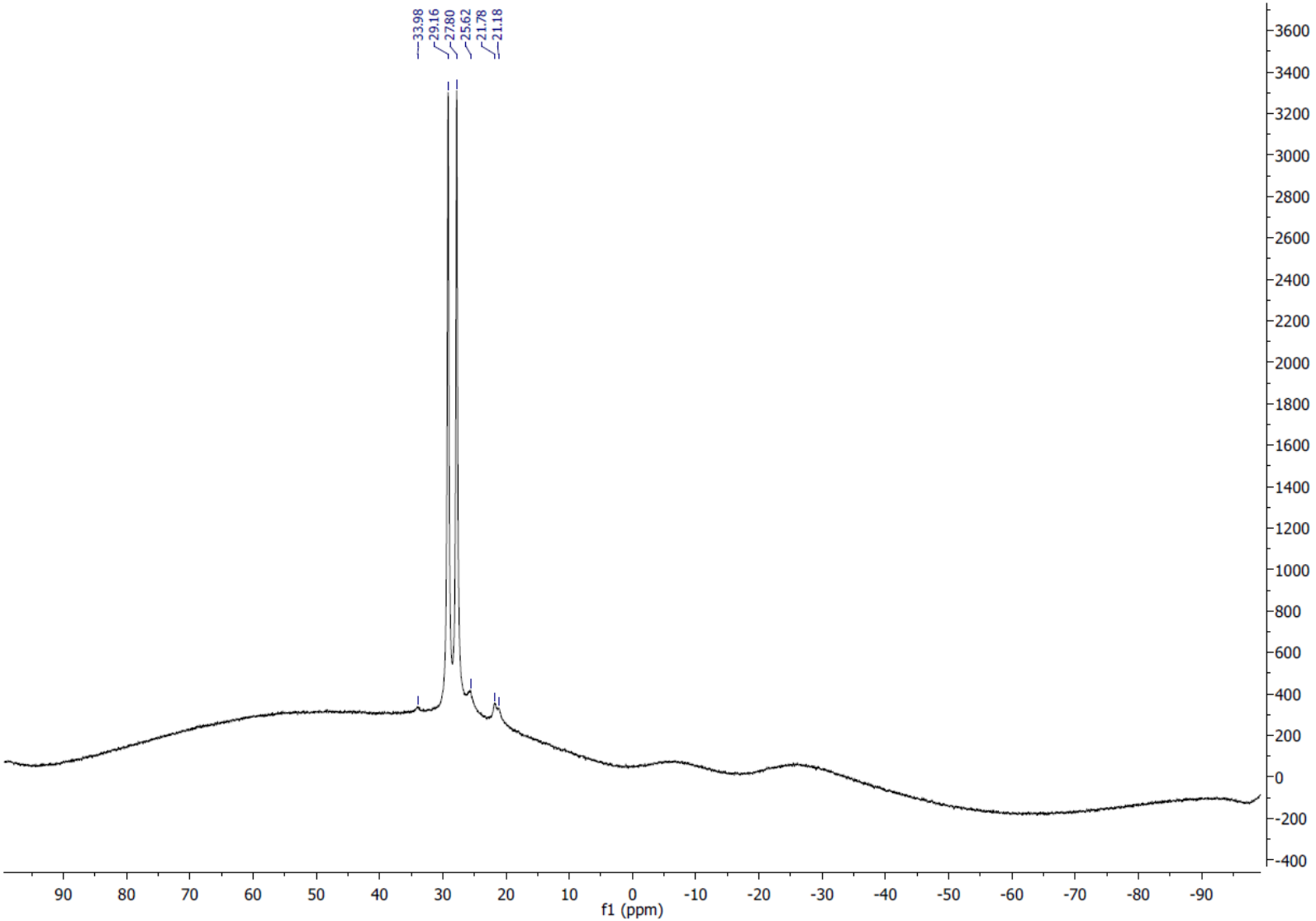

Figure S42: ^{11}B NMR (128 MHz, 298 K, C_6D_6/THF 9:1) of $Fe(Cl)_2(dmpe)_2$ (**1**) (8.2 µmol) treated by 2 equiv. of Na(hmds) (premix 3 days) and 10 equiv. of pinBH after 7 days in the dark.

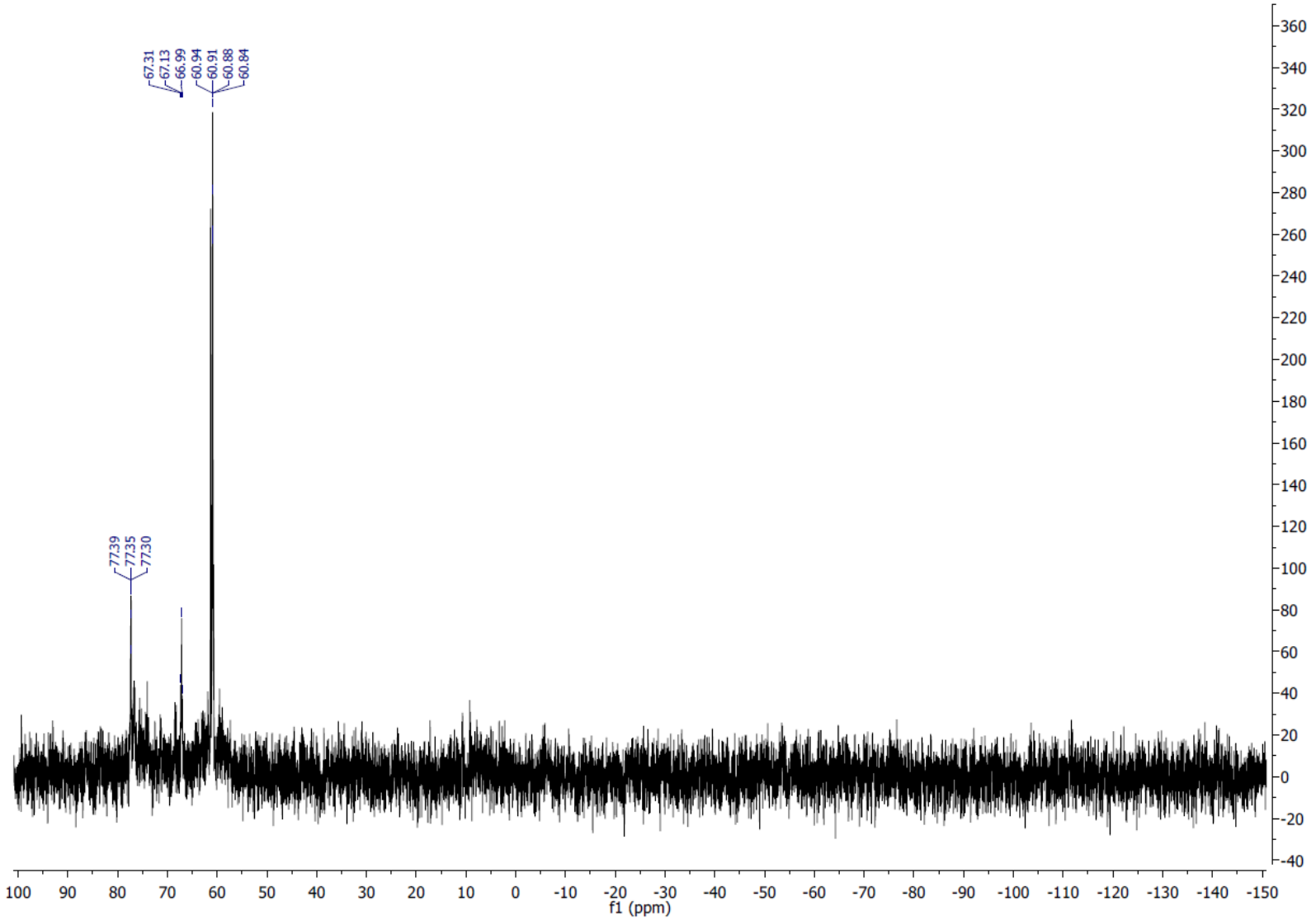

Figure S43: $^{31}P\{^{1}H\}$ NMR (162 MHz, 298 K, C_6D_6/THF 9:1) of $Fe(Cl)_2(dmpe)_2$ (**1**) (8.2 µmol) treated by 2 equiv. of Na(hmds) (premix 3 days) and 10 equiv. of pinBH after 7 days in the dark. It shows the presence of (**3'**), (**3''**), $Fe(H)_2(dmpe)_2$ and $Fe(H)(D)(dmpe)_2$.

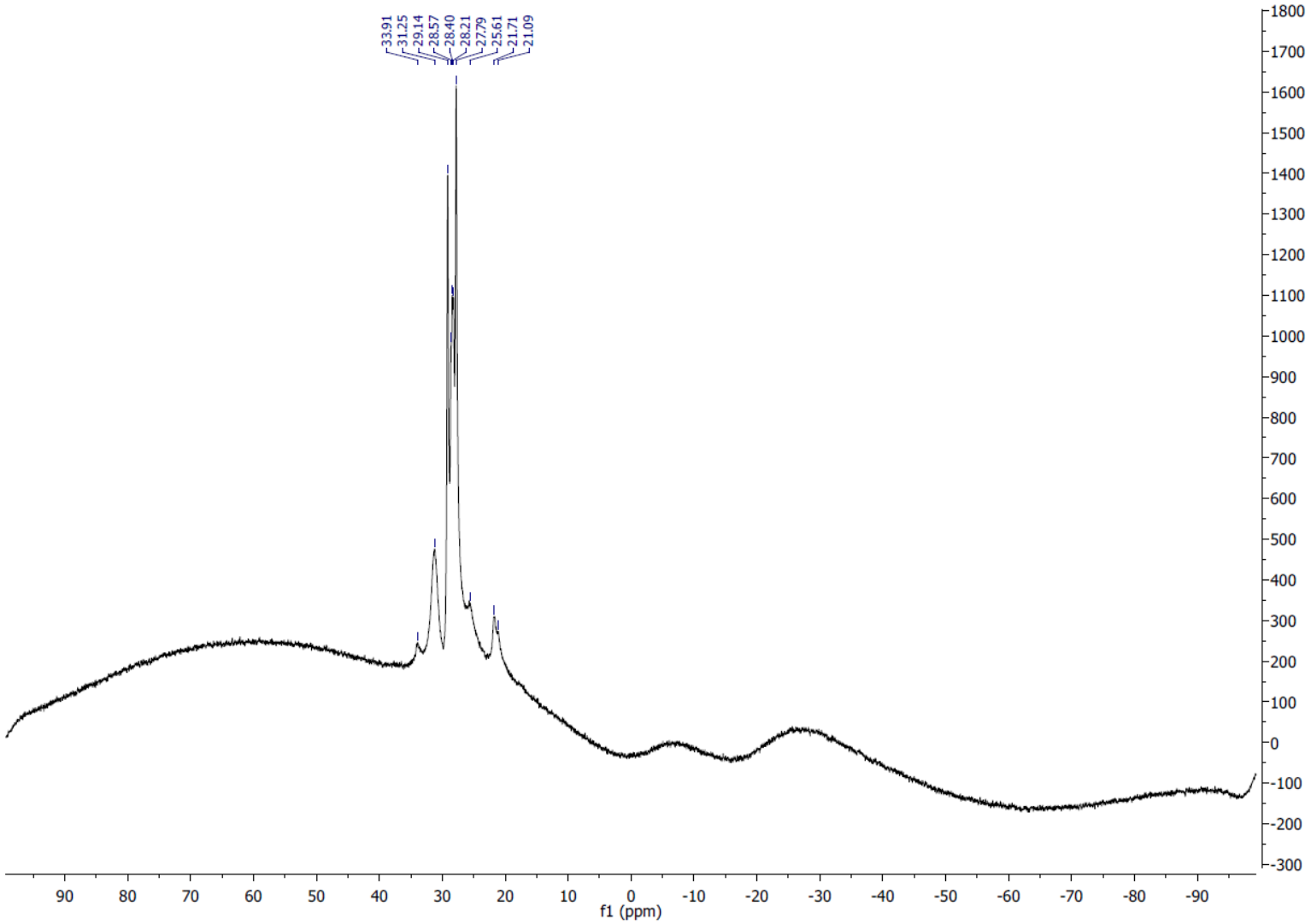

Figure S44: ^{11}B NMR (128 MHz, 298 K, C_6D_6/THF 9:1) of $Fe(Cl)_2(dmpe)_2$ (**1**) (8.2 µmol) treated by 2 equiv. of Na(hmds) (premix 3 days) and 10 equiv. of pinBH after 7 days upon photolysis (350 nm). It shows the presence of Ph-Bpin (s, 31.25 ppm) and pinBD (t, 28.4 ppm).

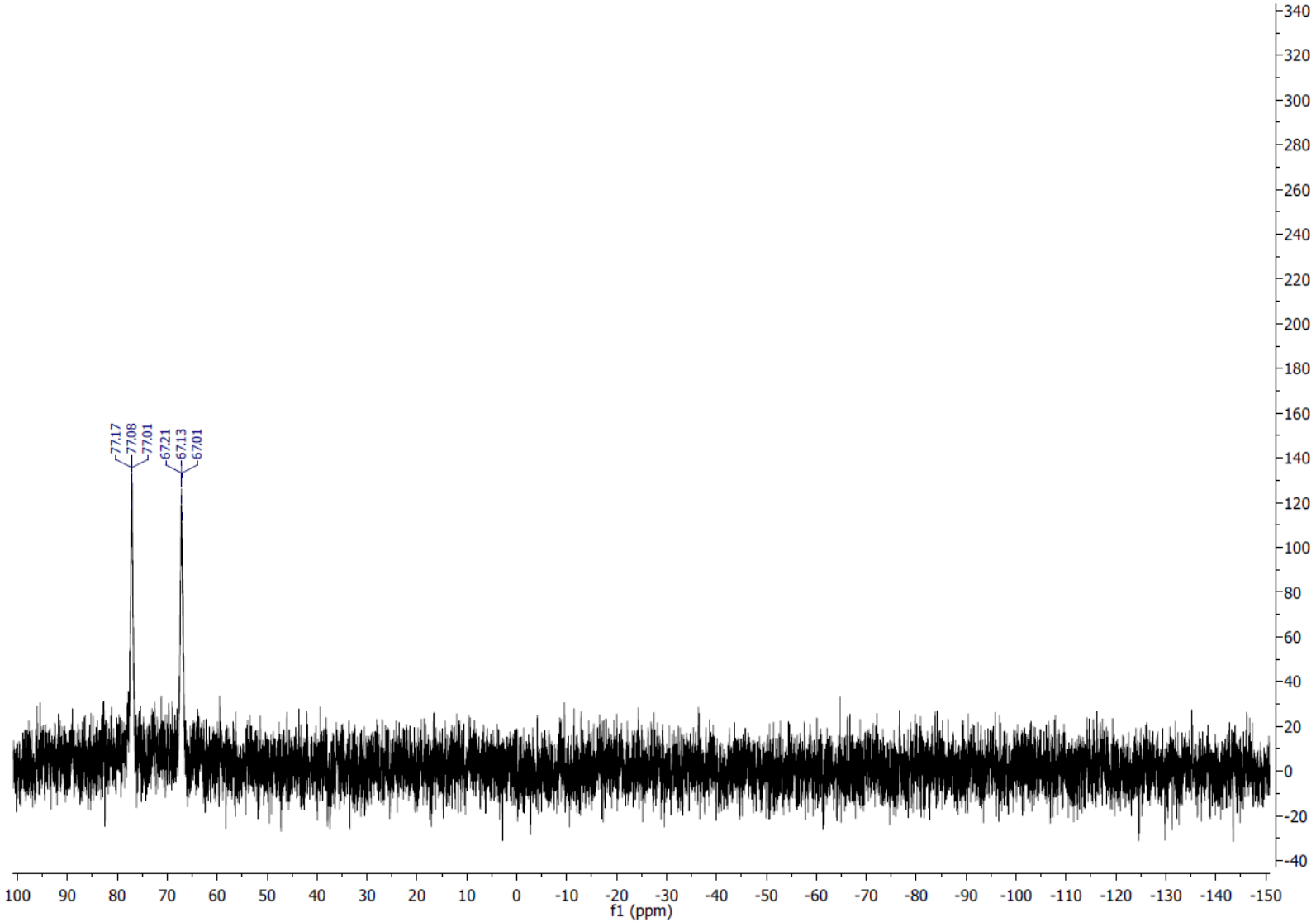

Figure S45: $^{31}P\{^{1}H\}$ NMR (162 MHz, 298 K, C_6D_6/THF 9:1) of $Fe(Cl)_2(dmpe)_2$ (**1**) (8.2 µmol) treated by 2 equiv. of Na(hmds) (premix 3 days) and 10 equiv. of pinBH after 7 days upon photolysis (350 nm). It shows only the presence of $Fe(H)_2(dmpe)_2$ and $Fe(H)(D)(dmpe)_2$.

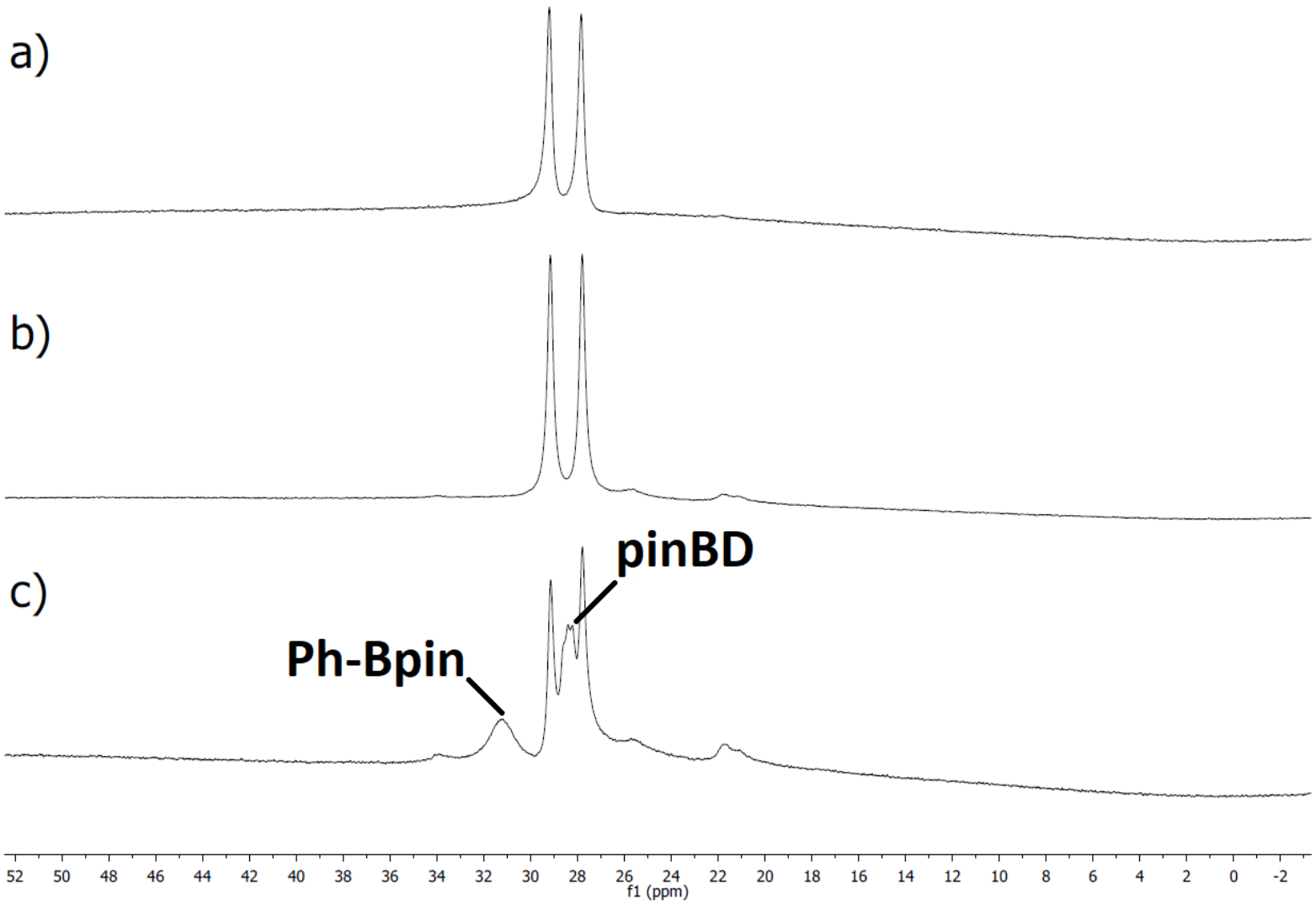

Figure S46: ^{11}B NMR (128 MHz, 298 K, C_6D_6/THF 9:1) of pinBH (a), **1** (8.2 µmol) treated by 2 equiv. of Na(hmds) (premix 3 days) and 10 equiv. of pinBH after 7 days in the dark (b) and (**1**) (8.2 µmol) treated by 2 equiv. of Na(hmds) (premix 3 days) and 10 equiv. of pinBH after 7 days upon photolysis (350 nm) (c).

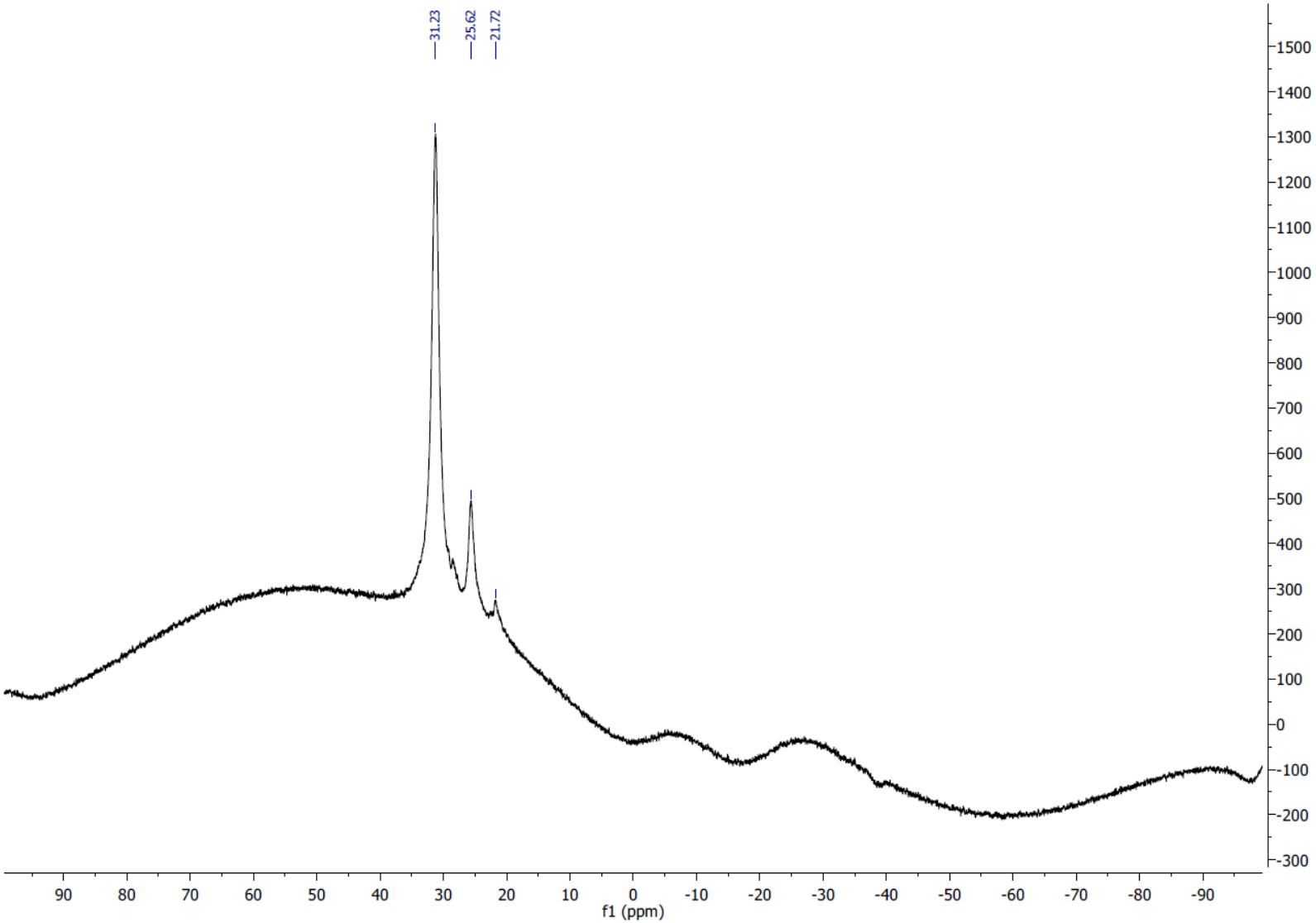

Figure S47: ^{11}B NMR (128 MHz, 298 K, C_6D_6/THF 9:1) of $Fe(Cl)_2(dmpe)_2$ (**1**) (8.7 µmol) treated by 2 equiv. of Li(hmds) (premix 3 days) and 10 equiv. of pinBH after 6 days upon photolysis (350 nm). It shows the presence of Ph-Bpin (s, 31.23 ppm).

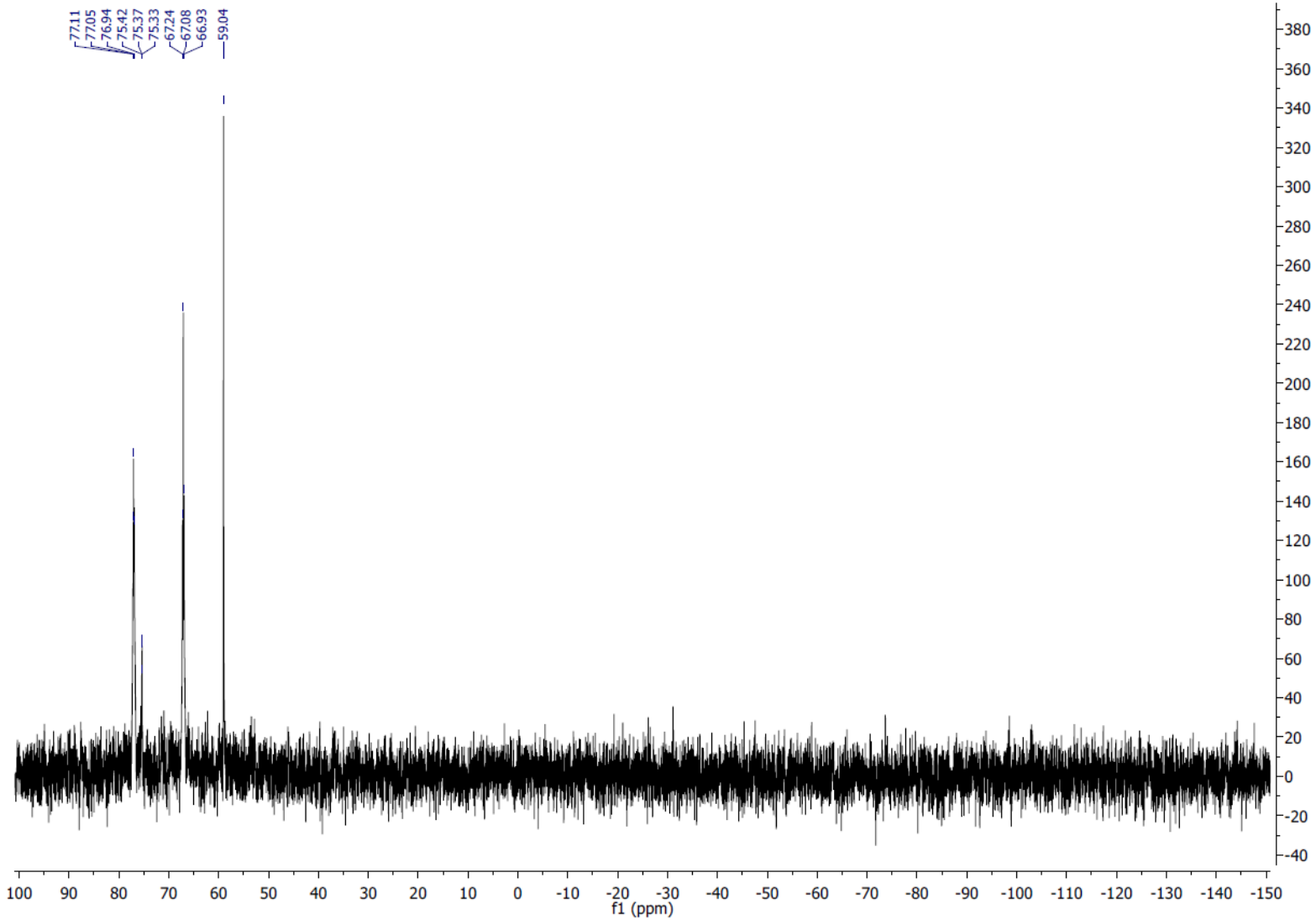

Figure S48: $^{31}P\{^{1}H\}$ NMR (162 MHz, 298 K, C_6D_6) of $Fe(Cl)_2(dmpe)_2$ (**1**) (8.7 µmol) treated by 2 equiv. of Li(hmds) (premix 3 days) and 10 equiv. of pinBH after 10 days upon photolysis (350 nm). It shows the presence of (**$4_{C6D5,D}$**), starting $FeCl_2(dmpe)_2$, $Fe(H)_2(dmpe)_2$ and $Fe(H)(D)(dmpe)_2$, and unreacted **1**.

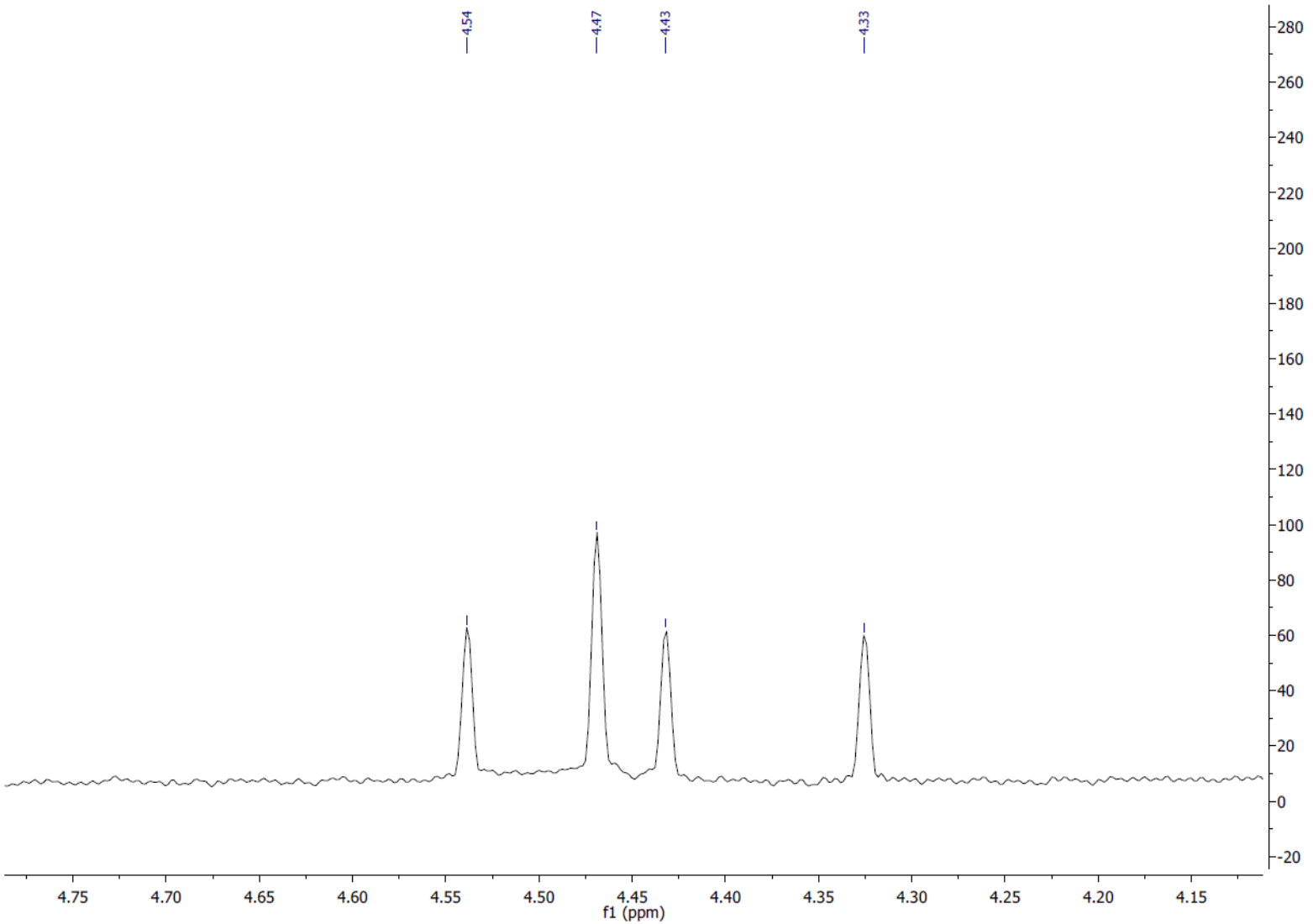

Figure S49: ^{1}H NMR (400 MHz, 298 K, C_6D_6) of $Fe(Cl)_2(dmpe)_2$ (**1**) (8.7 µmol) treated by 2 equiv. of Li(hmds) (premix 3 days) and 10 equiv. of pinBH after 10 days upon photolysis (350 nm). It shows the presence of H_2 (s, 4.47 ppm) and HD (t, 4.54-4.33, $J(^{1}H\text{-}^{2}D)$ = 42.7 Hz).

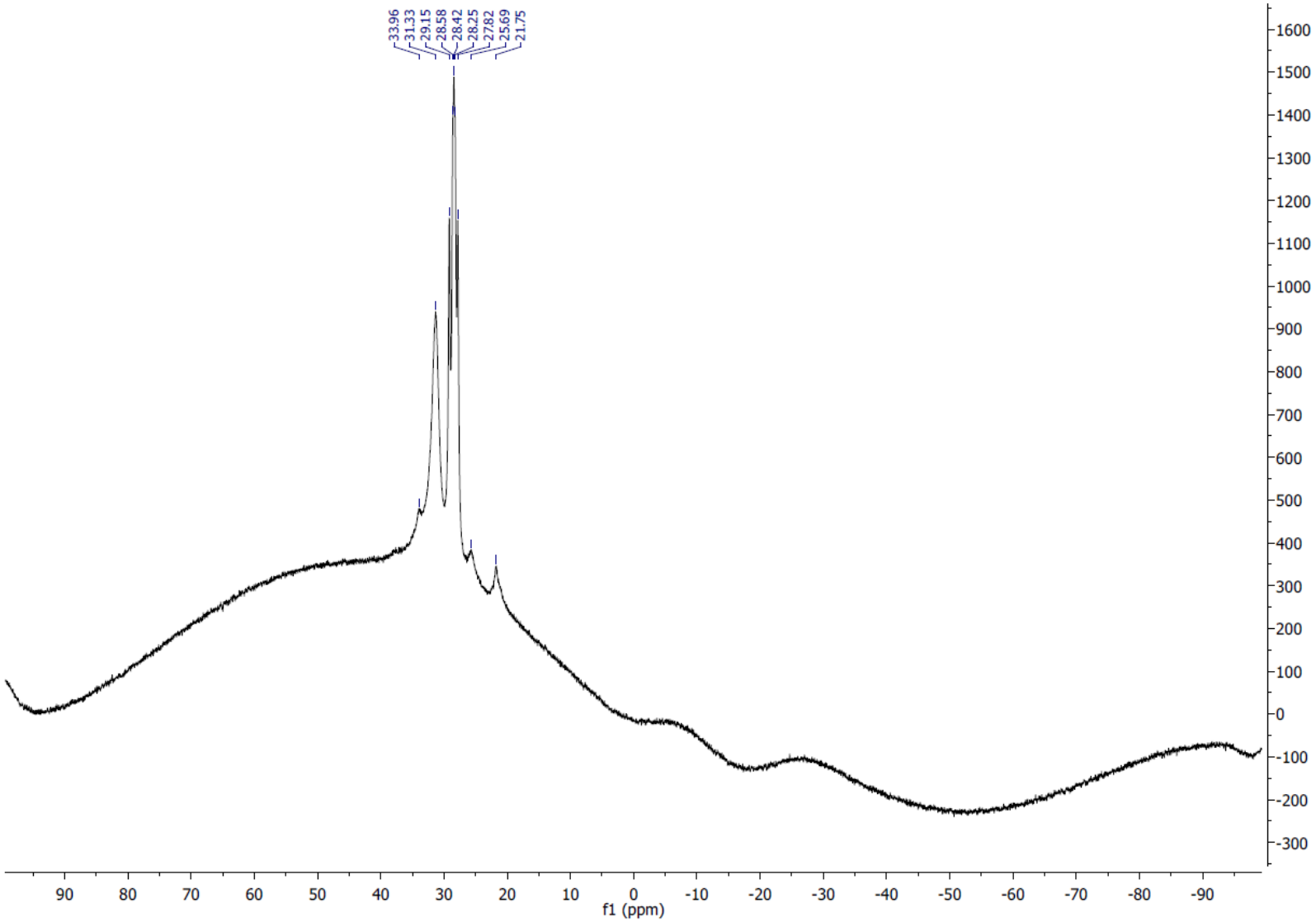

Figure S50: ^{11}B NMR (128 MHz, 298 K, C_6D_6/THF 9:1) of $Fe(Cl)_2(dmpe)_2$ (**1**) (8.7 µmol) treated by 2 equiv. of Na(hmds) (premix 3 days) and 10 equiv. of pinBH after 10 days upon photolysis (350 nm). It shows the presence of Ph-Bpin, pinBD and starting pinBH.

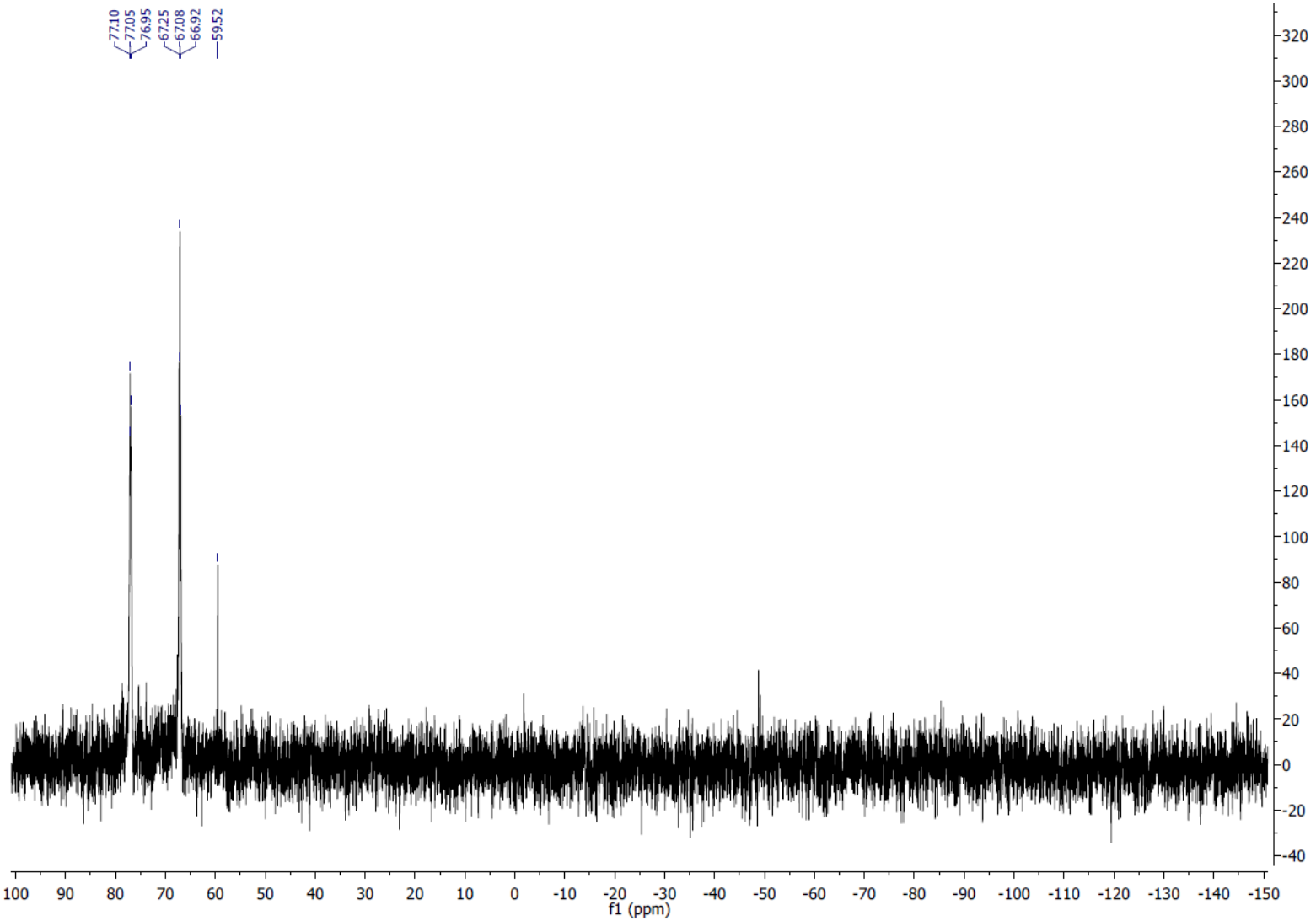

Figure S51: $^{31}P\{^{1}H\}$ NMR (162 MHz, 298 K, C_6D_6/THF 9:1) of $Fe(Cl)_2(dmpe)_2$ (**1**) (8.7 µmol) treated by 2 equiv. of Na(hmds) (premix 3 days) and 10 equiv. of pinBH after 10 days upon photolysis (350 nm). It shows the presence of $Fe(H)_2(dmpe)_2$ and $Fe(H)(D)(dmpe)_2$, and unreacted **1**.

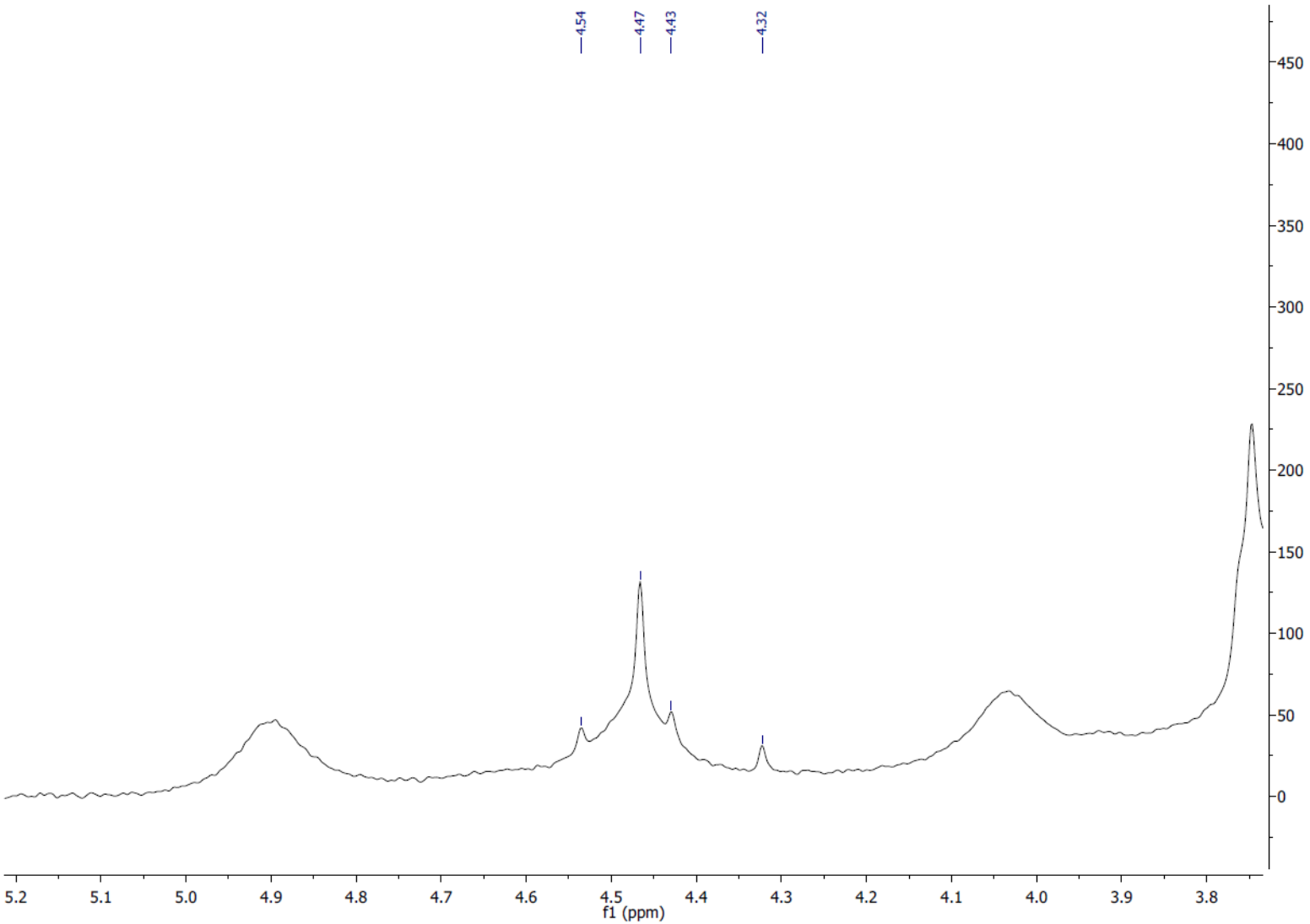

Figure S52: ^{1}H NMR (400 MHz, 298 K, C_6D_6/THF 9:1) of $Fe(Cl)_2(dmpe)_2$ (**1**) (8.7 µmol) treated by 2 equiv. of Na(hmds) (premix 3 days) and 10 equiv. of pinBH after 10 days upon photolysis (350 nm). It shows the presence of H_2 (s, 4.47 ppm), HD (t, 4.54-4.33, $J(^{1}H\text{-}^{2}D)$ = 42.7 Hz) and starting pinBH.

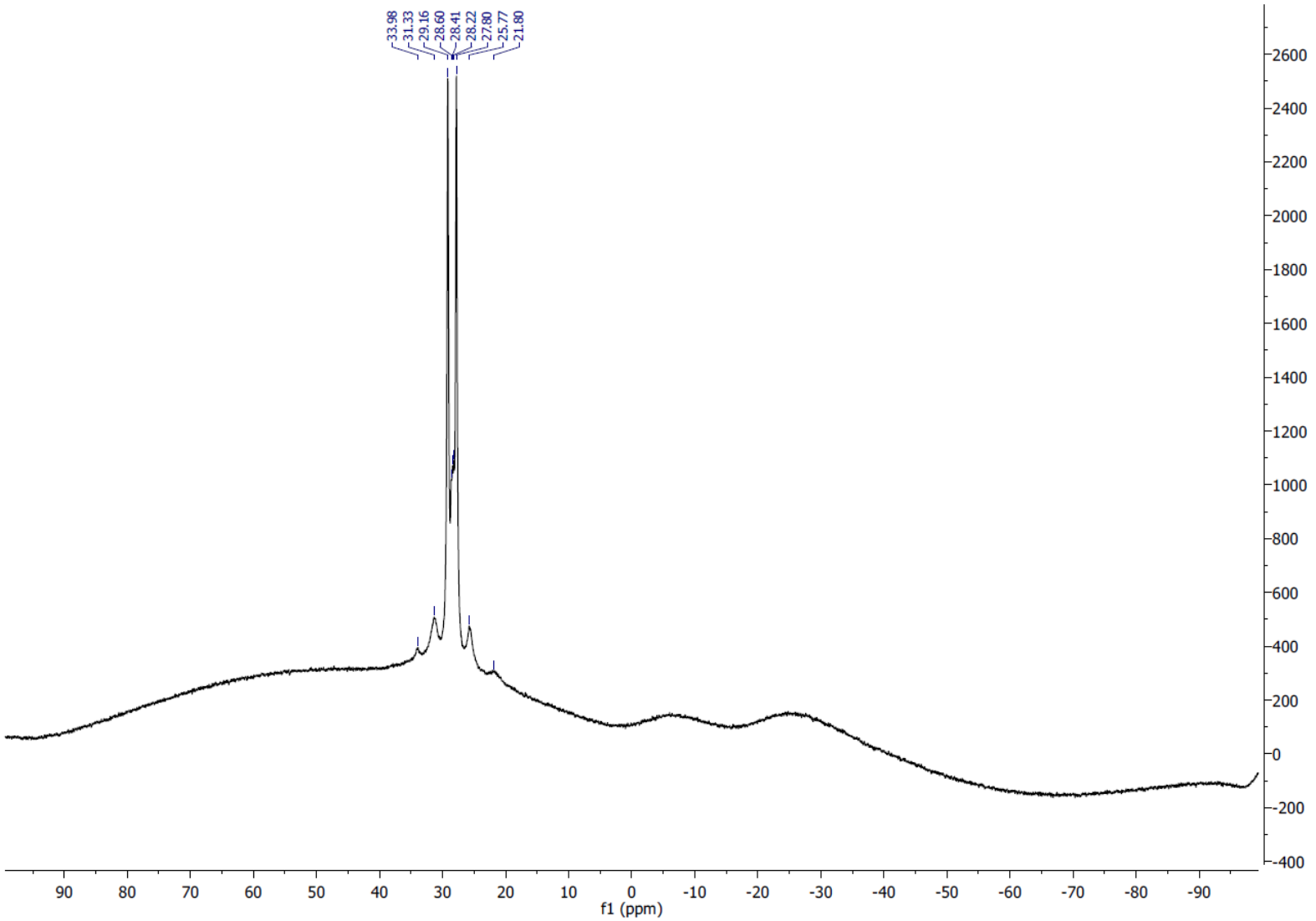

Figure S53: ^{11}B NMR (128 MHz, 298 K, C_6D_6/THF 9:1) of $Fe(Cl)_2(dmpe)_2$ (**1**) (9.6 µmol) treated by 2 equiv. of K(hmds) (premix 3 days) and 10 equiv. of pinBH after 10 days upon photolysis (350 nm). It shows the presence of Ph-Bpin, pinBD and starting pinBH.

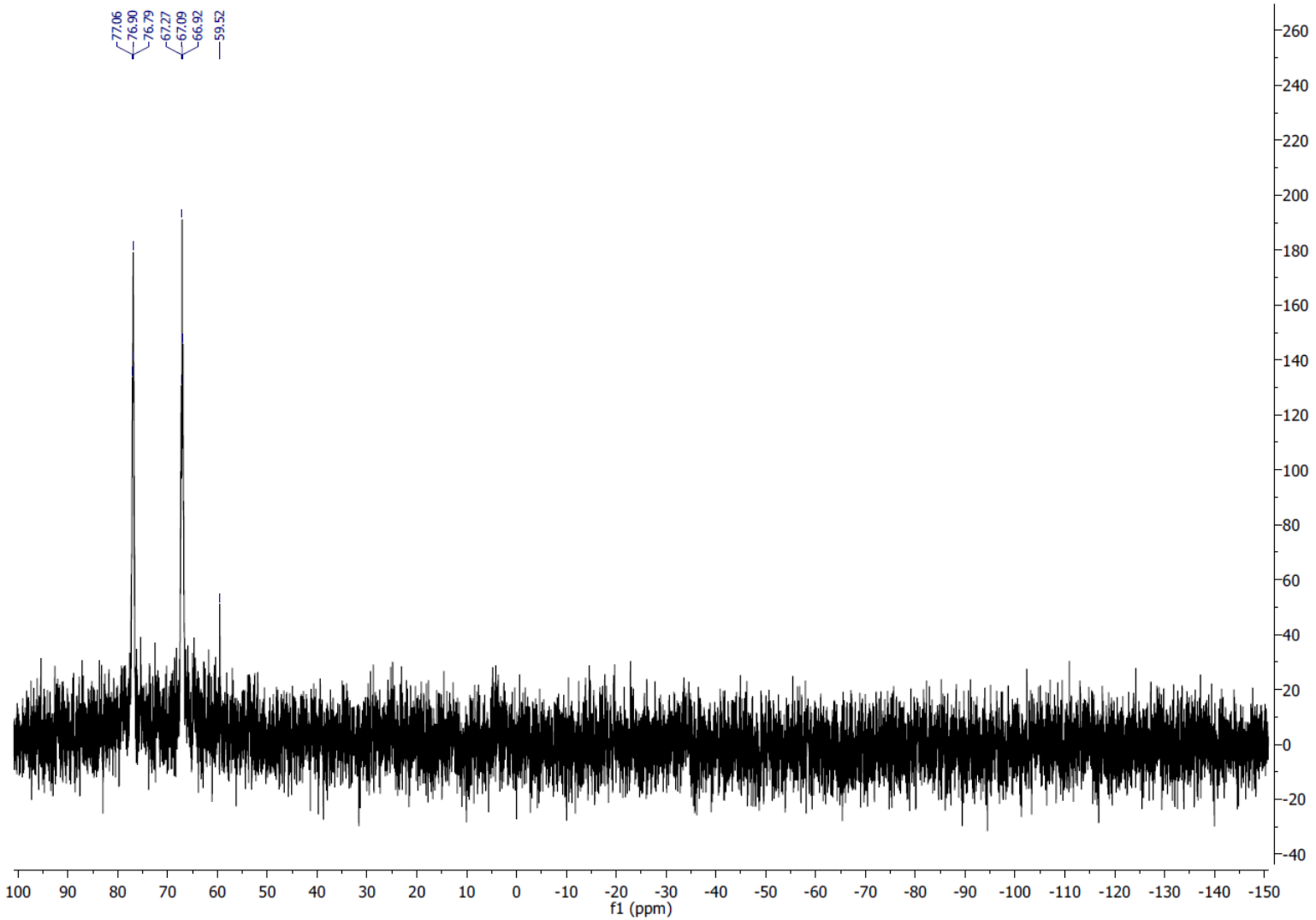

Figure S54: $^{31}P\{^{1}H\}$ NMR (162 MHz, 298 K, C_6D_6/THF 9:1) of $Fe(Cl)_2(dmpe)_2$ (**1**) (9.6 µmol) treated by 2 equiv. of K(hmds) (premix 3 days) and 10 equiv. of pinBH after 10 days upon photolysis (350 nm). It shows the presence of $Fe(H)_2(dmpe)_2$ and $Fe(H)(D)(dmpe)_2$, and unreacted **1**.

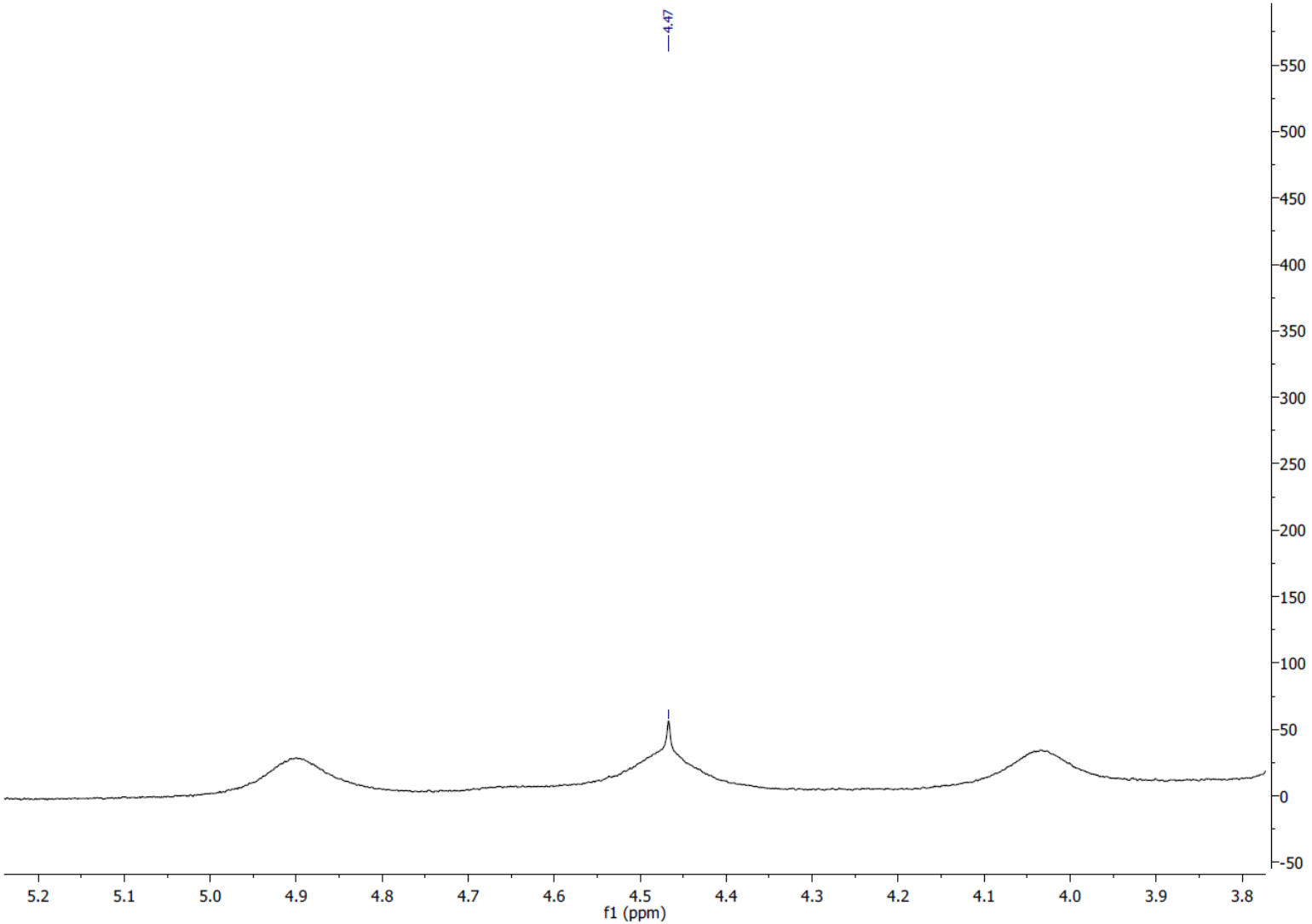

Figure S55: ^{1}H NMR (400 MHz, 298 K, C_6D_6/THF 9:1) of $Fe(Cl)_2(dmpe)_2$ (**1**) (9.6 µmol) treated by 2 equiv. of K(hmds) (premix 3 days) and 10 equiv. of pinBH after 10 days upon photolysis (350 nm). It shows the presence of H_2 (s, 4.47 ppm) and starting pinBH.

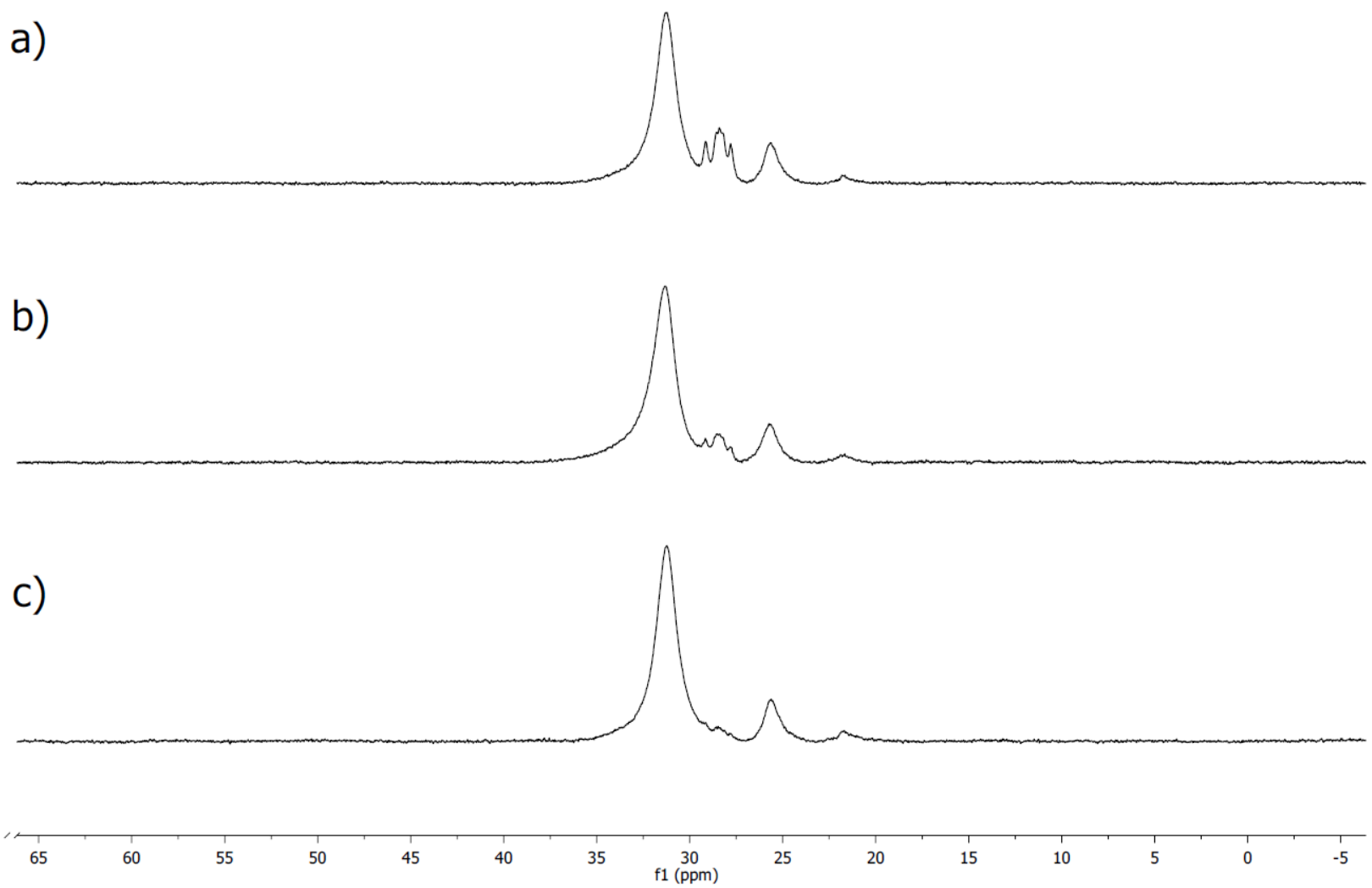

Figure S56: ^{11}B NMR (128 MHz, 298 K, C_6D_6/THF 9:1) of $Fe(Cl)_2(dmpe)_2$ (**1**) (8.7 µmol) treated by 2 equiv. of Li(hmds) (premix 3 days) and 10 equiv. of pinBH after 3 days (a), 4 days (b) and 6 days (c) upon photolysis (350 nm).

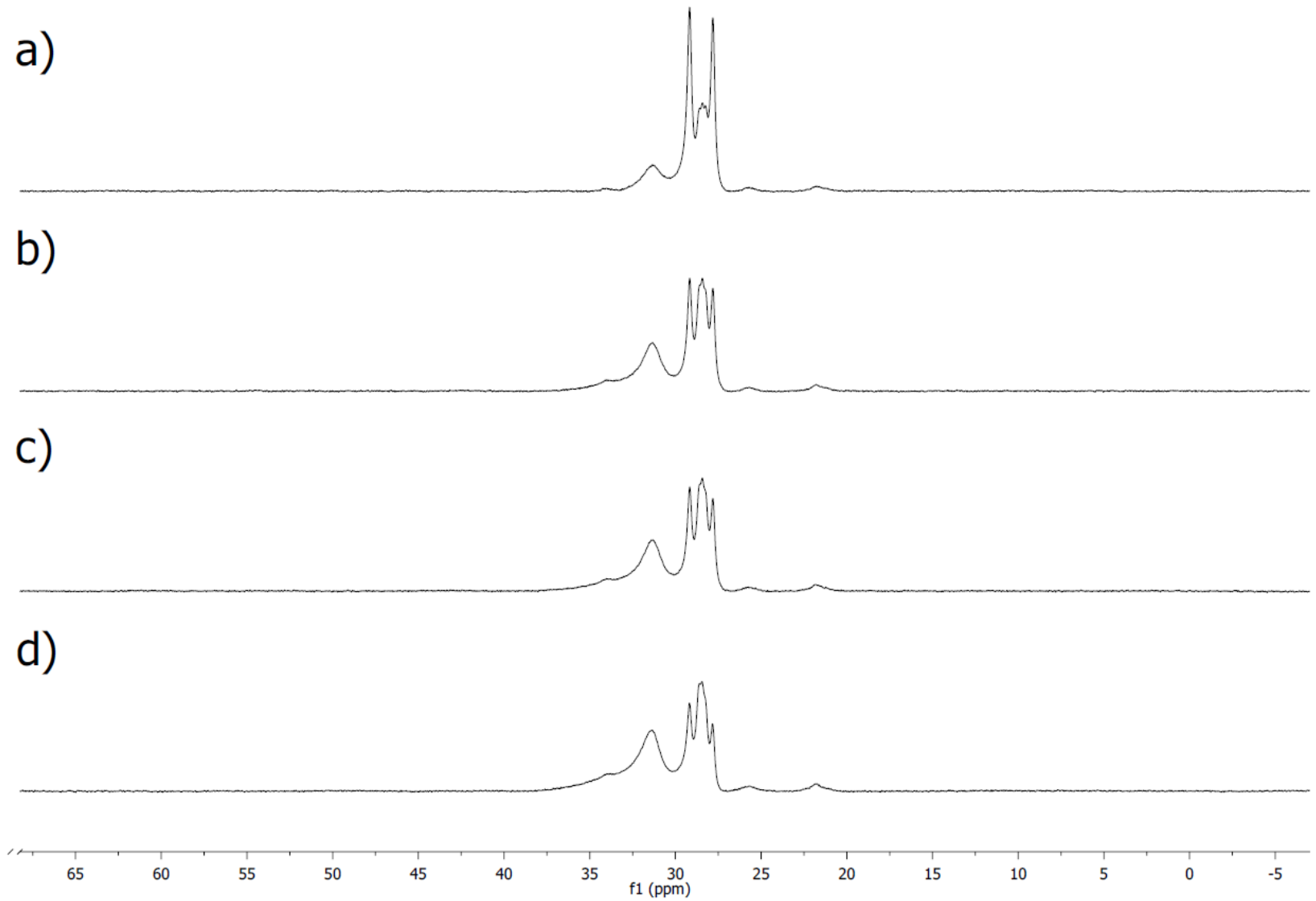

Figure S57: ^{11}B NMR (128 MHz, 298 K, C_6D_6/THF 9:1) of $Fe(Cl)_2(dmpe)_2$ (**1**) (8.7 µmol) treated by 2 equiv. of Na(hmds) (premix 3 days) and 10 equiv. of pinBH after 3 days (a), 6 days (b), 7 days (c) and 10 days (d) upon photolysis (350 nm).

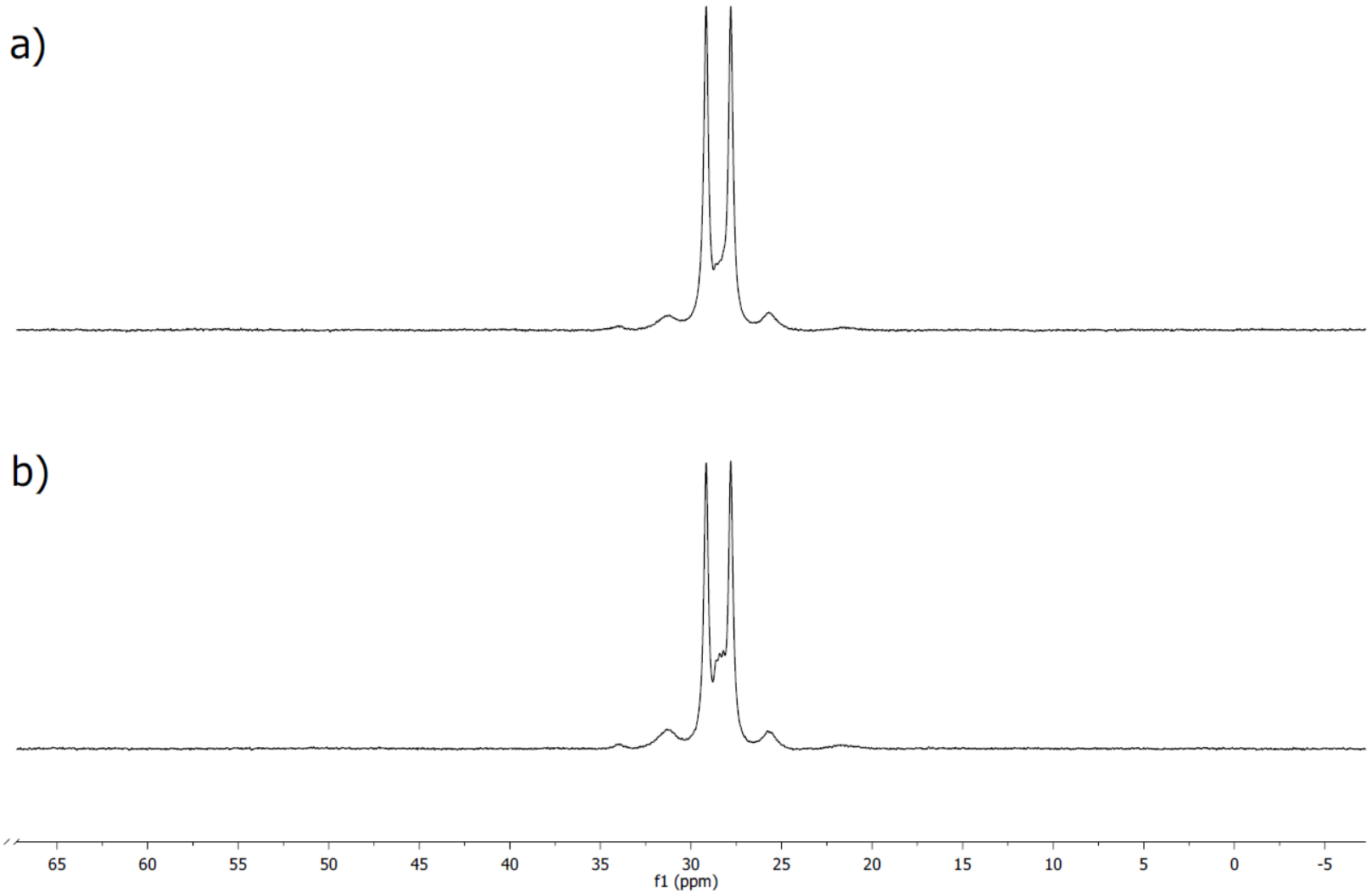

Figure S58: ^{11}B NMR (128 MHz, 298 K, C_6D_6/THF 9:1) of $Fe(Cl)_2(dmpe)_2$ (**1**) (9.6 µmol) treated by 2 equiv. of K(hmds) (premix 3 days) and 10 equiv. of pinBH after 4 days (a) and 10 days (b) upon photolysis (350 nm).

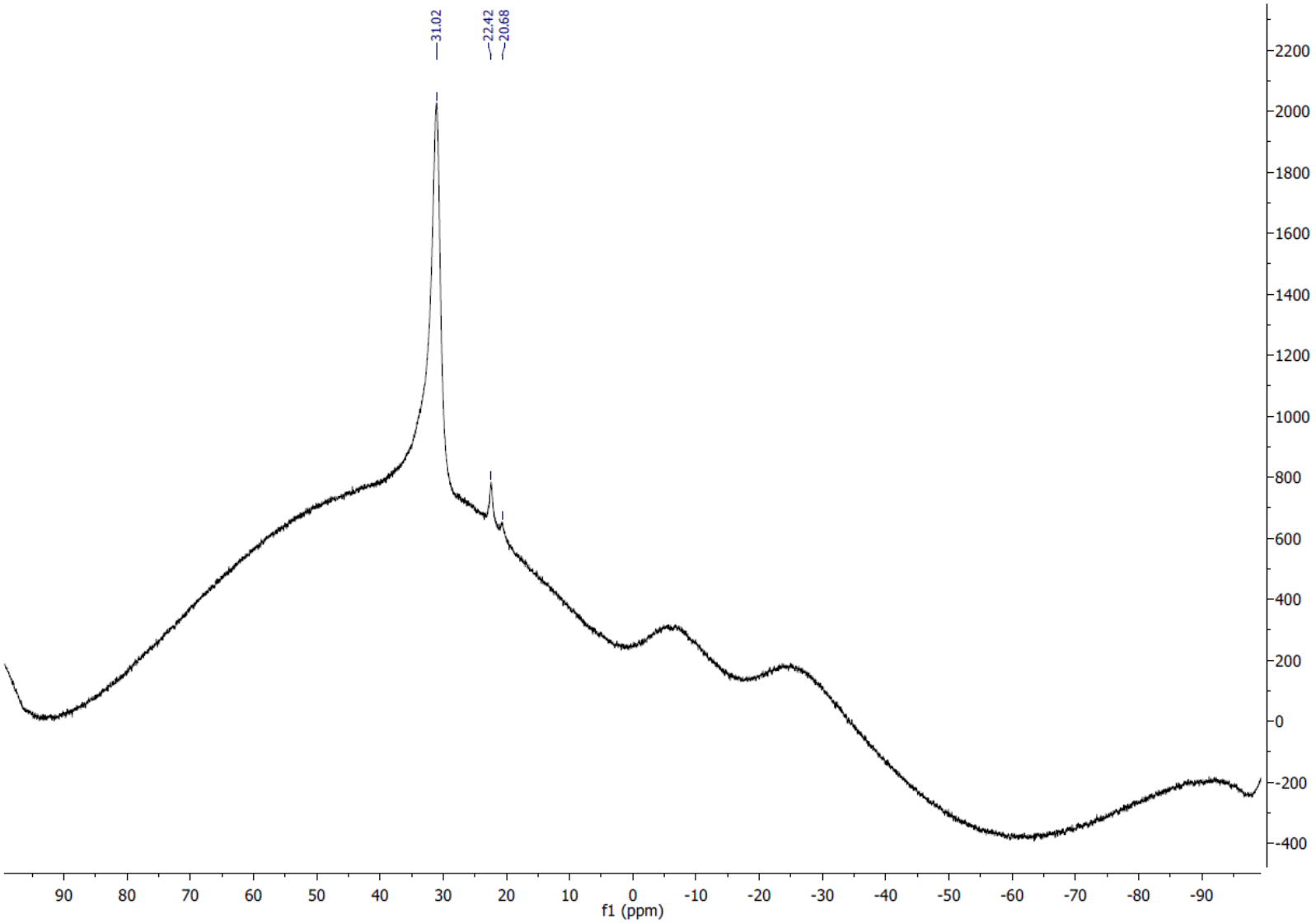

Figure S59: ^{11}B NMR (128 MHz, 298 K, $CDCl_3$) of $Fe(Cl)_2(dmpe)_2$ (**1**) (8.4 µmol) treated by 2 equiv. of Li(hmds) (premix 3 days) and 10 equiv. of pinBH after 10 days upon photolysis (350 nm), quench with H_2O, extraction with MTBE and evaporation of the solvent.

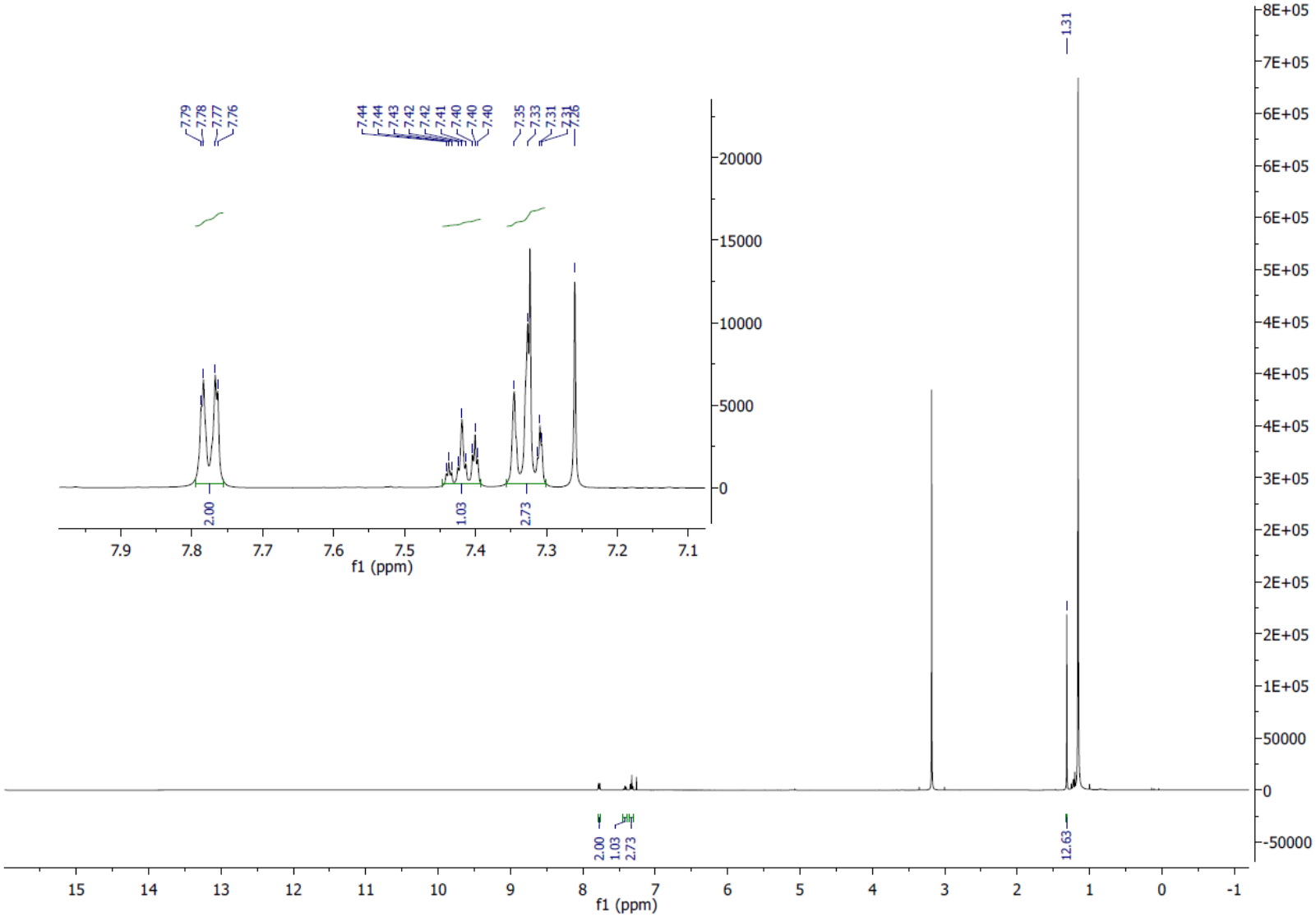

Figure S60: ^{1}H NMR (400 MHz, 298 K, $CDCl_3$) of $Fe(Cl)_2(dmpe)_2$ (**1**) (8.4 µmol) treated by 2 equiv. of Li(hmds) (premix 3 days) and 10 equiv. of pinBH after 10 days upon photolysis (350 nm), quench with H_2O, extraction with MTBE and evaporation of the solvent.

6) Crystallography

PhMgBr (THF solution, 1M) was added by 0.25 equiv. aliquots to a solution of **1** in benzene at -30°C; the solution was left at RT overnight. The solution was concentrated under vacuo (ca. 3 mL) in the glovebox, and was layered with 3 mL of *n*-pentane. This was placed in the glovebox freezer at -35°C for 3 days, allowing the formation of red crystals trapped in the frozen benzene.

A red block-like single crystal of compound $\mathbf{2_{Ph}}$, was selected, mounted onto a cryoloop, and transferred in the cold nitrogen gas stream of an Oxford Cryostream. Intensity data were collected with a BRUKER Kappa-APEXII diffractometer with micro-focused Cu-Kα radiation (λ=1.54178 A) at 200K. APEX 3 suite and SAINT program (BRUKER) were used to carry out data collection, unit-cell parameters refinement, integration and data reduction. SADABS (BRUKER) was used for scaling and multi-scan absorption corrections. In the Olex2 suite,**[R9]** the structure was solved with SHELXT-14 program **[R10]** and refined by full-matrix least-squares methods using SHELXL-17.**[R11]** All non-hydrogen atoms were refined anisotropically. Hydrogen atoms, although visible on the Fourier difference map, were placed at calculated positions and refined with a riding model.

CCDC 2248606 contain the supplementary crystallographic data for this paper. The data can be obtained free of charge from The Cambridge Crystallographic Data Centre via www.ccdc.cam.ac.uk/structures.

Table 1 Crystal data and structure refinement for vw479_0m.

Identification code	vw479_0m
Empirical formula	$C_{24}H_{43}BrFeP_4$
Formula weight	591.22
Temperature/K	200.0
Crystal system	monoclinic
Space group	$P2_1/c$
a/Å	9.4919(7)
b/Å	13.0523(9)
c/Å	22.5297(15)
α/°	90
β/°	92.497(3)
γ/°	90
Volume/Å^3	2788.6(3)
Z	4
ρ_{calc}g/cm^3	1.408
μ/mm^{-1}	8.249
F(000)	1232.0
Crystal size/mm^3	0.25 × 0.15 × 0.12
Radiation	CuKα (λ = 1.54178)

2Θ range for data collection/°	7.83 to 136.87
Index ranges	$-8 \leq h \leq 11$, $-15 \leq k \leq 15$, $-27 \leq l \leq 26$
Reflections collected	32155
Independent reflections	5121 [R_{int} = 0.0359, R_{sigma} = 0.0243]
Data/restraints/parameters	5121/0/280
Goodness-of-fit on F^2	1.132
Final R indexes [I>=2σ (I)]	R_1 = 0.0429, wR_2 = 0.1139
Final R indexes [all data]	R_1 = 0.0453, wR_2 = 0.1156
Largest diff. peak/hole / e Å^{-3}	0.43/-1.14

Table 2 Fractional Atomic Coordinates (×10^4) and Equivalent Isotropic Displacement Parameters (Å^2×10^3) for vw479_0m. U_{eq} is defined as 1/3 of the trace of the orthogonalised U_{IJ} tensor.

Atom	*x*	*y*	*z*	U(eq)
Br1	6984.5(6)	1564.8(4)	2569.1(2)	47.94(17)
Fe1	7190.7(6)	2124.2(4)	3665.1(2)	18.72(15)
P1	8932.3(10)	3161.3(8)	3400.5(4)	28.0(2)
P2	5755.6(10)	3442.3(7)	3428.9(4)	24.0(2)
P3	8618.0(10)	783.2(7)	3840.8(4)	27.3(2)
P4	5426.3(10)	1046.1(7)	3828.8(4)	24.8(2)
C1	7361(3)	2571(3)	4551.7(14)	17.0(6)
C2	7370(4)	3592(3)	4731.1(16)	27.5(8)
C3	7431(4)	3901(3)	5321.5(18)	33.2(9)
C4	7483(4)	3186(4)	5777.2(17)	35.8(10)
C5	7488(4)	2169(4)	5620.1(17)	34.9(9)
C6	7436(4)	1874(3)	5024.5(16)	28.0(8)
C7	8153(5)	4241(3)	2977.0(19)	35.9(9)
C8	6812(4)	4586(3)	3271.8(17)	32.2(9)
C9	10093(5)	3806(4)	3949(2)	45.8(11)
C10	10262(5)	2723(4)	2891(2)	47.4(12)
C11	4447(5)	3934(4)	3932(2)	39.1(10)
C12	4639(5)	3416(4)	2745(2)	43.8(11)
C13	7603(5)	-305(3)	4137.4(18)	34.5(9)
C14	6124(5)	-274(3)	3844.5(19)	36.2(9)
C15	10171(4)	890(4)	4348(2)	40.9(10)
C16	9433(6)	111(4)	3231(2)	48.9(12)
C17	4406(4)	1117(3)	4498.2(18)	34.7(9)
C18	3941(5)	894(4)	3291(2)	44.1(11)
C19	7557(5)	6704(4)	4633.0(19)	40.4(10)
C20	8821(5)	6758(4)	4359.3(19)	39.2(10)
C21	8832(4)	6964(3)	3758.9(19)	36.8(9)

Table 2 Fractional Atomic Coordinates ($\times 10^4$) and Equivalent Isotropic Displacement Parameters ($Å^2 \times 10^3$) for vw479_0m. U_{eq} is defined as 1/3 of the trace of the orthogonalised U_{IJ} tensor.

Atom	*x*	*y*	*z*	U(eq)
C22	7579(5)	7127(3)	3441.7(19)	37.4(9)
C23	6314(4)	7074(3)	3719(2)	35.4(9)
C24	6299(4)	6862(3)	4317(2)	36.7(9)

Table 3 Anisotropic Displacement Parameters ($Å^2 \times 10^3$) for vw479_0m. The Anisotropic displacement factor exponent takes the form: $-2\pi^2[h^2a^{*2}U_{11}+2hka^*b^*U_{12}+\ldots]$.

Atom	U_{11}	U_{22}	U_{33}	U_{23}	U_{13}	U_{12}
Br1	62.7(3)	55.4(3)	25.6(2)	-6.8(2)	0.5(2)	9.9(2)
Fe1	23.9(3)	18.7(3)	13.7(3)	-0.49(19)	2.4(2)	3.1(2)
P1	27.9(5)	33.5(5)	23.2(5)	5.0(4)	7.8(4)	1.0(4)
P2	28.3(5)	24.3(5)	19.3(4)	2.0(3)	-0.3(3)	6.1(4)
P3	32.0(5)	26.4(5)	23.8(5)	0.5(4)	5.1(4)	10.2(4)
P4	28.7(5)	22.7(5)	22.9(4)	-3.3(4)	-0.4(4)	-2.0(4)
C1	14.6(14)	22.7(17)	13.7(15)	-0.2(13)	2.6(11)	0.6(12)
C2	30.2(19)	30(2)	22.3(18)	-2.0(15)	1.7(14)	2.9(15)
C3	30.3(19)	37(2)	32(2)	-15.6(17)	2.1(16)	-0.9(17)
C4	27.4(19)	62(3)	17.9(18)	-11.3(18)	1.0(14)	1.8(19)
C5	32(2)	53(3)	20.1(18)	6.9(17)	0.2(15)	0.7(18)
C6	31.7(19)	32(2)	20.6(18)	0.7(15)	0.8(15)	1.0(16)
C7	44(2)	30(2)	34(2)	10.3(17)	8.8(18)	0.4(18)
C8	44(2)	24.2(19)	27.9(19)	9.8(15)	3.1(17)	4.7(17)
C9	36(2)	58(3)	44(3)	2(2)	4.5(19)	-11(2)
C10	40(2)	59(3)	44(3)	8(2)	22(2)	7(2)
C11	38(2)	43(2)	37(2)	1.9(19)	7.0(18)	11.1(19)
C12	49(3)	47(3)	34(2)	4.0(19)	-14.9(19)	8(2)
C13	47(2)	22.3(19)	34(2)	1.2(16)	3.8(18)	7.6(17)
C14	50(2)	20.2(19)	38(2)	-4.8(16)	0.4(19)	-1.3(17)
C15	31(2)	51(3)	41(2)	11(2)	1.6(18)	11.9(19)
C16	64(3)	43(3)	41(2)	-2(2)	18(2)	24(2)
C17	33(2)	38(2)	33(2)	0.9(17)	6.9(17)	-6.3(17)
C18	45(2)	48(3)	38(2)	-4(2)	-11.0(19)	-9(2)
C19	37(2)	53(3)	31(2)	2.5(19)	1.3(17)	3(2)
C20	32(2)	50(3)	35(2)	1.6(19)	-3.0(17)	5.7(19)
C21	32(2)	40(2)	38(2)	1.3(18)	5.2(17)	0.2(18)
C22	47(2)	33(2)	32(2)	5.1(17)	-2.1(18)	-1.7(18)
C23	36(2)	25(2)	44(2)	-1.7(17)	-7.9(18)	-1.2(16)

Table 3 Anisotropic Displacement Parameters ($Å^2×10^3$) for vw479_0m. The Anisotropic displacement factor exponent takes the form: $-2\pi^2[h^2a^{*2}U_{11}+2hka^*b^*U_{12}+\ldots]$.

Atom	U_{11}	U_{22}	U_{33}	U_{23}	U_{13}	U_{12}
C24	31(2)	36(2)	43(2)	-5.2(19)	4.3(17)	0.8(17)

Table 4 Bond Lengths for vw479_0m.

Atom	Atom	Length/Å	Atom	Atom	Length/Å
Br1	Fe1	2.5742(7)	P4	C17	1.830(4)
Fe1	P1	2.2375(11)	P4	C18	1.829(4)
Fe1	P2	2.2439(10)	C1	C2	1.392(5)
Fe1	P3	2.2381(11)	C1	C6	1.401(5)
Fe1	P4	2.2304(11)	C2	C3	1.389(5)
Fe1	C1	2.081(3)	C3	C4	1.386(6)
P1	C7	1.839(4)	C4	C5	1.374(6)
P1	C9	1.825(5)	C5	C6	1.395(5)
P1	C10	1.834(4)	C7	C8	1.530(6)
P2	C8	1.841(4)	C13	C14	1.525(6)
P2	C11	1.834(4)	C19	C20	1.374(6)
P2	C12	1.833(4)	C19	C24	1.379(6)
P3	C13	1.857(4)	C20	C21	1.380(6)
P3	C15	1.830(4)	C21	C22	1.377(6)
P3	C16	1.830(4)	C22	C23	1.380(6)
P4	C14	1.845(4)	C23	C24	1.376(6)

Table 5 Bond Angles for vw479_0m.

Atom	Atom	Atom	Angle/°	Atom	Atom	Atom	Angle/°
P1	Fe1	Br1	86.69(3)	C15	P3	C13	104.5(2)
P1	Fe1	P2	85.46(4)	C16	P3	Fe1	120.95(16)
P1	Fe1	P3	94.11(4)	C16	P3	C13	98.4(2)
P2	Fe1	Br1	88.28(3)	C16	P3	C15	98.6(2)
P3	Fe1	Br1	88.17(3)	C14	P4	Fe1	108.69(15)
P3	Fe1	P2	176.44(4)	C17	P4	Fe1	122.17(14)
P4	Fe1	Br1	87.33(3)	C17	P4	C14	103.5(2)
P4	Fe1	P1	174.01(4)	C18	P4	Fe1	121.41(16)
P4	Fe1	P2	94.04(4)	C18	P4	C14	100.2(2)
P4	Fe1	P3	86.01(4)	C18	P4	C17	97.6(2)
C1	Fe1	Br1	179.80(10)	C2	C1	Fe1	123.1(2)
C1	Fe1	P1	93.37(9)	C2	C1	C6	113.7(3)

Table 5 Bond Angles for vw479_0m.

Atom	Atom	Atom	Angle/°	Atom	Atom	Atom	Angle/°
C1	Fe1	P2	91.92(9)	C6	C1	Fe1	123.1(3)
C1	Fe1	P3	91.63(9)	C3	C2	C1	123.7(4)
C1	Fe1	P4	92.61(9)	C4	C3	C2	120.9(4)
C7	P1	Fe1	108.46(14)	C5	C4	C3	117.4(3)
C9	P1	Fe1	122.00(15)	C4	C5	C6	121.0(4)
C9	P1	C7	102.4(2)	C5	C6	C1	123.4(4)
C9	P1	C10	99.0(2)	C8	C7	P1	108.9(3)
C10	P1	Fe1	120.98(18)	C7	C8	P2	108.3(3)
C10	P1	C7	100.7(2)	C14	C13	P3	107.8(3)
C8	P2	Fe1	109.72(13)	C13	C14	P4	110.9(3)
C11	P2	Fe1	122.82(15)	C20	C19	C24	120.9(4)
C11	P2	C8	102.9(2)	C19	C20	C21	119.6(4)
C12	P2	Fe1	120.54(16)	C22	C21	C20	119.7(4)
C12	P2	C8	98.8(2)	C21	C22	C23	120.4(4)
C12	P2	C11	98.3(2)	C24	C23	C22	120.0(4)
C13	P3	Fe1	110.02(13)	C23	C24	C19	119.4(4)
C15	P3	Fe1	121.07(16)				

Table 6 Torsion Angles for vw479_0m.

A	B	C	D	Angle/°	A	B	C	D	Angle/°
Fe1	P1	C7	C8	40.9(3)	C9	P1	C7	C8	-89.3(3)
Fe1	P2	C8	C7	34.4(3)	C10	P1	C7	C8	168.9(3)
Fe1	P3	C13	C14	34.1(3)	C11	P2	C8	C7	166.7(3)
Fe1	P4	C14	C13	36.8(3)	C12	P2	C8	C7	-92.6(3)
Fe1	C1	C2	C3	177.6(3)	C15	P3	C13	C14	165.5(3)
Fe1	C1	C6	C5	-177.1(3)	C16	P3	C13	C14	-93.3(3)
P1	C7	C8	P2	-46.9(3)	C17	P4	C14	C13	-94.5(3)
P3	C13	C14	P4	-44.2(3)	C18	P4	C14	C13	165.1(3)
C1	C2	C3	C4	-0.2(6)	C19	C20	C21	C22	0.9(7)
C2	C1	C6	C5	1.2(5)	C20	C19	C24	C23	0.1(7)
C2	C3	C4	C5	0.7(6)	C20	C21	C22	C23	-0.7(7)
C3	C4	C5	C6	-0.3(6)	C21	C22	C23	C24	0.2(6)
C4	C5	C6	C1	-0.7(6)	C22	C23	C24	C19	0.1(6)
C6	C1	C2	C3	-0.7(5)	C24	C19	C20	C21	-0.6(7)

Table 7 Hydrogen Atom Coordinates (Å×10^4) and Isotropic Displacement Parameters (Å^2×10^3) for vw479_0m.

Atom	*x*	*y*	*z*	U(eq)
H2	7333.04	4106.99	4432.64	33
H3	7437.5	4611.02	5414.39	40
H4	7513.81	3391.81	6182.12	43
H5	7528.14	1659.37	5921.52	42
H6	7452.68	1162.57	4934.88	34
H7A	8833.85	4814.5	2969.55	43
H7B	7924.07	4026.58	2562.36	43
H8A	6264.43	5055.01	3004.25	39
H8B	7058.75	4956.04	3645.66	39
H9A	10576.97	3294.37	4201.93	69
H9B	9532.93	4257.45	4194.34	69
H9C	10790.99	4213.81	3744.65	69
H10A	10767.89	3316.16	2739.09	71
H10B	9796.85	2353.8	2557.96	71
H10C	10930.4	2266.29	3102.55	71
H11A	3630.1	3474.64	3925.66	59
H11B	4145.87	4619.76	3803.54	59
H11C	4867.32	3969.95	4337	59
H12A	5222.68	3278.8	2405.37	66
H12B	4168.39	4079.92	2689.71	66
H12C	3927.99	2875.77	2772.86	66
H13A	8069.05	-961.55	4046.48	41
H13B	7552.88	-243.9	4574	41
H14A	5490.23	-720.02	4067.24	43
H14B	6152.77	-539.19	3433.56	43
H15A	10894.7	1299.18	4160.36	61
H15B	10544.29	204.07	4437.28	61
H15C	9906.86	1222.31	4716.41	61
H16A	8695.57	-141.02	2949.58	73
H16B	9986.78	-468.28	3389.5	73
H16C	10051.79	583.15	3026.33	73
H17A	3928.68	1782.2	4512.19	52
H17B	5040.18	1040.37	4850.37	52
H17C	3702.07	567.58	4490.67	52
H18A	3455.96	247.38	3365.9	66
H18B	4289.98	888.04	2887.68	66
H18C	3282.49	1465.71	3330.41	66
H19	7550.48	6555.47	5045.7	49
H20	9682.28	6654.02	4582.12	47

Table 7 Hydrogen Atom Coordinates (Å×10^4) and Isotropic Displacement Parameters (Å^2×10^3) for vw479_0m.

Atom	*x*	*y*	*z*	U(eq)
H21	9700.01	6993.75	3565.08	44
H22	7586.17	7276.27	3029.17	45
H23	5452.83	7185.27	3497.44	42
H24	5430.76	6823.85	4510.02	44

7) Mössbauer spectroscopy

All samples were prepared in an inert atmosphere glovebox equipped with a liquid nitrogen fill port to enable sample freezing to 77 K within the glovebox. Each sample was loaded into a Delrin Mössbauer sample cup for measurements and loaded under liquid nitrogen. Low temperature ^{57}Fe Mössbauer measurements were performed using a See Co. MS4 Mössbauer spectrometer integrated with a Janis SVT-400T He/N2 cryostat for measurements at 80 K. Isomer shifts were determined relative to α-Fe at 298 K. All Mössbauer spectra were fit using the program WMoss (SeeCo). Errors of the fit analyses were the following: $\delta \pm 0.02$ mm/s and $\Delta EQ \pm 3\%$. For multi-component fits the quantitation errors were ± 3% (e.g. 70 ± 3%).

8) References

[R1] Chatt, J.; Hayter, R. G. Some hydrido-complexes of iron(II). *J. Chem. Soc.* **1961**, 5507−5511. doi.org/10.1039/JR9610005507.

[R2] Tolman, C. A.; Ittel, S. D.; English, A. D.; Jesson, J. P. The chemistry of 2-naphthyl bis[bis(dimethylphosphino)ethane] hydride complexes of iron, ruthenium, and osmium. 1. Characterization and reactions with hydrogen and Lewis base ligands. *J. Am. Chem. Soc.* **1978**, *100*, 13, 4080–4089. doi.org/10.1021/ja00481a016.

[R3] Tolman, C. A.; Ittel, S. D.; English, A. D.; Jesson, J. P. Chemistry of 2-naphthyl bis[bis(dimethylphosphino)ethane] hydride complexes of iron, ruthenium, and osmium. 3. Cleavage of sp2 carbon-hydrogen bonds. *J. Am. Chem. Soc.* **1979**, *101*, 7, 1742–1751. doi.org/10.1021/ja00501a017.

[R4] Maddock, L. C. H.; Cadenbach, T.; Kennedy, A. R.; Borilovic, I.; Aromí, G.; Hevia, E. Accessing Sodium Ferrate Complexes Containing Neutral and Anionic N-Heterocyclic Carbene Ligands: Structural, Synthetic, and Magnetic Insights. *Inorg. Chem.* **2015**, *54*, 18, 9201−9210. doi.org/10.1021/acs.inorgchem.5b01638.

[**R5**] Yang, C.-T.; Zhang, Z.-Q.; Liu, Y.-C.; Liu, L. Copper-Catalyzed Cross-Coupling Reaction of Organoboron Compounds with Primary Alkyl Halides and Pseudohalides. *Angew. Chem. Int. Ed.* **2011**, *50*, 3904–3907. doi.org/10.1002/anie.201008007.

[**R6**] Chen, K.; Chen, W.; Yi, X.; Chen, W.; Liu, M.; Wu, H. Sterically hindered N-heterocyclic carbene/palladium(ii) catalyzed Suzuki–Miyaura coupling of nitrobenzenes. *Chem. Commun.* **2019**, *55*, 9287–9290. doi.org/10.1039/C9CC04634H.

[**R7**] Scherpf, T.; Steinert, H.; Großjohann, A.; Dilchert, K.; Tappen, J.; Rodstein, I.; Gessner, V. H. Efficient Pd-Catalyzed Direct Coupling of Aryl Chlorides with Alkyllithium Reagents. *Angew. Chem. Int. Ed.* **2020**, *59*, 20596–20603. doi.org/10.1002/anie.202008866.

[R8] Dombray, T.; Werncke, C. G.; Jiang, S.; Grellier, M.; Vendier, L.; Bontemps, S.; Sortais, J.-B.; Sabo-Etienne, S.; Darcel, C. Iron-Catalyzed C–H Borylation of Arenes. *J. Am. Chem. Soc.* **2015**, *137*, 12, 4062–4065. doi.org/10.1021/jacs.5b00895.

[R9] O. V. Dolomanov, L. J. Bourhis, R. J. Gildea, J. A. K. Howard, H. Puschmann, *J. Appl. Cryst.* **2009**, *42*, 339–341.

[R10] G. M. Sheldrick, *Acta Crystallographica Section A* **2015**, *71*, 3–8.

[R11] G. M. Sheldrick, *Acta Crystallographica Section C* **2015**, *71*, 3–8.